

Characterization of $\alpha 4\beta 7$ integrin and CD32 expression of CD4⁺ memory T-cell subsets at different stages of HIV infection.

Dissertation

Zur Erlangung des Doktorgrades (Dr. rer. nat.)
im Fachbereich Biologie
der Fakultät für Mathematik, Informatik und Naturwissenschaften
der Universität Hamburg

vorgelegt von
Melanie Wittner
Hamburg, 2020

1. Gutachter: PD Dr. med. Julian Schulze zur Wiesch

2. Gutachter: Prof. Dr. Thomas Dobner

Datum der Disputation: 14.08.2020

Eidesstattliche Versicherung

Hiermit erkläre ich, dass ich die vorliegende Arbeit persönlich, selbstständig und unter Offenlegung der erhaltenen Hilfen angefertigt habe. Die vorliegende Arbeit wurde an keiner anderen Hochschule als Dissertation eingereicht. Ich habe früher noch keinen Promotionsversuch unternommen.

Hamburg, 30.04.2020

Melanie Wittner

TABLE OF CONTENTS

LIST OF FIGURES	I
LIST OF TABLES	III
ZUSAMMENFASSUNG	IV
ABSTRACT	VI
1 Introduction	1
1.1 The Acquired Immune Deficiency Syndrome	1
1.2 The HI Virus	2
1.3 The course of HIV infection	3
1.4 The human immune system	7
1.5 Treatment of the HIV infection	16
1.5.1 Antiretroviral therapy.....	16
1.5.2 The viral reservoir	18
1.5.3 Recent approaches to curing HIV.....	19
1.6 The gut: a crucial site for dissemination of the HIV infection	21
1.6.1 Homing of T cells to the gut-associated lymphoid tissue	22
1.6.2 The integrin $\alpha 4\beta 7$	25
1.7 The Fc γ receptor CD32, a potential marker of latently HIV-infected cells	27
1.8 Aims	28
2 Material und Methods	31
2.1 Material	31
2.1.1 Lab equipment.....	31
2.1.2 Consumables.....	31
2.1.3 Reagents, chemicals and buffers.....	32
2.1.4 Buffers and media	32
2.1.5 Antibodies.....	33
2.2 Clinical cohorts	34
2.3 Methods	39
2.3.1 Acquisition and cryopreservation of PBMC and isolation of LNMC	39
2.3.2 Acquisition of gut biopsies and preparation of lamina propria lymphocytes	39
2.3.3 Surface staining for flow cytometry	40
2.3.4 Flow Cytometry.....	41
2.3.5 <i>In vitro</i> experiments	41
2.4 Data analysis	43
2.4.1 Analysis of cytometric data.....	43
2.4.2 Statistical analysis	43

3	Results	44
3.1	Phenotypic characterization of peripheral blood and lymph nodal CD32⁺ CD4⁺ T cells from healthy individuals and HIV-infected patients	45
3.1.1	Frequency of CD32 ⁺ T cells in the peripheral CD4 ⁺ and CD8 ⁺ memory T-cell compartment.....	45
3.1.2	Expression of the HIV co-receptors on CD4 ⁺ CD32 ⁺ versus CD4 ⁺ CD32 ⁻ T cells	47
3.1.3	Immune activation was associated with the frequency of CD32 ⁺ CD4 ⁺ T cells and CD32 ⁻ CD4 ⁺ T cells were more activated than CD32 ⁻ CD4 ⁺ T cells.....	48
3.1.4	The copy number of integrated HIV-DNA in peripheral CD4 ⁺ T cells of patients with primary infection did not correlate with the frequency of CD32 ⁺ CD4 ⁺ T cells	50
3.1.5	Higher frequency of PD-1 ⁺ and TIGIT ⁺ cells among CD32 ⁺ CD4 ⁺ T cells from HIV-infected individuals	51
3.2	Comparison of the integrin $\alpha 4\beta 7$ expression pattern of memory T-cell subsets during HIV infection and in patients with ulcerative colitis	53
3.2.1	Vedolizumab blocked the binding site of the $\alpha 4\beta 7$ -specific antibody clone Act1.....	54
3.2.2	Definition of $\alpha 4\beta 7$ ⁺ T-cell populations.....	58
3.2.3	Frequency of $\alpha 4\beta 7$ ⁺ CD4 ⁺ T effector memory populations differed in HIV-infected versus healthy individuals	60
3.2.4	The frequency of $\alpha 4\beta 7$ ⁺ CD4 ⁺ T cells was upregulated after <i>in vitro</i> stimulation with bead bound anti-CD3/CD28.....	63
3.2.5	Evaluation of the HLA-DR ⁺ frequency as marker for activated cells.....	65
3.2.6	Frequency of PD-1 ⁺ cells was higher among $\alpha 4\beta 7$ ⁺ T cells of HIV-infected individuals.....	67
3.2.7	Expression of the HIV co-receptor CCR5 on $\alpha 4\beta 7$ ⁺ and $\alpha 4\beta 7$ ⁻ CD4 ⁺ T cells	68
3.2.8	The frequency of $\alpha 4\beta 7$ ⁺ CD4 ⁺ T cells was decreased in the naïve CD4 ⁺ T-cell compartment of patients with UC after treatment with Vedolizumab	69
3.2.9	Longitudinal study of $\alpha 4\beta 7$ expression by CD4 ⁺ T cells from an HIV-infected patient with UC treated with Vedolizumab	75
4	Discussion	81
5	Conclusion and Outlook	104
6	Appendix.....	107
6.1	List of abbreviations.....	114
6.2	References.....	116
7	Acknowledgements	134

LIST OF FIGURES

Figure 1: Electron micrograph of HIV-1.	1
Figure 2: Schematic structure of the HI virus.....	2
Figure 3: Binding and entry of HIV into a host cell.	4
Figure 4: Schematic showing the natural course of HIV infection with regard to plasma viral load and CD4 ⁺ T-cell count.....	5
Figure 5: Spread of HIV in the body via DCs.....	8
Figure 6: T-cell differentiation.....	13
Figure 7: Formation of the latent reservoir.	18
Figure 8: Schematic overview of the "shock and kill" approach.	20
Figure 9: Gut-specific imprinting of CD4 ⁺ T cells in the gut-associated lymphoid tissue.....	22
Figure 10: Leukocyte adhesion cascade.....	23
Figure 11: Main conformations of $\alpha\beta$ -integrins.	25
Figure 12: Overview of Fc receptor family.....	27
Figure 13: Frequency of CD32 ⁺ T cells in the CD4 ⁺ and CD8 ⁺ compartment.	45
Figure 14: Expression of the HIV co-receptors CXCR4 and CCR5 on CD32 ⁺ versus CD32 ⁻ cells.....	47
Figure 15: Correlation between frequencies of activated HLA-DR ⁺ CD8 ⁺ T cells and CD32 ⁺ CD4 ⁺ T cells....	48
Figure 16: Frequency of HLA-DR ⁺ CD4 ⁺ CD32 ⁺ and CD32 ⁻ T cells.....	49
Figure 17: Frequency of peripheral CD4 ⁺ CD32 ⁺ T cells versus total HIV-DNA in CD4 ⁺ T cells in patients with primary HIV infection.....	50
Figure 18: Frequency of PD-1 ⁺ (A) and TIGIT ⁺ (B) CD4 ⁺ CD32 ⁺ and CD32 ⁻ T cells.....	51
Figure 19: Vedolizumab blocks binding of the $\alpha4\beta7$ -specific antibody clone Act1 in <i>ex vivo</i> samples from UC patients.....	54
Figure 20: Percentage of $\alpha4\beta7$ expressing CD4 ⁺ T cells after <i>in vitro</i> incubation with Vedolizumab.....	55
Figure 21: Comparison of the $\alpha4\beta7$ -specific clone Act1 and the $\alpha4$ -specific clone 7.2R in combination with a separate $\beta7$ -specific antibody.	56
Figure 22: Correlation of the $\alpha4\beta7$ frequencies detected with the $\alpha4\beta7$ -specific clone Act1 and the $\alpha4$ -specific clone 7.2R in combination with a separate $\beta7$ -specific antibody.....	57
Figure 23: Exemplary plots of $\alpha4\beta^{\text{intermediate}}$ and $\alpha4\beta7^{\text{high}}$ cells as well as $\alpha4^{\text{intermediate}}/\alpha4^{\text{high}}$ and $\beta7^{\text{intermediate}}/\beta7^{\text{high}}$ cells.....	58
Figure 24: Gating of samples from an HIV-infected patient (A) and a patient with UC (B).....	59

Figure 25: Frequency of $\alpha 4\beta 7^+$ cells does not differ in total $CD4^+$ or $CD8^+$ T cells from PBMC of HIV-infected patients compared to healthy individuals.	60
Figure 26: Distribution of $CD4^+$ T-cell subsets in different cohort groups.	61
Figure 27: Frequency of $\alpha 4\beta 7^+$ cells differs in different effector memory $CD4^+$ T-cell populations in PBMC from HIV-infected patients compared to healthy individuals.....	62
Figure 28: Upregulation of $\alpha 4\beta 7^+$ $CD4^+$ T cells after <i>in vitro</i> stimulation with bead-bound anti-CD3/CD28.	63
Figure 29: Comparative analysis of HLA-DR on $\alpha 4\beta 7^+$ and $\alpha 4\beta 7^-$ cells of healthy controls, patients with UC and HIV-infected individuals.	65
Figure 30: Comparative analysis of PD-1 on $\alpha 4\beta 7^+$ and $\alpha 4\beta 7^-$ cells from healthy controls, HIV-infected individuals and patients with UC.....	67
Figure 31: Comparative analysis of CCR5 on $\alpha 4\beta 7^+$ and $\alpha 4\beta 7^-$ $CD4^+$ T cells from healthy controls, patients with UC and HIV-infected individuals.	68
Figure 32: Frequency of $\alpha 4\beta 7^+$ cells is significantly decreased on naïve $CD4^+$ T cells from patients with UC treated with Vedolizumab compared to untreated patients.....	69
Figure 33: Frequency of $\alpha 4\beta 7^+$ cells does not differ between naïve and memory $CD4^+$ T-cell populations of gut derived lymphocytes of healthy individuals and patients with UC.	71
Figure 34: Frequency of $\alpha 4\beta 7^+$ cells does not differ between naïve and memory $CD4^+$ T-cell populations of lymph node mononuclear cells from HIV-infected and uninfected individuals.....	73
Figure 35: $\alpha 4\beta 7$ is not correlated with activation, $CD4^+$ T-cell count or plasma viral load in HIV.....	74
Figure 36: Longitudinal study of the frequencies of $\alpha 4\beta 7^+$ $CD4^+$ and $CD8^+$ T cells from an HIV patient with concomitant UC.....	76
Figure 37: Frequencies of $\alpha 4\beta 7$ $CD4^+$ T cells within different $CD4^+$ T-cell compartments over the course of therapy.....	77
Figure 38: Changes in the frequency of $CCR9^+$ $CD4^+$ T cells during Vedolizumab therapy.	78
Figure 39: Activation as indicated by HLA-DR expression of $CD8^+$ and $CD4^+$ $\alpha 4\beta 7^{+/-}$ T cells.	79
Figure 40: Activation/exhaustion of $CD4^+$ $\alpha 4\beta 7^+$ T cells as indicated by PD-1 expression.	80

LIST OF TABLES

Table 1: Overview of equipment used.....	31
Table 2: Overview of consumables used.	31
Table 3: Overview of reagents/chemicals and buffers as well as media used.....	32
Table 4: Overview of the compositions of buffers and media used.....	32
Table 5: Overview of antibodies used.	33
Table 6: Summarized clinical data from patients with HIV infection and healthy subjects who participated in the CD32 study.	34
Table 7: Clinical details of patients with UC who participated in the $\alpha 4\beta 7$ study.....	35
Table 8: Clinical details of patients with HIV infection who participated in the $\alpha 4\beta 7$ study.....	37
Table 9: Summarized clinical data from patients with HIV infection and uninfected controls.....	38
Table 10: Overview of the literature on CD32(a).	85
Table 11: Overview of the literature on $\alpha 4\beta 7$	93

ZUSAMMENFASSUNG

Das Humane Immundefizienz-Virus (HIV) verursacht eine chronische Infektion, die unbehandelt zu Acquired Immune Deficiency Syndrome (AIDS) fortschreitet. AIDS resultiert aus der induzierten Abnahme der Anzahl von CD4⁺ Helfer-T-Zellen, wodurch es zu einem schweren Immundefekt kommt, der den Körper für eine Vielzahl potenziell tödlicher Infektionen und für insbesondere viral induzierte Krebsarten anfällig macht, z.B. das Kaposi-Sarkom¹.

Latent infizierte CD4⁺ T-Zellen, die während der Infektion persistieren, sind dauerhaft stabil und enthalten replikationskompetentes Provirus. Da latent infizierte CD4⁺ T-Zellen nur wenig oder keine virale Genexpression aufweisen, ist es für das Immunsystem schwierig, sie zu erkennen und zu eliminieren. Es wird angenommen, dass bestimmte T-Zell-Untergruppen, wie z.B. Zentrale-Gedächtnis-T-Zellen entscheidend sind für die Bildung des beständigen Virusreservoirs latent infizierter T-Zellen. Darüber hinaus wurden mehrere neuartige Markermoleküle zur Bestimmung latent HIV-infizierter Zellen vorgeschlagen²⁻⁶.

Diese Arbeit zielte darauf ab, das Expressionsmuster und die mögliche Rolle von zwei Molekülen zu untersuchen, von denen in vorherigen Untersuchungen beschrieben wurde, dass sie Indikatormoleküle latent infizierter Zellen (CD32a) oder an der Bildung des Reservoirs ($\alpha 4\beta 7$) in CD4⁺ Gedächtnis-T-Zell-Subpopulationen beteiligt sind. Dazu wurde eine große Kohorte von HIV-infizierten Personen mit unterschiedlichem klinischen Krankheitsverlauf (HIV-Patienten mit nachweisbarer Virämie, antiretrovirale Therapie- (ART-) behandelte Patienten mit nicht nachweisbarer Viruslast, Elite-Controller, die die Infektion ohne Medikamente kontrollieren) untersucht. Neben mononukleären Zellen des peripheren Blutes (PBMC) wurden auch mononukleäre Zellen des Lymphknotens (LNMC) sowie Lymphozyten der Lamina propria des Darms (LPL) hinsichtlich der Oberflächenexpression von CD32 und $\alpha 4\beta 7$ untersucht. T-Zell-Subpopulationen von PBMC und LPL von Patienten mit Colitis ulcerosa (UC) wurden hinsichtlich der Homing-Kapazität einer bestimmten T-Zell-Subpopulation in den Darm sowie der Eignung eines therapeutischen, $\alpha 4\beta 7$ -spezifischen Antikörpers zur potenziellen Hemmung der Bildung des HIV-Reservoirs innerhalb des Darms untersucht.

Der Fc-Rezeptor CD32a wurde kürzlich in einer einzelnen Studie als exklusiver Marker für latent HIV-infizierte T-Zellen beschrieben, jedoch fehlten weitere Details des Expressionsmusters von CD32(a) auf Gedächtnis-T-Zell-Subpopulationen von gesunden und HIV-infizierten Patienten. Daher wurde in dieser Arbeit eine umfassende phänotypische Charakterisierung von CD32 mittels Multiparameter-Durchflusszytometrie von PBMC und LNMC von Patienten mit HIV-Infektion und nicht infizierten Personen durchgeführt. Insgesamt konnten nur geringe Unterschiede in der Häufigkeit peripherer Gesamt-CD4⁺ CD32⁺ T-Zellen zwischen gesunden und HIV-infizierten Personen mit Virämie sowie HIV-infizierten ART-behandelten Patienten festgestellt werden. Darüber hinaus korrelierte die CD32-Expression mit dem Aktivierungsstatus der CD8⁺ T-Zellen.

Parallel dazu wurde das Expressionsmuster des Integrins $\alpha 4\beta 7$, welches das T-Zell-Homing von CD4⁺ und CD8⁺ T-Zellen in den Magen-Darm-Trakt ermöglicht, mittels Durchflusszytometrie analysiert. Periphere CD4⁺ T-Zellen von Patienten, die einen $\alpha 4\beta 7$ -spezifischen Antikörper (Vedolizumab, VDZ) als Behandlung für ihre UC erhielten, wurden mittels Durchflusszytometrie auf die Expression von $\alpha 4\beta 7$, sowie auf Homing-, Erschöpfungs- und Aktivierungsmarker im Vergleich zu Proben von gesunden und HIV-infizierten Personen untersucht. Zusätzlich wurden Zellen, gewonnen aus dem Lymphknoten und der Lamina propria des Darmes, von Personen mit UC und HIV-infizierten Patienten sowie longitudinale PBMC Proben eines einzelnen HIV-infizierten Patienten untersucht, der wegen gleichzeitiger UC mit Vedolizumab behandelt wurde. Vedolizumab verringerte hauptsächlich die Häufigkeit von naiven $\alpha 4\beta 7^+$ CD4⁺ T-Zellen bei Patienten mit UC, während bei virämischen und avirämischen HIV-infizierten Patienten ein signifikanter Verlust der CD4⁺ Gedächtnis-T-Zell-Subpopulationen nachweisbar war.

Die Ergebnisse dieser Arbeit legen nahe, dass CD32(a) nicht ausschließlich ruhende, latent infizierte CD4⁺ T-Zellen zu markieren scheint. Darüber hinaus helfen die erhaltenen Resultate, Vedolizumab als mögliche Behandlung einer primären HIV-Infektion zu bewerten.

ABSTRACT

The human immunodeficiency virus (HIV) causes a chronic infection that, if left untreated, progresses to Acquired Immune Deficiency Syndrome (AIDS). AIDS results from decreasing numbers of CD4⁺ helper T cells causing a severe immunodeficiency that leaves the body susceptible to a variety of potentially fatal infections and mainly viral-induced cancers, e.g. Kaposi's Sarcoma¹.

Latently infected CD4⁺ T cells that persist during infection are highly stable over time and contain replication-competent provirus. Since there is little to no viral gene expression in latently infected CD4⁺ T cells, it is difficult for the immune system to recognize and eliminate them. It has been suggested that certain T cell subsets, such as central memory T cells, are crucial in the formation of the stable viral reservoir of latently infected T cells. Furthermore, several novel marker molecules to designate latently HIV-infected cells have been proposed²⁻⁶.

The aim of this thesis was to investigate the expression pattern and potential role of two molecules that could indicate latently infected cells (CD32a) or be involved in the formation of the reservoir ($\alpha 4\beta 7$) in CD4⁺ T cell memory subsets in a large cohort of HIV-infected individuals with different clinical disease course (HIV patients with detectable viremia, antiretroviral therapy- (ART-) suppressed patients with undetectable viral load and elite controllers controlling the infection without medication). In addition to peripheral blood mononuclear cells (PBMC), lymph node mononuclear cells (LNMC) as well as gut lamina propria lymphocytes (LPL) were studied with regard to the surface expression of CD32 and $\alpha 4\beta 7$. T-cell subsets of PBMC and LPL from patients with ulcerative colitis (UC) were studied to investigate the homing capacity of a certain T-cell subset to the gut as well as the eligibility of a therapeutic $\alpha 4\beta 7$ -specific antibody to potentially inhibit the HIV reservoir formation within the gut.

The Fc receptor CD32a has recently been described in a single study to be an exclusive marker of latently HIV-infected T cells but further details of the expression pattern of CD32(a) on T cell memory subsets of healthy and HIV-infected patients were missing. Therefore, a comprehensive phenotypic characterization of CD32 via multicolour flow cytometry of PBMC and LNMC from patients with HIV infection and uninfected individuals was carried out in this thesis. Overall, only small differences in the frequency of peripheral total CD4⁺ CD32⁺ T cells could be detected between healthy and HIV viremic individuals as well as HIV-infected patients on ART. Moreover, CD32 expression correlated with the activation status of the CD8⁺ T cells.

In parallel, the expression pattern of the integrin $\alpha 4\beta 7$ that facilitates T cell homing of CD4⁺ and CD8⁺ T cells to the gastrointestinal tract was analysed by flow cytometry. Peripheral CD4⁺ T cells from patients receiving an $\alpha 4\beta 7$ -specific antibody (Vedolizumab, VDZ) as a medical treatment for their UC were studied by flow cytometry for the expression of $\alpha 4\beta 7$ as well as for homing, exhaustion and activation markers in comparison to samples from healthy and HIV-infected individuals. Additionally, lymph node and gut lamina propria-derived cells of individuals with UC and HIV-infected patients, as well as longitudinal PBMC samples from a single HIV-infected patient who was being treated with Vedolizumab for concomitant UC were studied.

Vedolizumab mainly decreased the frequency of naïve $\alpha 4\beta 7^+$ CD4⁺ T cells in patients with UC, whereas a significant loss of CD4⁺ T cell memory populations was detectable in viremic and aviremic HIV-infected patients.

The results of this thesis suggest that CD32(a) does not seem to exclusively mark resting, latently infected CD4⁺ T cells. Furthermore, the observed effect of Vedolizumab mainly on naïve T cells helps to evaluate Vedolizumab as a possible treatment of primary HIV infection.

1 Introduction

1.1 The Acquired Immune Deficiency Syndrome

In 1981, the first cases of a rare lung infection (*Pneumocystis carinii* pneumonia) and other opportunistic infections as well as an unusual, aggressive type of cancer (Kaposi's Sarcoma) were reported in the United States by Dr. Gottlieb and Dr. Friedman-Kien and colleagues⁷. Two years later, Dr. Barré-Sinoussi *et al.*, together with Dr. Gallo and colleagues first identified the virus that causes Acquired Immune Deficiency Syndrome (AIDS): the human immunodeficiency virus (HIV), shown in an electron micrograph in **Figure 1**⁸.

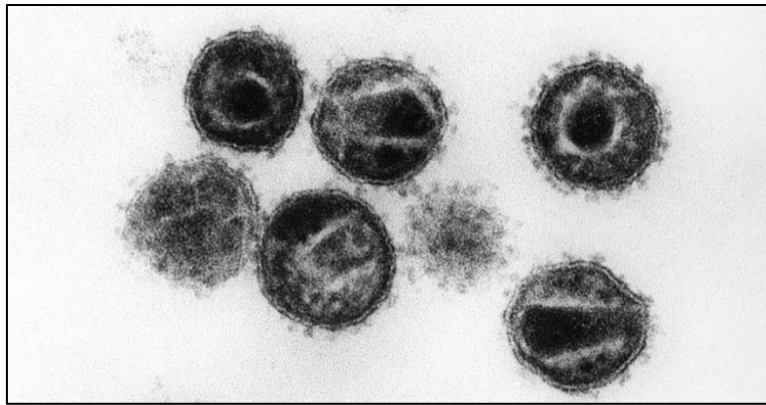


Figure 1: Electron micrograph of HIV-1. Courtesy of Hans R. Gelderblom/Robert Koch Institut, reproduced with permission.

In 2018, globally approximately 37.9 million people were living with HIV, of whom only 23.3 million had access to antiretroviral therapy (ART) (UNAIDS Data 2019). In the same year, 1.7 million new HIV infections were recorded, and 770 000 people died from AIDS-related illnesses (UNAIDS Data 2019).

Although HIV has become a manageable chronic infection in Western countries, there is still no protective vaccine and no cure available. Thus, further efforts are being made to better understand the persistence of the virus in the human body and to eradicate infected cells.

1.2 The HI Virus

HIV is an enveloped retrovirus and belongs to the genus *Lentivirus*. There are two types, HIV-1 and HIV-2, which are phylogenetically different^{8,9}. HIV-2 is considered less pathogenic than HIV-1 and accounts for less than 1 % of infections worldwide (mostly in West-Africa). Further classification of HIV-1 is done according to groups (M, N, O and P) and clades (A-D and F-J). Using the *env* gene as an example, inter-clade variations differ by 20 to 30 % within the M subgroups^{10,11}. More than 90 % of HIV infections are caused by group M (major).

Figure 2 shows the schematic structure of an HI virus.

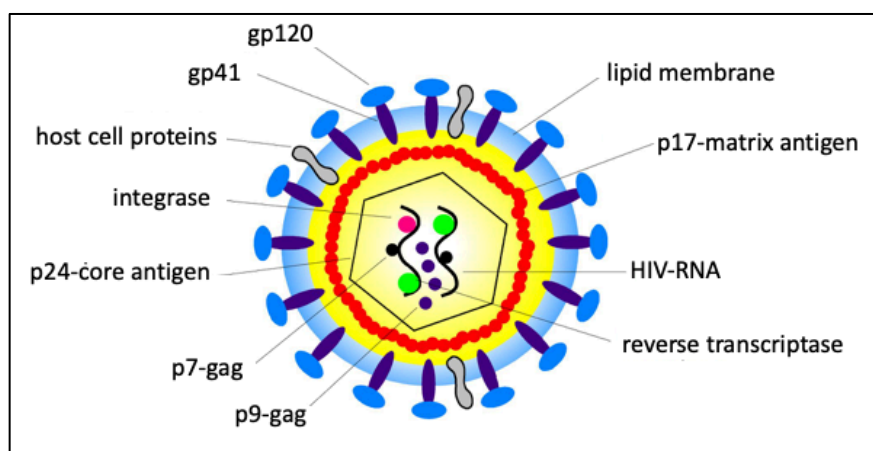


Figure 2: Schematic structure of the HI virus. Figure adapted from Hoffmann, Rockstroh *et al.*²⁶⁰.

The envelope consists of a host cell-derived lipid bilayer membrane that contains so-called (envelope protein) spikes formed by one gp120 and three molecules of gp41 which anchor the protein complex into the membrane^{12,13}. Gp120 initiates target cell contact by binding to the CD4 molecule and one of the chemokine receptors CXCR4 or CCR5, whereas gp41 is a membrane-spanning protein that mediates the fusion of viral particle and target cells¹⁴⁻¹⁶.

There are two copies of the single-stranded HIV-1 RNA, each of which is nine kilobases long. Out of the nine genes *gag*, *pol*, *env*, *vif*, *vpu*, *vpr*, *tat*, *rev* and *nef*, three are essential: *gag* ("group antigen"), *pol* ("polymerase") and *env* ("envelope"). *Pol* encodes for reverse transcriptase and other (additional) enzymes, whereas *gag* and *env* code for the nucleocapsid and the proteins of the viral envelope. The focus in this thesis is on different aspects of the interaction of the immune system with HIV-1, which will from now on be referred to as HIV.

1.3 The course of HIV infection

HIV is present in the semen, vaginal fluid, blood and breast milk of untreated, infected individuals. Furthermore, rectal fluid can contain high concentrations of the virus^{17,18}. Thus, infection can occur through sexual intercourse, usage of contaminated needles for injection, or breastfeeding. Also, HIV-infected mothers can transmit the virus to their babies during pregnancy and birth^{19,20}. Many people were also infected by receiving contaminated blood products before donated blood was routinely screened for HIV in 1985²¹.

The most common way of transmission is sexual intercourse. The mucosae of the female genital tract, the male foreskin and the rectum contain numerous viral target cells, such as activated CD4⁺CCR5⁺ T cells and dendritic cells (DC)²². DC subsequently transport the virus to proximal lymph nodes, where they present it to activated CD4⁺ T cells which become infected (see also section 1.4). For productive infection, the target cells need to be activated, so that the viral RNA can be reversely transcribed and integrated into the host cell.

The CD4 molecule is the primary HIV receptor and constitutes part of the T-cell receptor/CD3 complex. Binding of the viral envelope protein gp120 to CD4 induces a conformational change of the viral envelope and triggers intracellular signal cascades^{23,24}. In addition, the binding of a co-receptor which defines the tropism of the virus is required. X4 tropic strains bind the chemokine receptor CXCR4; CCR5 is used by R5 tropic viruses. It has been shown that the tropism of HIV changes as the infection progresses: in the early phase, mostly R5 tropic virus can be isolated from infected patients, whereas the majority of the virus in the chronic phase was found to be X4 tropic²⁵. After binding both to the CD4 molecule and one of the co-receptors, the viral and host cell membrane fuse and the viral core is released into the cytoplasm²⁶.

In the cytoplasm, the viral RNA is reversely transcribed into proviral DNA before it is transported and integrated into the host DNA (**Figure 3**).

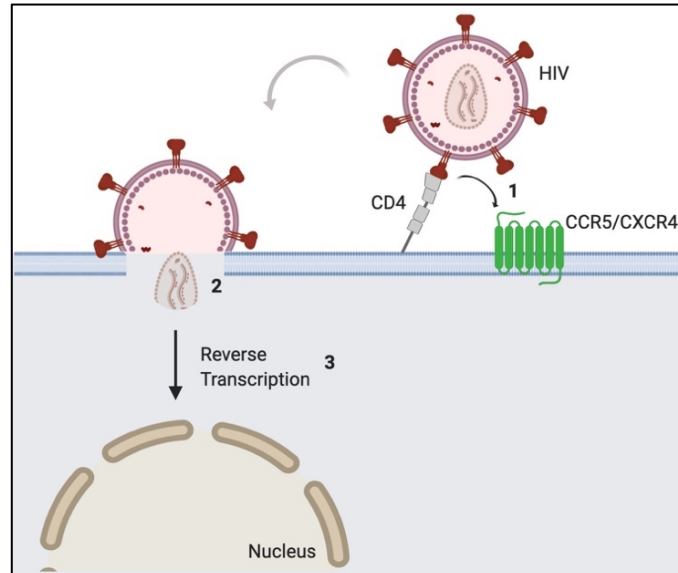


Figure 3: Binding and entry of HIV into a host cell. The viral envelope protein (Env) binds to the CD4 molecule and one of the co-receptors CCR5 or CXCR4 of the host cell (1). This binding initiates fusion of the viral and the host cell membranes (2), followed by reverse transcription of the viral RNA (3). The converted DNA is then integrated into the host genome (not shown).

How the virus is disseminated on a cellular and anatomical level will be described in the following sections (1.4 and 1.6).

Two clinical parameters that are used to monitor the course of the disease are the **CD4⁺ T-cell count** and the HIV **plasma viral load**. The CD4⁺ T-cell count is a surrogate parameter for the immune function and disease progression; one of the parameters that define AIDS is a CD4⁺ T-cell count < 200 CD4⁺ T cells/ μ L. It is furthermore used in determining the necessity for ART or prophylaxis against opportunistic infections. The plasma viral load is measured regularly to monitor the efficacy of antiviral therapy.

The **viral set point** is a relatively steady level of viremia, caused by a balance between the viral turnover and the counteracting immune response. Early treatment with ART has been shown to be associated with a lower viral set point and a smaller reservoir size^{27,28}.

The course of the disease can be divided into two phases, the acute and the chronic. These two phases are illustrated in **Figure 4**.

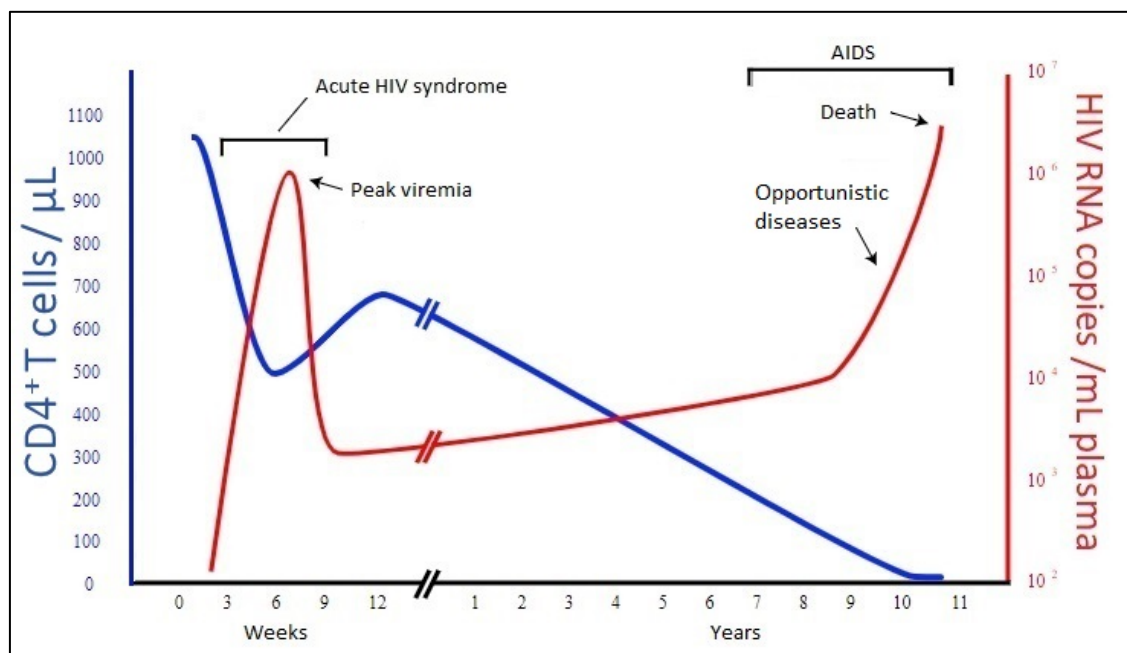


Figure 4: Schematic showing the natural course of HIV infection with regard to plasma viral load and CD4⁺ T-cell count. The course of HIV infection without ART. The blue line shows changes in the number of CD4⁺ T cells/ μ L blood, the red line depicts the number of HIV RNA copies/mL plasma.

In the **primary HIV infection**, influenza-like symptoms such as fever, swollen lymph nodes and joint and muscle aches can be experienced (“acute HIV syndrome”). High numbers of virus present in the blood plasma lead to the expansion of circulating CD4⁺ T cells and to an activation of cytotoxic CD8⁺ T cells. Large numbers of CD4⁺ T cells are depleted during primary infection, due to the following mechanisms: First, cells die due to cytopathic effects caused by the virus; second, infected cells are killed by virus-specific CD8⁺ T cells; and third, it is hypothesized that infected cells are more sensitive to the initiation of apoptosis²⁹. This results in an inverted CD4:CD8 T cell ratio caused by the depletion of CD4⁺ and the expansion of CD8⁺ T cells^{30–32}. CD4⁺ T cells orchestrate the production of neutralizing antibodies against the envelope proteins gp120 and gp41 by B cells^{33,34}. The time at which these HIV-specific antibodies can be detected in the patients’ blood is termed seroconversion. The onset of the adaptive immune response then lowers the plasma viral load.

The symptoms of the acute infection usually subside after three to four months. After that, patients enter a phase without clinical symptoms, termed **clinical latency**. Even if left untreated, the virus can persist in the body for months or years before the infection becomes symptomatic. During this period, the number of CD4⁺ T cells steadily decreases because the generation and differentiation as well as homeostasis of CD4⁺ T-cell subsets is impaired³⁵. At the same time, the function of the remaining memory CD4⁺ T cells is compromised.

Clinical symptoms re-appear once the CD4⁺ T-cell counts fall below about 500 cells/ μ L which is accompanied by increasing plasma viral loads. At this point, opportunistic infections and AIDS-specific cancers can spread which the patient eventually dies of. Typical infections are e.g. caused by *Candida* spp. and *Mycobacterium tuberculosis*, resulting in oral candidiasis and tuberculosis^{36,37}. AIDS-specific cancers comprise Kaposi's sarcoma or AIDS-related lymphoma caused by Epstein-Barr virus³⁸.

1.4 The human immune system

The immune system of vertebrates has evolved potent mechanisms to fight pathogens (viruses, bacteria, fungi, protozoa and parasites). The following section gives a short overview of the cellular **innate and adaptive immune response** of the human immune system, with a focus on the anti-viral immune response.

The **innate immune response** is the first-line defence against pathogens. As such, it is fast, but non-specific. There are two main components of the innate immune system: the **humoral** and the **cellular** system. The latter consists of DCs, natural killer cells (NK cells), granulocytes (neutrophils, basophils and eosinophils) and monocytes as well as macrophages. The humoral system entails macromolecular mechanisms, such as antimicrobial peptides and the complement system that consists of precursor proteins circulating in the blood.

Unlike adaptive immune responses that rely on a huge repertoire of specific receptors, innate immune cells are well conserved. Importantly, antigens can be recognized as a whole and do not require processing and presentation by other cells (see the adaptive immune system). Instead, general patterns are recognized on pathogens (e.g. bacterial lipopolysaccharides) which serve as “nonself” signals. These so-called pathogen-associated molecular patterns (PAMPs) are identified by pathogen-recognition receptors (PRRs) and trigger innate immune responses. It has been demonstrated that gp120 is recognized by the PRR C-type lectin DC-SIGN (Dendritic Cell-Specific Intercellular adhesion molecule-3-Grabbing Non-integrin) and that HIV-RNA can be detected by the Toll-like receptors (TLR) 7 and 8³⁹⁻⁴¹.

When viral products are recognized by the innate immune system, type I and type III interferons as well as proinflammatory cytokines and chemokines are produced. This causes innate immune cells such as NK cells and macrophages to be activated and recruited in the proximity of the infected cell. The secretion of interferons also serves as a signal for nearby cells to activate anti-viral processes, e.g. the expression of RNase L which is capable of cleaving RNA or the up-regulation of p53, which promotes apoptosis^{42,43}.

NK cells are able to rapidly identify virus-infected cells, e.g. by direct recognition of viral proteins or virus-induced stress ligands which are recognized by activating killer cell immunoglobulin-like receptors (KIRs). In HIV infection, human leukocyte antigen-class I (HLA-class I) molecules that act

as ligands for inhibitory KIRs are downregulated by the virus. Thus, infected cells are killed by perforin and granzyme secretion from NKs.

Unfortunately, other innate immune cells aid in the spread of HIV in the body. DCs are antigen-presenting cells (APCs) present in high numbers at mucosal surfaces where they take up and process antigens which they subsequently present to T- and B-cells to trigger a response by the adaptive immune system. It has been demonstrated that HIV can bind to the lectin DC-SIGN on lamina propria DCs which absorb it into early endosomes and transport it through the small intestinal mucosa^{44,45}. The DCs then migrate into lymph nodes where the infectious virions are presented to CD4⁺ T cells (see **Figure 5**).

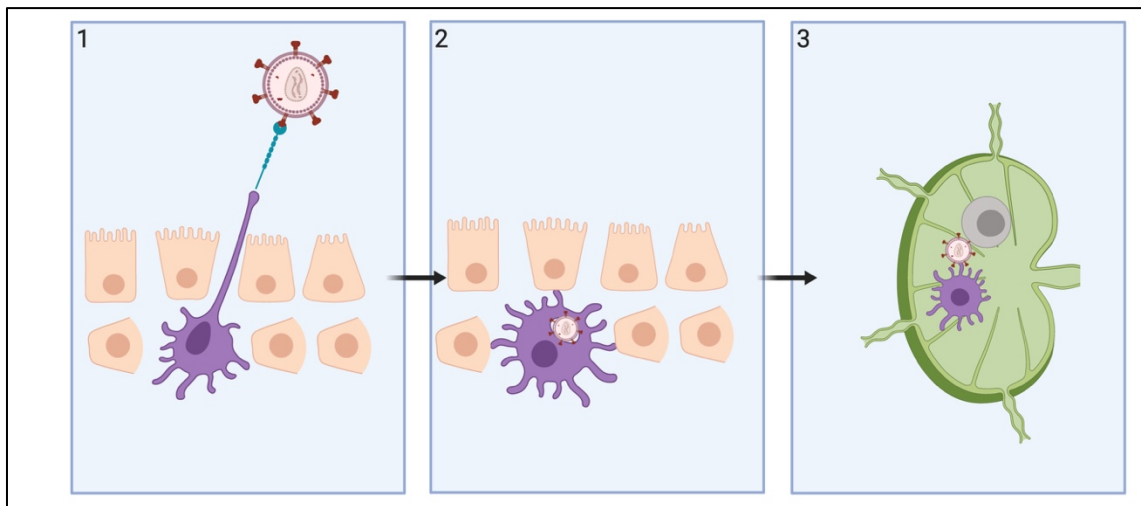


Figure 5: Spread of HIV in the body via DCs. (1) HIV (depicted in pink) is recognized and bound by intraepithelial DC-SIGN (in blue) on DCs (in purple). (2) HIV is taken up by the DCs into early endosomes. (3) After migration into lymph nodes (in green), DCs present HIV to CD4⁺ T cells (in grey), which then become infected. Figure adapted from Janeway Immunobiology, 9th edition, Garland Science 2008²⁹.

Another crucial host defence mechanism against viral infections is **restriction factors** which target most steps of the viral replication cycle⁴⁶. These intracellular proteins are germline-encoded and can be found in almost all cell types. Some are constitutively expressed, while others are upregulated upon interferon stimulation. Since most of the viral components targeted are highly conserved, restriction factors can be active against different viral species. Nevertheless, viruses have developed mechanisms to evade this response or to counteract restriction factors.

An example of restriction factors is DNA-cytosine deaminases that convert viral cytosine to uracil, which results in guanine to adenosine exchanges and ultimately mutation of the viral genome⁴⁷. This mutagenic conversion is facilitated by apolipoprotein B mRNA editing catalytic polypeptide-like (APOBEC) enzymes. In the human genome, eleven APOBEC proteins are encoded, four of which can interfere with HIV infection⁴⁸. They get transported to new target cells in the HIV virion and act during reverse transcription of viral RNA into DNA. The HIV protein Vif (virion infectivity factor) can counteract the antiviral response of APOBEC enzymes by mediating their polyubiquitination, which marks the protein for degradation in cellular proteasomes^{49,50}.

Another restriction factor that suppresses reverse transcription in non-dividing myeloid cells is sterile a motif domain-, HD domain-containing protein 1 (SAMHD1) that works both by blocking deoxyribonucleotide triphosphates (dNTPs) required for cDNA synthesis and also possibly by degrading viral RNA^{51,52}. The counteracting viral protein is viral protein x (Vpx), which is unique to HIV-2 and simian immunodeficiency virus (SIV). It binds to SAMHD1 and causes its proteasomal degradation by interaction with a ubiquitin ligase complex⁵³.

Whilst APOBEC and SAMHD1 interfere with the reverse transcription of the viral RNA, tetherin inhibits the release of newly synthesized virions from the infected host cell^{54,55}. It carries a transmembrane anchor close to its N terminus and a glycosylphosphatidylinositol lipid anchor at its C terminus. It is hypothesized that one anchor is inserted into the viral envelope, whereas the other remains in the host cell. Following internalization, the virions accumulate in endosomes, where they are degraded. HIV uses Vpu (viral protein unknown) to counteract this mechanism, but the exact mode of action is still unknown.

In contrast to the innate immune system, the **adaptive immune** system targets evading pathogens with specialized and specific entities and forms a memory system. However, the generation of appropriate responses is slow and can take from days to weeks. The specificity with which it can detect an enormous diversity of antigens is achieved by somatically rearranged antigen receptor genes⁵⁶.

The adaptive immune system also consists of cellular and humoral components. **CD4⁺ and CD8⁺ T cells** orchestrate the cellular response, while antibodies produced by B cells constitute the humoral response. Since this thesis has aimed at investigating the role of T cells as potential reservoir cells of HIV infection, only T cells will be covered in this section.

In **acute**, non-persisting **viral infections**, e.g. those caused by influenza viruses, **CD8⁺ T cells** are capable of eliminating infected cells by cytotoxic activity. Naïve T cells are first primed by matching antigens presented on major histocompatibility complex (MHC) class I molecules on APCs such as DCs in peripheral lymphatic organs. They bind to the MHC/antigen complex via their T cell receptor (TCR) which is composed of two polypeptide chains, $TCR\alpha$ and $TCR\beta$ that resemble the Fab fragment of IgG. They then undergo differentiation to effector cells, whilst being retained in the lymphatic tissue.

Once back in circulation, the CD8⁺ effector T cells are capable of detecting the complex of their specific antigen presented via MHC-I molecules on infected target cells via their specific TCR and form a so-called immunological synapse with the target cell. The CD8 molecule is needed as a co-receptor whose MHC-I-specific binding results in a hundredfold increase in the T cell's sensitivity towards the presented antigen. Target cells are killed off either by induction of apoptosis via interaction of Fas (on the target cell) and Fas-ligand (on the effector cell) or by secretion of cytotoxic granules (perforin, granzyme and granulysin). In addition, cytokines which activate and recruit macrophages (TNF- α and lymphotoxin (LT)- α) and inhibit viral replication directly (IFN- γ) and indirectly by enhancing the expression of MHC-I molecules are produced. Other chemokines like CCL3, CCL4 and CCL5 can block the entry of CCR5-tropic viruses⁵⁷. These non-cytolytic mechanisms also contribute to the (anti-viral) immune response.

HIV-specific CD8⁺ T cells play a crucial role in the host defence against HIV. Upon CD8⁺ T cell depletion in SIV infected rhesus monkeys, plasma viremia rose markedly and was quickly followed by the appearance of new virus-specific CD8⁺ T cells⁵⁸. Also, viral mutants that escape the CD8⁺ T cell response form quickly during acute infection which indicates that the CD8⁺ T cell response exerts a considerable selection pressure⁵⁹. Since HIV causes a **chronic infection**, pathogen-specific CD8⁺ effector T cells become functionally exhausted as a consequence of persistent exposure to HIV antigens. Furthermore, support from CD4⁺ T-cells, which has been shown to be crucial in the maintenance of the virus-specific CD8⁺ T-cell response and prevention of CD8⁺ T-cell dysfunction during chronic infection, is lacking⁶⁰. Exhausted cells are transcriptionally distinct from regular effector cells: they upregulate e.g. inhibitory receptors such as programmed cell death protein 1 (PD-1) and co-inhibitory molecules like lymphocyte-activation gene 3 (LAG-3) and T cell immunoglobulin and mucin domain-containing protein 3 (Tim-3)^{61,62}. As a consequence, the effector response is poor and the infection cannot be controlled properly⁶³.

After an initial strong response against HIV, impaired function and decreased proliferation can be observed soon after peak viremia. Without treatment, the loss of viral control and continuous activation of CD8⁺ T cells leads to disease progression and eventually to AIDS⁶⁴. Under ART, some of the polyfunctionality of CD8⁺ T cell responses can be regained and a partial down-regulation of activation and exhaustion markers is observed^{65,66}. However, full cytotoxic and proliferative capacity cannot be regained, even if viral control is achieved under ART⁶⁷. Also, the expanded CD8⁺ T-cell compartment does not return to normal levels; instead a high proportion of terminally differentiated effector cells (T_{EM}) are found, which represent CD8⁺ T cells in a sort of “hyperproliferation state” after full differentiation and expansion^{68,69}. These cells are impaired in their antiviral activity and contribute to the pool of exhausted cells. Most importantly, CD8⁺ T cells are not capable of destroying latently infected cells that comprise the reservoir and persist during ART. Paradoxically, this could be partially due to the non-cytolytic activity that suppresses viral replication.

The binding of pathogen-derived peptides to HLA proteins is crucial for the onset of the adaptive immune system and is strongly influenced by polymorphisms of the HLA gene. Some individuals in the group of so-called “elite controllers” (EC), who are able to control HIV infection without ART, have been shown to carry a distinct HLA allele (HLA B*5701 class I) that promotes a more durable CD8⁺ T-cell response and thus a better immunological control of the infection⁷⁰. Similar effects have been found regarding the HLA allele B*27 that is associated with a slower progression to AIDS⁷¹. Other genetic determinants possess a protective function against HIV infection. Individuals with a homozygous $\Delta 32$ mutation in the CCR5 gene lack 32 base pairs resulting in a non-functional protein that is not expressed on the cell surface. As these people do not express any CCR5 receptor, they are protected from infection by M-tropic HIV⁷².

CD4⁺ T lymphocytes, also termed **T helper cells**, mainly orchestrate the adaptive immune response by the release of cytokines. Additionally, it has been shown that CD4⁺ T cells can transform into a cytotoxic phenotype during viral infections (e.g. caused by Epstein Barr Virus or HIV), enabling them to kill infected MHC class II cells^{73,74}.

Like CD8⁺ T cells, CD4⁺ T cells are activated by antigen-presentation on MHC class II molecules by APCs. Yet, it should be noted that CD4⁺ and CD8⁺ T cells differentiate autonomously and that the kinetics and efficiency of CD4⁺ and CD8⁺ T-cell proliferation differ.

1.4.1.1.1 CD4⁺ T-cell differentiation

Broadly speaking, the term differentiation describes T cells' transition from being naïve cells to memory cells upon antigen exposure (see **Figure 6**).

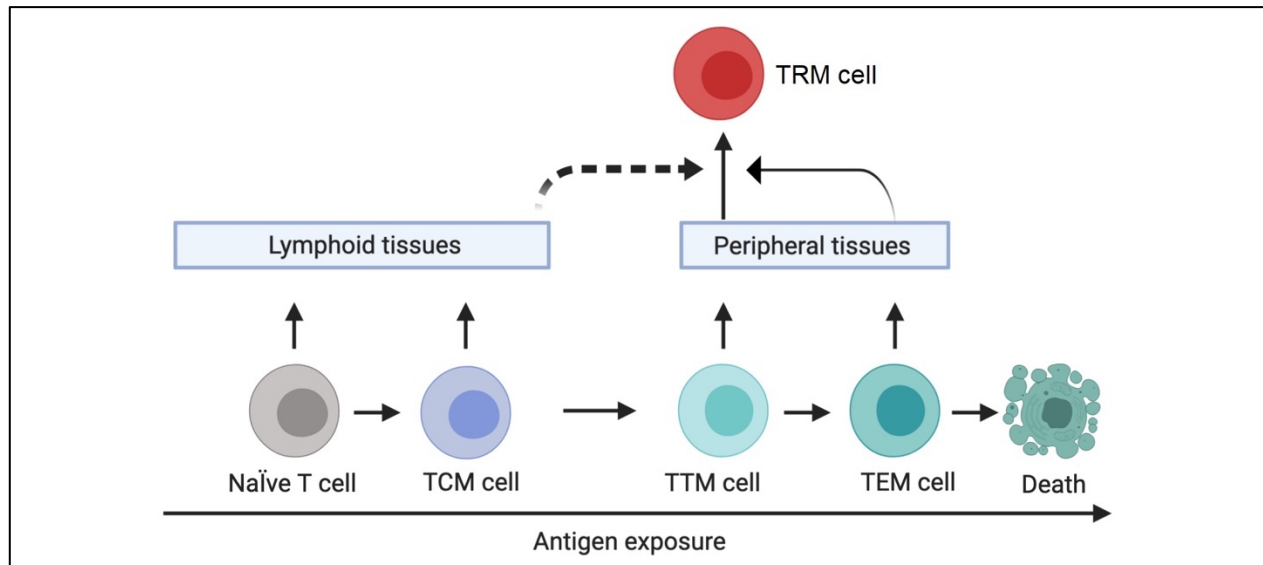


Figure 6: T-cell differentiation. Naïve T cells and central memory T cells (TCM) circulate in peripheral blood and through lymphatic tissue and can differentiate to transitional memory T cells (TTM) and effector memory T cells (TEM) upon antigen exposure. TTM and TEM can migrate to peripheral tissues. Tissue-resident memory T cells (TRM) that are derived from TTM or TEM remain in peripheral tissues and do not further differentiate into other memory T cells. Figure adapted from Farber *et al.*⁷⁵.

It also describes how T-cells develop into different lineages. In 1986, Mosmann and Coffman were the first to observe two separate sets of differentiated murine T-cell clones, namely **T Helper 1** (T_H1) and **T Helper 2** (T_H2)⁷⁶. Their distinction was mainly based on the cytokines that were produced, but also unique patterns of surface molecules became apparent. Over time, several other lineages have been discovered, such as T_H17 (see separate section below), T follicular helper (T_{FH}) cells and regulatory T cells (Tregs)^{77,78}. Lately, the group has been extended to include other subsets, e.g. T_H9 and T_H22^{79–81}.

The classification into the respective subset is made according to the cytokine signature that is produced. **T_H1 cells** produce IFN- γ , IL-2 and TNF- α , which aid in fighting viral and bacterial infections.

T_H2 cells express IL-4, IL-5 and IL-13 and can thereby defend the body against extracellular infections, such as parasites.

T_{FH} cells help to coordinate humoral immunity in germinal centres. Their differentiation is induced by the transcription factor Bcl-6⁸². They produce IL-21 which stimulates B cells and may produce IL-4 which triggers immunoglobulin class switching in the latter^{83,84}. Phenotypically, T_{FH} cells express CXCR5 together with PD-1 and/or inducible costimulator (ICOS)^{85,86}. Notably, T_{FH} cells were found to be crucial in both active replication of HIV and chronic infection^{87,88}.

Tregs express CD25 and FOXP3 and act in a suppressive manner on T effector cells, APCs, B cells, and monocytes. They balance immune reactions and sustain tolerance to self and foreign antigens, thereby preventing auto-immune diseases. This is facilitated by the secretion of IL-35, IL-9, IL-10 and TGF- β as well as cell-contact mediated inhibition and cytolytic activity⁸⁹⁻⁹³.

Cytokines released by antigen-presenting cells initiate the differentiation into the distinct subsets: IFN- γ and IL-12 trigger the differentiation into T_H1 cells, whereas IL-4 drives naïve cells into T_H2 differentiation. T_{FH} cells, on the other hand, are induced by the secretion of IL-21 and IL-6 and Tregs are either polarized peripherally by TGF- β and IL-2 or directly in the thymus during thymocyte development (natural Tregs)^{78,94}.

In consequence, the polarization into either subset was long considered mutually exclusive. Recently, the rigid separation into certain lineages has become mitigated: Panzer *et al.* demonstrated that both murine T_H1 and T_H17 cells can be repolarized into IL-4 expressing T_H2 cells *in vivo*⁹⁵. Also, T_H2 cells were shown to produce the T_H1 cytokine IFN- γ after the addition of IL-12, IFN- γ , and type I IFNs⁹⁶. This phenomenon is termed plasticity. Interestingly, a shift in immune response from T_H1 to T_H2 responses can be observed during the course of HIV infection⁹⁷.

1.4.1.1.2 T_H17 cells

A crucial subset of T helper cells that bridges innate and adaptive immunity are the T_H17 cells, that reside in the skin and in mucosal surfaces of organs like the gut and lung. They secrete IL-17A in response to IL-23 produced by DCs^{98,99}. The corresponding receptors are mostly expressed on epithelial and mesenchymal cells¹⁰⁰. Thus, IL-17A helps to maintain epithelial integrity¹⁰¹. In addition, other cytokines such as IL-17F, IL-22 and IL-26 can be produced in response to infection. Phenotypically, T_H17 can be identified by the surface expression of CCR6 which facilitates trafficking to the gut or other organs such as the brain^{102,103}. Different functional subsets can be distinguished by the expression of CCR4 and CXCR3¹⁰⁴.

By definition, a subset of T cells is defined as a separate lineage when specific effector functions are regulated by particular transcription factors¹⁰⁵. The main factor in T_H17 cells is retinoic acid-related orphan receptor gamma t (RORγt)¹⁰⁶. Others include signal transduction and activation of transcription (STAT3), basic leucine zipper transcription factor ATF-like (BATF), interferon regulatory factor 4 (IRF4) and aryl hydrocarbon receptor (AhR)^{99,107–109}.

The role of T_H17 cells in HIV infection is mainly defined by their non-existence, as this subset is massively depleted, mainly in the gastrointestinal tract¹¹⁰. The remaining cells are highly enriched for HIV-DNA¹¹¹. T_H17 cells, along with CCR6⁺ T cells, express the highest levels of the HIV co-receptor CCR5 compared to other cells in the gut mucosa which makes them a preferred target for HIV infection and subsequent depletion¹¹². Also, the expansion of Tregs during HIV infection and associated expression of FOXP3 which downregulates RORγt contributes to the low frequency of T_H17 cells in the gut of HIV-infected individuals. In elite controllers, however, the T_H17/Treg ratio remains unchanged¹¹³.

As mentioned above, T_H17 cells are crucial in maintaining mucosal barrier functions and their loss allows for translocation of microbial products from the gut into the bloodstream¹¹⁴. This in turn triggers systemic and chronic inflammation. Interestingly, the frequency of T_H17 cells is conserved in long-term non-progressors¹¹⁵.

1.5 Treatment of the HIV infection

People living with HIV have a higher risk of developing certain illnesses that are not directly related to their infection; so-called “non-AIDS-defining” conditions like atherosclerosis, osteoporosis, certain cancers or neurocognitive disorders such as HIV-associated dementia¹¹⁶⁻¹¹⁹. Other associated diseases include pulmonary and renal diseases as well as diabetes, hyperlipidaemia and lipodystrophy¹²⁰.

Another critical factor for patients is the still existing stigma of HIV infection that, depending on how well the person is connected to the community or supported by family and friends, often results in severe depression¹²¹.

1.5.1 Antiretroviral therapy

Antiretroviral therapy (ART) was developed shortly after the start of the pandemic and since then has improved continuously¹²². Azidothymidine, a direct-acting dideoxynucleoside reverse transcriptase inhibitor, was the first single drug approved for the treatment of HIV infection in 1987¹²³. As early monotherapeutic drug regimens were associated with considerable toxicity and rapid development of resistant virus strains, dual combination therapies were established where e.g. two nucleosides were administered together¹²⁴. Considerable advances were made in 1996, when the protease inhibitor Indinavir was approved; this marked the onset of the highly active antiretroviral therapy (HAART) era¹²⁵. In 1998, a landmark study reported the efficacy of triple combination antiretroviral therapy in reducing both mortality and morbidity in the patients being treated¹²⁶.

Starting with several doses multiple times per day, many patients now only need to take a single tablet once daily (so-called single tablet regimens). Current standard regimens for initial ART consist of a combination of antivirally active components, usually two nucleoside/nucleotide reverse transcriptase inhibitors together with a third active drug from one of the following classes: protease inhibitor, non-nucleoside reverse transcriptase inhibitor or integrase strand transfer inhibitor¹²⁷.

However, the initial hope that antiretroviral medication could be curative was not met, since viral loads in the blood quickly rebound after cessation of treatment. A stringent, life-long adherence to the drug regime is crucial and although side effects with second and third generation drugs are usually mild, the long-term side-effects of life-long ART are not fully understood due to the relatively short time-span they have been applied.

Future developments of ART comprise the introduction of highly potent STRs consisting of only two components and longer-acting forms of drug administration such as intramuscular injections or drug-eluting implants¹²⁸⁻¹³⁰.

The adherence to and efficacy of ART is influenced by several factors, such as depression and alcohol abuse but is also dependent on the ability of the drug to permeate certain tissues¹³¹. Notably, only about 2 % of the body's lymphocytes circulate in the body, whereas the rest remains in tissues¹³². The brain, for example, is poorly penetrated by drugs due to the blood-brain barrier. A study by Lamers *et al.* investigating various tissues from autopsies revealed that virus remained in all brain samples studied¹³³. Drug-resistant virus variants pose another significant problem in the treatment of the infection and the eradication of the virus^{134,135}.

1.5.2 The viral reservoir

HIV infects activated $CD4^+$ T cells that express one of the HIV co-receptors CXCR4 or CCR5. Although antiretroviral drugs can inhibit active virus replication and prevent the infection of new cells, the biggest obstacle to finding a cure is the presence of infected cells that reside in the body without producing viral components. This non-productive but reversible state of infection is defined as (viral) **latency**. Latently infected cells form the **viral reservoir**.

A schematic overview is given in **Figure 7**.

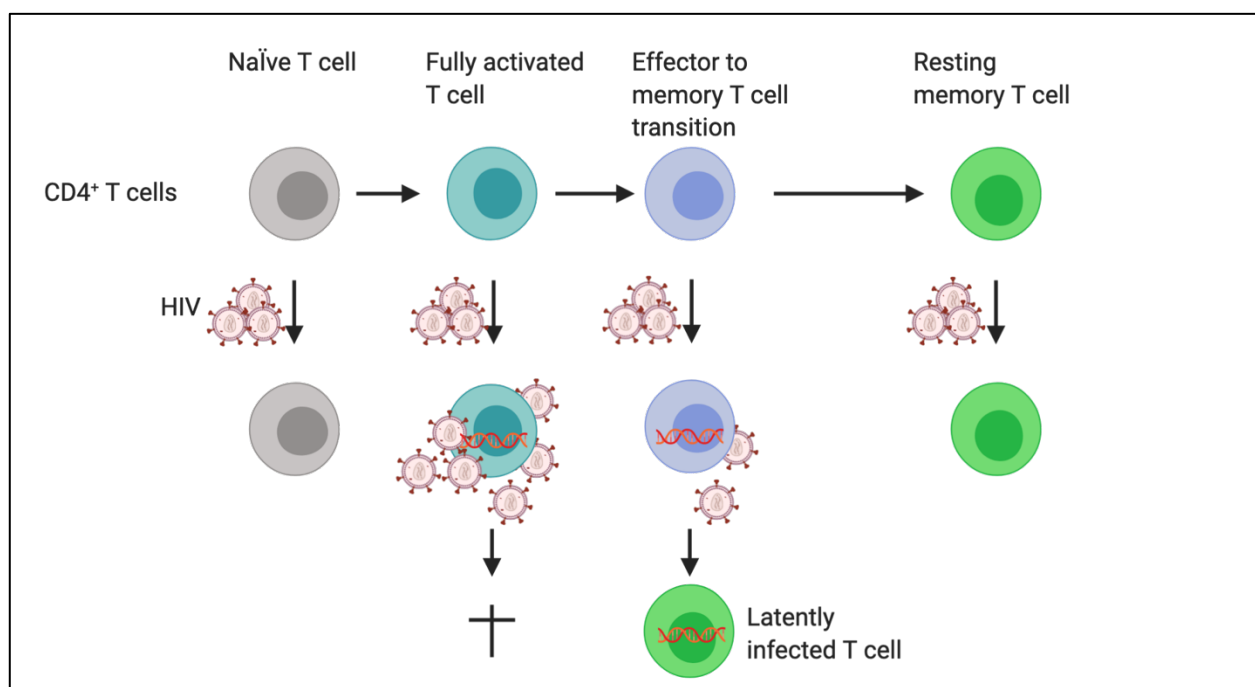


Figure 7: Formation of the latent reservoir. Whereas naïve and resting memory $CD4^+$ T cells are resistant to infection by HIV, activated $CD4^+$ T cells are infected and die. Some cells transition from an effector to a memory phenotype and thus become latently infected. Figure adapted from Sengupta *et al.*¹³⁶.

Early studies suggested that resting memory T cells formed the major cellular reservoir^{137,138}. Later, HIV proviral DNA was detected in TCM and (to a lesser extent) in TTM $CD4^+$ T cells¹³⁹. Central memory T cells persist in the body for years and are thus ideal for maintaining the virus. It has been calculated that the mean half-life of the viral reservoir under ART is approximately 44 months^{138,140}.

Another important factor that ensures the survival of latently infected cells for long time spans is the low-level proliferation and clonal expansion of latently infected cells^{139,141}. Also, CD4⁺ T cells with stem cell-like properties have been shown to contribute to the viral reservoir¹⁴².

Since the virus is transcriptionally silent in latently infected cells, no proteins are produced that can be presented via MHC class I molecules. In consequence, the infected cells are not recognized and cleared by the immune system and do not die from cytopathic effects. Once therapy is stopped, latently infected cells can be reactivated by mechanisms that are not fully understood yet and start to produce virus (“viral rebound”)¹³⁶. Over the last few years, numerous T-cell and non-T-cell types such as epithelial cells have been found to carry proviral DNA, making a targeted approach even more difficult¹⁴³.

1.5.3 Recent approaches to curing HIV

Despite adequate and efficient treatment of HIV infections, patients are afflicted with comorbidities such as neurocognitive disorders or lipodystrophy^{116,117,120}. Therefore, research continues to aim for the eradication of the virus from the infected host. Potential approaches to a cure can be subdivided into **sterilizing** (removal of all proviruses that can reinitiate infection) and **functional** (achieving long-term virologic control after treatment interruption) strategies.

The single case of the so-called “Berlin patient” showed that a sterilizing cure is technically possible¹⁴⁴. This patient was diagnosed with HIV in 1995 and had an undetectable viral load when he was diagnosed with acute myeloid leukaemia in 2007. He underwent two allogeneic hematopoietic stem cell transplantations after myeloablation with donor cells that carried a mutation in the CCR5 gene (CCR5 Δ 32/ Δ 32) which confers resistance to HIV. ART was stopped at the time of the first transplantation without a detectable rebound in viremia in either plasma or other anatomical reservoirs such as the intestinal lamina propria¹⁴⁴. However, this approach cannot be applied to the majority of HIV-infected individuals.

Another proposed way to reduce the number of latently infected cells is the “shock and kill” strategy. Here, virus replication in latently infected CD4⁺ T cells is pharmaceutically reactivated to prompt an elimination of these cells^{145–147}.

A schematic overview of the "shock and kill" approach is shown in **Figure 8**.

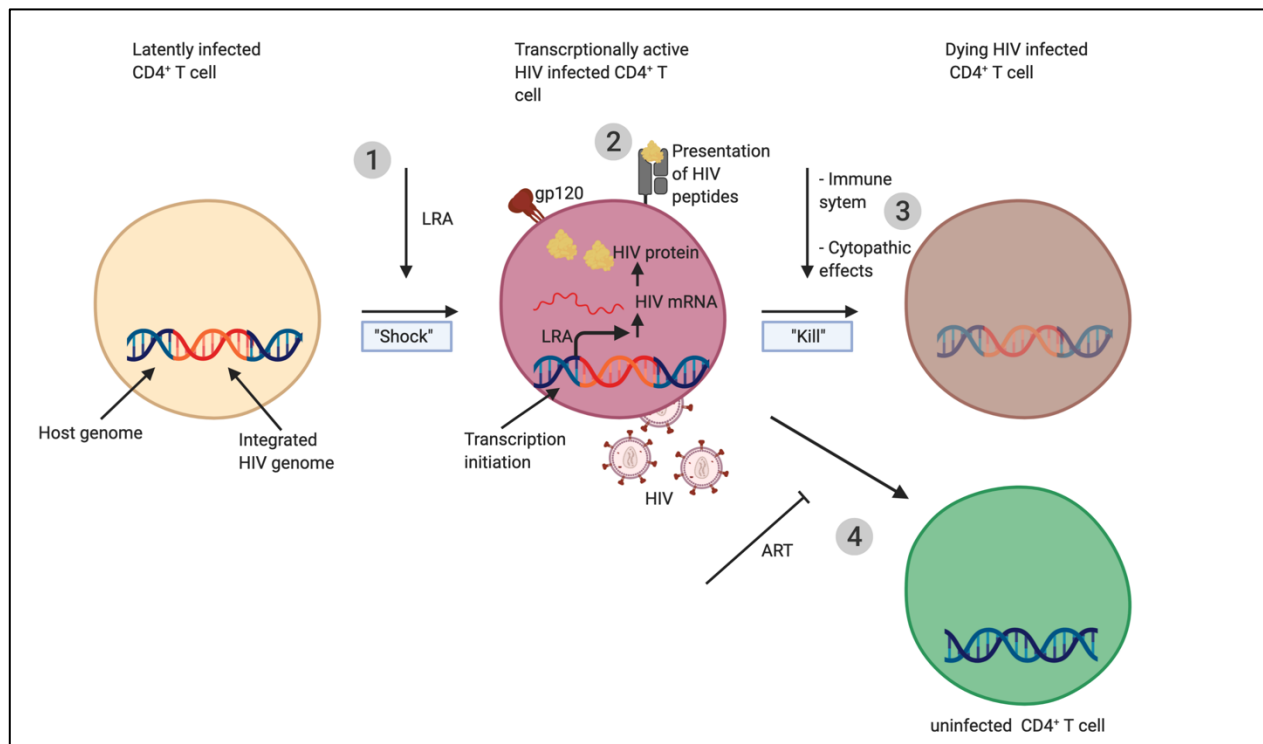


Figure 8: Schematic overview of the "shock and kill" approach. Latently infected CD4⁺ T cells are "shocked"/activated by latency reversing agents (LRA) (1) which leads to the transcription of HIV-DNA and ultimately to the presentation of viral proteins via MHC class I molecules (2). This means that the infected cell can either be recognized and killed by the immune system or dies due to cytopathic effects (3). New infection of uninfected cells is prevented by the administration of antiretroviral therapy (ART) (4). Figure adapted from Perreau *et al.*¹⁴⁸.

In short, latently infected cells are triggered by latency-reversing agents (LRA, e.g. histone deacetylase inhibitors), causing viral DNA to be transcribed and translated into viral protein. Once HIV peptides are presented on MHC class I molecules, the infected cells can be recognized and killed by either cytotoxic CD8⁺ T cells or NK cells, or die due to cytopathic effects. *De novo* infection of uninfected cells is prohibited by continuous ART.

It has been shown that LRA (e.g. valproic acid) can lead to an outgrowth of HIV from resting CD4⁺ T cells of aviremic patients *in vitro* as well as SIV in rhesus macaques *in vivo*^{149–152}. However, clinical trials have so far failed to reduce the reservoir size *in vivo* in humans¹⁵³. The following sections will introduce the anatomical site that has been the focus of this thesis and explain why targeting leukocyte migration might be a suitable intervention for HIV infection.

1.6 The gut: a crucial site for dissemination of the HIV infection

The human **mucosa** contains organized and dispersed **lymphoid tissues** that are closely connected with the mucosal epithelial surface. The immune response generated at one location is transferred throughout the mucosa by lymphocytes programmed to home to regional effector sites (see following section). In the gut, highly structured lymphoid components make up the gut and the **gut-associated lymphoid tissue** (GALT): mesenteric lymph nodes, Peyer's patches, fat-associated lymphoid tissues, cryptopatches and isolated lymphoid follicles as well as the lamina propria¹⁵⁴. Most of the effector lymphocytes reside in the epithelium and the lamina propria. The latter also contains other immune cells such as plasma cells, macrophages and DCs. Tight regulatory mechanisms prevent misdirected immune responses.

The GALT was rapidly identified as critical site of HIV replication and CD4⁺ T-cell depletion during primary infection^{155–158}. This has various reasons: firstly, there are a high number of activated lymphocytes with a central memory or effector memory phenotype present, due to the high prevalence of microbial and food antigens. Secondly, upon binding to MAdCAM (see section below), the HIV co-receptor CCR5 is upregulated¹⁵⁹. Thirdly, the gut is devised in a way that promotes antigen presentation. It has been demonstrated that intestinal DCs play an important role in transporting HIV through the intestinal mucosa and subsequently transmitting it to T cells (see also section on innate immunity)⁴⁵.

Certain cell types that are known to be important in maintaining the mucosal integrity are depleted during natural HIV infection, such as CD4⁺ T_H17 cells in the gut. By secreting IL-17 and IL-22, they support the production of tight junction proteins and thereby renew and maintain the intestinal epithelial barrier^{101,160}. Once these cells are missing, the barrier function is compromised and microbial components like LPS can enter the bloodstream. This phenomenon, known as “leaky gut syndrome”, leads to a systemic activation (providing more activated target cells) and eventually exhaustion of the immune system. Another CD4⁺ T-cell subset that are present in the healthy gut are mucosal-associated invariant T (MAIT) cells. These contribute to defence against pathogens by producing TNF- α , IFN- γ , IL-17 and granzyme B^{161,162}. During HIV infection, these cells are diminished and do not recover under ART^{163–165}. It is hypothesized that their loss further enhances the translocation of microbial products and promotes systemic activation.

1.6.1 Homing of T cells to the gut-associated lymphoid tissue

The term homing describes the targeted distribution of cells between the circulation, lymphoid organs and peripheral tissues, such as those in the gut or the skin¹⁶⁶. The gut is one of the organs where tissue-specific imprinting takes place. Different adhesion molecules (e.g. selectins and **integrins**, see section below) play a role in this process.

Naïve T lymphocytes expressing CCR7 leave the thymus without a specific imprint for a compartment (see **Figure 9**).

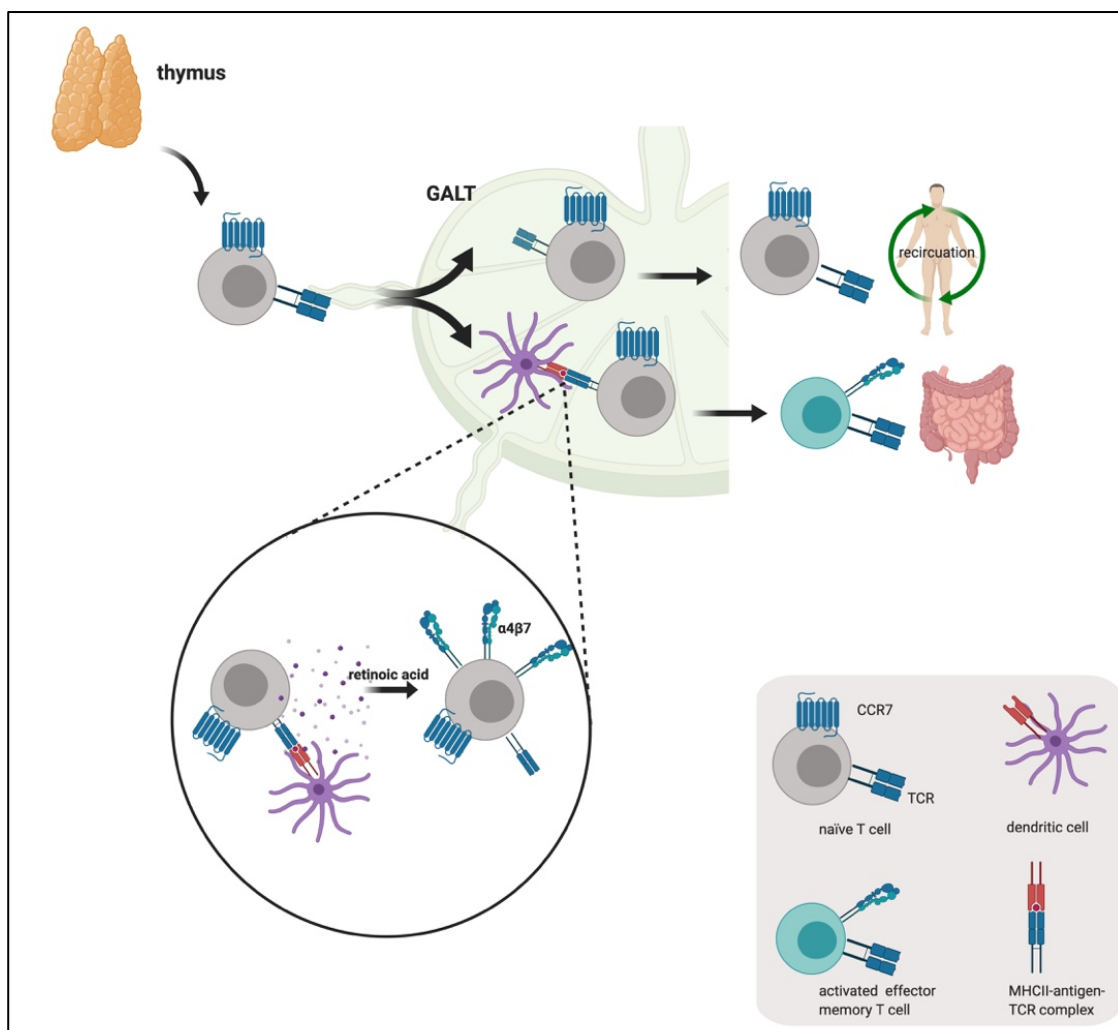


Figure 9: Gut-specific imprinting of CD4⁺ T cells in the gut-associated lymphoid tissue. Naïve CD4⁺ T cells expressing CCR7 circulate through peripheral blood and lymphatic tissues. If they encounter their specific antigen in the GALT, differentiation to memory T cells and expression of the gut-specific homing markers are induced.

CCR7 binds to cytokines CCL21 and CCL19 which are secreted by cells in peripheral lymphatic tissues, for example the GALT. If naïve cells do not encounter any antigen, they continue circulating. Antigens drive activation and antigen-induced differentiation of naïve cells, upon which CCR7 is lost (TEM) or preserved (TCM, retain the ability to circulate through all lymphoid tissues)¹⁶⁶. Only lymphocytes that encounter their antigen in the GALT are stimulated to express gut-specific homing markers such as C-C motif chemokine receptor 9 (CCR9) or $\alpha 4\beta 7$. The expression of $\alpha 4\beta 7$ is induced by retinoic acid produced by GALT-specific DCs at the time of antigen presentation to naïve lymphocytes^{167,168}. Next, the cells exit the compartment where they became activated via mesenteric lymph nodes, enter the bloodstream and selectively re-enter the mucosal tissue where the activation took place, in this example the GALT. A recirculation of TEM into secondary lymphatic organs is prevented by the loss of CCR7. To re-enter the lamina propria, the activated lymphocytes migrate across the epithelium of mucosal blood vessels (see **Figure 10**).

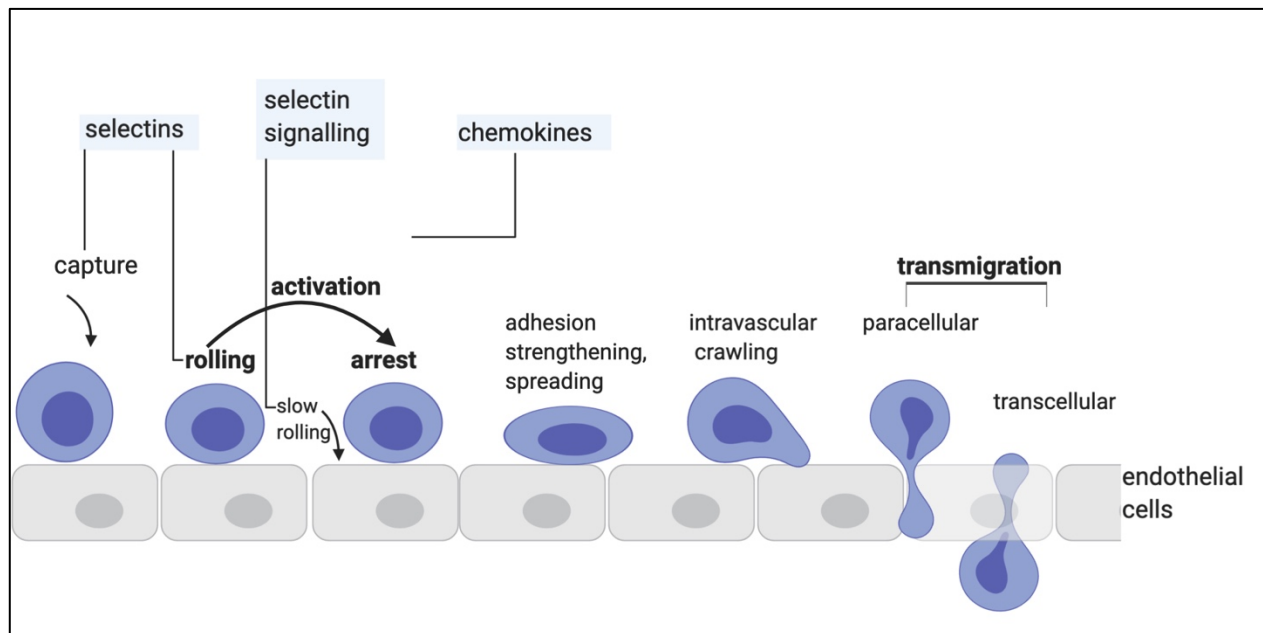


Figure 10: Leukocyte adhesion cascade. Leukocytes are slowed down by binding of selectins on the cell surface to selectin ligands on the endothelium. After that, integrins are activated by chemokines which results in cell arrest and enables transmigration through the epithelial barrier. Figure adapted from Ley *et al.*¹⁶⁹.

In the first phase of the adhesion cascade, known as **capture and rolling**, circulating lymphocytes are slowed down and adhere to the endothelium by loose binding of selectins to the corresponding selectin ligands on endothelial cells¹⁶⁹. E-selectin and P-selectin are the most important molecules on the latter. Afterwards, the **activation of integrins and adhesion** take place. Activation is caused by chemokines and results in increased ligand-binding capability by conformational changes of the integrin heterodimers. Once cells are rolling, they get activated via chemokines which trigger firm adhesion mediated by the binding of integrins to addressins (e.g. $\alpha 4\beta 7$ to MAdCAM-1)¹⁷⁰. The last step is the **transmigration** or diapedesis, where lymphocytes migrate to the lamina propria through the endothelium either paracellularly or transcellularly.

1.6.2 The integrin $\alpha 4 \beta 7$

Integrins are heterodimers expressed on the surface of leukocytes and consist of one noncovalently linked alpha (α) and one beta (β) subunit¹⁷¹. To date, 18 α and eight β subunits have been described in humans which can form 24 transmembrane heterodimers¹⁷². By mediating cell adhesion, they are crucial for the directed homing of leukocytes to tissues. Integrins exist in at least three conformations with different affinities towards their ligand. The “bent” conformation displays the lowest affinity, the “extended conformation with closed head piece” an intermediate one, whereas the “extended conformation with open head piece” conveys the highest affinity (see **Figure 11**).

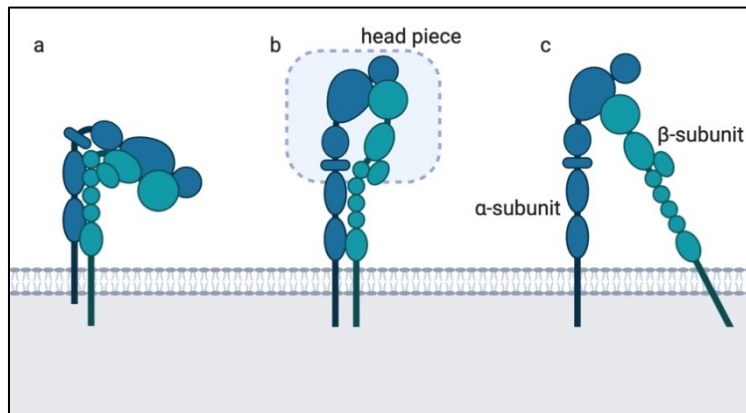


Figure 11: Main conformations of $\alpha\beta$ -integrins. Integrins consist of two noncovalently linked, transmembrane subunits. (a) Bent conformation with low affinity, (b) extended conformation with closed head piece with intermediate affinity and (c) extended conformation with open head piece with high affinity.

To prevent non-specific adhesion, the default conformation of integrins on most leukocytes is the bent one. Upon extracellular or intracellular signals, the high-affinity conformation is adopted which fosters ligand binding (integrin activation).

T cells express a variety of integrins that are engaged in activation, trafficking and retention in a tissue. The main ones are $\alpha 4 \beta 1$, which binds to vascular cell adhesion protein-1 (VCAM-1) and $\alpha L \beta 2$ which binds to intercellular adhesion molecule-1 (ICAM-1)^{173,174}.

The group of $\alpha 4$ integrins promotes recirculation through secondary lymphoid organs¹⁷⁵. Once T cells are activated, the expression of integrins changes in a fashion that allows for the entry of T cells in nonlymphoid compartments.

The molecule that has been studied in this thesis is $\alpha 4\beta 7$ which binds to MAdCAM-1, thus facilitating homing of $\alpha 4\beta 7^+$ cells to the gut. MAdCAM-1 is expressed on high endothelial venules of mesenteric lymph nodes and Peyer's patches at steady-state and becomes highly upregulated on intestinal venules during inflammation^{176,177}.

Importantly, the gut and GALT are critical sites of HIV replication and CD4⁺ T-cell depletion¹⁵⁵⁻¹⁵⁸. Several studies have reported that $\alpha 4\beta 7^{\text{high}}$ CD4⁺ T cells are highly susceptible to HIV and SIV infection, and are preferentially depleted in the blood and the gut during primary HIV infection¹⁷⁸⁻¹⁸¹. Remarkably, HIV particles were demonstrated to transport $\alpha 4\beta 7$ on their surface after budding, aiding homing of the virions to the gastrointestinal tract (GIT)¹⁸².

Even the acquisition and progression of HIV can be predicted by the $\alpha 4\beta 7$ expression of peripheral blood CD4⁺ T cells¹⁷⁸. In a study in macaques it was shown that ART and subsequent administration of an $\alpha 4\beta 7$ -specific antibody led to virologic control of SIV for up to 50 weeks after the withdrawal of both antibody and ART¹⁸³.

A similar therapeutic antibody (Vedolizumab/Entyvio) to the one used in the aforementioned macaque study was approved for the treatment of inflammatory bowel diseases (IBD, i.e. Crohn's disease/UC) several years ago. Furthermore, several trials of Vedolizumab are being carried out to explore this drug's potential in treating HIV (2018-000497-30, 2017-003081-27, NCT02788175, NCT02972450).

In parallel, large efforts are being made to identify phenotypic markers for latently infected cells. One of the candidate molecules will be discussed in the next section.

1.7 The Fc γ receptor CD32, a potential marker of latently HIV-infected cells

The Fc γ receptor II (Fc γ RII, CD32) family is formed mainly by membrane receptor proteins that are encoded by three genes: *FCGR2A*, *FCGR2B* and *FCGR2C*¹⁸⁴. The resulting surface proteins recognize and bind the Fc portion of IgGs with low affinity and are mostly expressed on B cells, monocytes, neutrophils, and eosinophils^{185–187}. Several isoforms of CD32 (a, b and c) exist in humans, which can be activating (a, c) or inhibitory (b), depending on whether the associated cytoplasmic sequence contains an ITAM (immunoreceptor tyrosine-based activation motif) or ITIM (immunoreceptor tyrosine-based inhibition motif) sequence (see also **Figure 12**)¹⁸⁸.

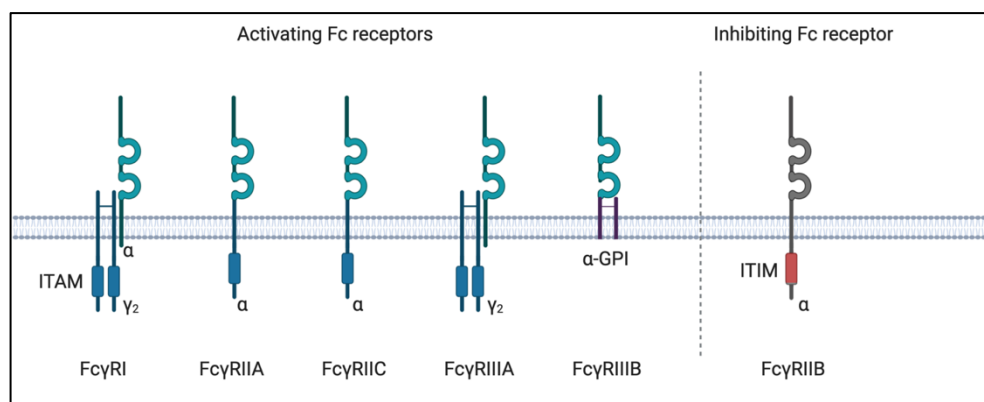


Figure 12: Overview of Fc receptor family. Figure adapted from Nimmerjahn *et al.*¹⁸⁹.

It is notable that Fc γ RIIA also acts as a receptor for pentraxins, which plays a crucial role in infection and inflammation processes¹⁹⁰. By 2007, the Fc γ RIIA RR genotype had already been linked to a faster progression of HIV infection by Forthal *et al.*¹⁹¹. Men carrying this specific polymorphism, i.e. arginine (R) at amino acid position 131, were reported to progress to low CD4⁺ T-cell counts more quickly than others who had the RH or HH genotype. In 2017, Descours *et al.* identified CD32a, an activating receptor, as a potential “marker of a CD4⁺ T cell HIV reservoir harbouring replication-competent proviruses *in vitro*”⁶. The group found a 50-fold upregulation of the corresponding RNA (*FCGR2A*) in resting latently HIV-infected versus uninfected cells. Previous studies did not report any expression of CD32a on T lymphocytes and indeed the frequencies found in peripheral blood are very low¹⁸⁷.

1.8 Aims

Although potent antiretroviral therapy is broadly available and effectively inhibits active HIV replication, there is currently no treatment option which specifically and completely targets latently infected cells. HIV infection is accompanied by various comorbidities and the constant exposure to viral antigen, even at a low level, causes a chronic inflammatory response in the body. There is a consensus that CD4⁺ T cells form the main reservoir for HIV, although other CD4-expressing cell populations have also been shown to contain provirus, e.g. macrophages or unconventional T cells such as $\gamma\delta$ ^{192,193}. Reservoir-harboring cells such as TCM and, to a lesser extent, TTM CD4⁺ T cells, are long-lived and proliferate slowly¹³⁹. Among the functional CD4⁺ T subsets, T_H17 cells, Tregs and T_{FH} cells have been identified¹⁹⁴. Still, there are knowledge gaps about the relative contribution of distinct CD4⁺ T-cell subtypes to the overall HIV reservoir.

Thus, efforts continue to identify further surface markers of latently infected cells to enable targeted therapy and an elimination of this pool of cells. It is also understood that these cellular reservoirs are predominantly located in different tissues (lymph nodes, gut), rather than in the blood. There, the frequency of (latently) infected cells is low: only 1 in 10⁴-10⁵ cells expresses viral proteins or mRNA^{26,195}.

Overall, a better understanding of the homing mechanisms of CD4⁺ T cells to certain tissues is needed. Recently, two landmark studies have proposed additional candidate molecules that might be involved in the formation of the reservoir and could pose novel targets for eradication strategies.

Within this thesis, the expression pattern of these two potential markers of latently infected cells and cellular homing have been characterized for the first time in a detailed way on a number of T-cell subsets in large cohorts of HIV patients with different disease course and in different tissues.

The receptor protein **CD32** is a low-affinity receptor for the IgG Fc fragment and is mostly expressed on monocytes, neutrophils and eosinophils. In a recent study it was postulated that CD32a is expressed on non-activated, latently HIV-infected CD4⁺ T cells with correlation to infection frequency, whereby no detectable expression on uninfected bystander cells was measured⁶.

The aim in this **first part** of this thesis was to phenotype peripheral blood and lymph nodal CD32⁺ CD4⁺ T cells from healthy individuals and HIV-infected patients in a way that would allow deductions as to whether these cells are latently infected.

In particular, the following questions were addressed:

- Do CD4⁺ CD32⁺ T cells notably differ from their CD32⁻ counterparts in terms of frequency, phenotype (e.g. HIV co-receptor expression), differentiation, activation or exhaustion status?
- Do peripheral CD4⁺ CD32⁺ T cells notably differ from lymph nodal CD4⁺ CD32⁺ T cells in terms of their frequency, phenotype, differentiation, activation or exhaustion status?
- Are there associations between a general activation of the immune system or disease progression markers (i.e. CD4⁺ T-cell count and HIV plasma viral load) and the frequency of CD32⁺ CD4⁺ T cells?

In the **second part** of the thesis, the expression pattern of integrin **$\alpha 4\beta 7$** which is expressed on circulating CD4⁺ T cells and enables homing to gastrointestinal tissues was investigated on different T-cell populations in different patient groups. It has been demonstrated that the viral envelope protein gp120 can bind to $\alpha 4\beta 7$ on cell surfaces and that $\alpha 4\beta 7$ can even be exploited by HIV to selectively home to the gut^{181,182}. This integrin-mediated homing to the gut can be disrupted by a therapeutic antibody which has already been approved for the treatment of IBD (Vedolizumab). Studies in macaques have shown that blockade of $\alpha 4\beta 7$ with an antibody similar to Vedolizumab mitigated the progression of the infection in SIV-infected monkeys and delayed viral rebound after cessation of ART¹⁸³. This finding suggests that one approach to limiting the size of the reservoir that becomes established during primary infection would be to hinder the migration of activated CD4⁺ T target cells to the gut.

The second part of this thesis was conducted with two cohorts: HIV-infected individuals as well as patients with UC receiving Vedolizumab. Both peripheral blood and gut samples from these individuals were examined and compared to healthy individuals. In detail, the following questions were addressed:

- Does the frequency of $\alpha 4\beta 7^+$ T cells in peripheral blood and lymph nodes change during HIV infection? (Comparison of healthy controls, viremic and aviremic patients as well as elite controllers.)
- How are $\alpha 4\beta 7^+$ T cells differentiated in peripheral blood and lymph nodes of the above-mentioned cohort?
- Which phenotype do T cells that home to the gut display? How are they differentiated? Is the status of $\alpha 4\beta 7^+$ T cells more exhausted and/or activated than $\alpha 4\beta 7^-$ T cells?
- Does Vedolizumab reduce the frequency of $\alpha 4\beta 7^+$ T cells in the gut? Are other homing markers (such as CCR9) upregulated instead?
- Can a beneficial role of Vedolizumab in primary HIV infection be extrapolated from these findings?

2 Material und Methods

2.1 Material

2.1.1 Lab equipment

The following **Tables 1-5** depict the equipment, consumables, reagents and antibodies used.

Table 1: Overview of equipment used.

Piece of equipment	Manufacturer
Centrifuge Sigma 4K15	Sigma Laborzentrifugen GmbH, Osterode am Harz, Germany
Incubator Heracell	Heraeus, Hannover, Germany
Laminar flow hood HeraSafe KS15	Thermo Fisher Scientific, Waltham, USA
Microscope Olympus CK2	Olympus Europa SE, Hamburg, Germany
Mini-Rocker Shaker MR-1	Biosan, Riga, Latvia
Multicolour cytometer LSR Fortessa	BD Biosciences, Heidelberg, Germany
Neubauer counting chamber	Carl Roth, Karlsruhe, Germany
Pipettes	Eppendorf AG, Hamburg, Germany
Vortexer Lab Dancer S40	VWR International GmbH, Darmstadt, Germany
Water bath WNE-7	Memmert GmbH, Büchenbach, Germany

2.1.2 Consumables

Table 2: Overview of consumables used.

Product	Manufacturer
96-well cell culture plate, U bottom	Greiner Bio-One, Frickenhausen, Germany
24-well cell culture plate, flat bottom	Sarstedt AG & Co. KG, Nümbrecht, Germany
6-well cell culture plate, ultra-low attachment, flat bottom	Corning GmbH, Wiesbaden, Germany
Mononuclear Cell Preparation Tube (CPT™)	BD Biosciences, Heidelberg, Germany
Microcentrifuge tubes (1,5 mL)	Eppendorf, Hamburg, Germany
Falcon tubes (15 mL, 50 mL)	Merck, Darmstadt, Germany
Nunc cryotubes (1,8 mL)	Thermo Fisher Scientific, Waltham, USA
Parafilm	Bemis, Solgnies, Belgium
Plastic filter tips	Sarstedt, Nümbrecht, Germany
Polystyrene tubes (5 mL)	BD FALCON™, Heidelberg, Germany
Serological pipette tips	BD FALCON™, Heidelberg, Germany

2.1.3 Reagents, chemicals and buffers

Table 3: Overview of reagents/chemicals and buffers as well as media used.

Reagent/Chemical	Manufacturer
Amphotericin B	GIBCO, Thermo Fisher Scientific, Waltham, USA
Bovine Serum Albumin (BSA)	Merck, Darmstadt, Germany
Dimethylsulfoxid (DMSO)	Merck, Darmstadt, Germany
Ethylenediaminetetraacetic acid (EDTA)	Promega GmbH, Mannheim, Germany
Ethanol, 100 %	Merck, Darmstadt, Germany
Foetal calf serum (FCS)	Biochrom, Berlin, Germany
HBSS, no Ca ₂ ⁺ /Mg ₂ ⁺	GIBCO, Thermo Fisher Scientific, Waltham, USA
HEPES-Puffer	GIBCO, Thermo Fisher Scientific, Waltham, USA
Human BD Fc Block™	BD Biosciences, Heidelberg, Germany
L-Glutamine Roswell Park Memorial Institute Medium 1640 (RPMI)	GIBCO, Thermo Fisher Scientific, Waltham, USA
Sodium azide	Merck, Darmstadt, Germany
Paraformaldehyde (PFA)	Merck, Darmstadt, Germany
Piperacillin/Tazobactam	Fresenius Kabi AG, Bad Homburg, Germany
Penicillin-Streptomycin	GIBCO, Thermo Fisher Scientific, Waltham, USA
Trypan blue	GIBCO, Thermo Fisher Scientific, Waltham, USA
Zombie NIR™ fixable viability kit	BioLegend, San Diego, USA

2.1.4 Buffers and media

Table 4: Overview of the compositions of buffers and media used. Volume/volume percentages are given.

Buffer/Medium	Composition
Freezing medium	50 % FCS (heat inactivated), 30 % RPMI, 20 % DMSO
FACS buffer	1,2 mM EDTA, 2 % FCS, 1,8 % NaN ₃ (5 % stock) in PBS
Fixation buffer	0,5 % PFA (4 % stock) in PBS
Culture medium	1 % Penicillin/Streptomycin (10 000 Units/mL Penicillin, 10 000 µg/mL Streptomycin), 10 % FCS, 10 mM HEPES-buffer in RPMI

2.1.5 Antibodies

Table 5: Overview of antibodies used.

Antigen	Clone	Fluorochrome	Supplier	Cat. no.
CD19	H1B19	APC-Cy7	BioLegend, San Diego, USA	302218
CD14	M5E2	APC-Cy7	BioLegend	301819
CD4	SK3	BV510	BioLegend	344633
HLA-DR	L243	BV711	BioLegend	307644
PD-1	EH12.2H7	PE-Dazzle 594	BioLegend	329939
CCR5	2D7	BUV737	BD Biosciences, Heidelberg, Germany	565293
CD32	FUN-2	APC	BioLegend	303207
CD127	A019D5	BV605	BioLegend	351334
$\alpha 4$	7.2R	unconjugated	Novus Biologicals, Wiesbaden Nordenstadt, Germany	MAB1354-100
anti-mouse IgG1	X56	BUV395	BD Biosciences	742481
CCR7	G043H7	BV421	BioLegend	353208
CD45RA	HI100	BV650	BioLegend	304136
CD3	UCHT1	Alexa Fluor 700	BioLegend	300424
CD8	RPA-T8	BV785	BioLegend	301046
CD27	M-T271	FITC	BD Biosciences	555440
$\beta 7$	FIB504	PerCP Cy5.5	BioLegend	321220
CD39	A1	PE Cy7	BioLegend	328212
CCR9	L053E8	PE	BioLegend	358904
HLA-DR	L243	BV711	BioLegend	307644
CD4	SK3	PerCP Cy5.5	BioLegend	344607
CCR6	G034E3	PE-Cy7	BioLegend	353418
CXCR4	12G5	PE-Dazzle 594	BioLegend	306525
CD25	M-A251	PE	BioLegend	356104

2.2 Clinical cohorts

At the University Medical Center Hamburg-Eppendorf, written informed consent was obtained from all participants who were recruited for the experiments described below, which were approved by the local Institutional Review Board of the Ärztekammer Hamburg (MC-316/14, PV4444, PV4870, PV5798). Clinical and demographic information like CD4⁺ T-cell counts and plasma viral loads or treatment were extracted from the clinical database.

In total, samples were examined from 96 patients with HIV infection, 15 with UC and 37 healthy subjects who were used as controls. Patients with HIV infection were further stratified into “viremic” (detectable plasma viremia), “ART” (undetectable plasma viral load) and elite controllers, “elite ctrl” (control plasma viremia and maintain stable CD4⁺ T-cell counts without medication). Patients with UC were divided into Vedolizumab treatment-naïve (“UC baseline”) and Vedolizumab treated (“UC + VDZ”). “Healthy” depicts patients without HIV infection or UC. Types of sample included peripheral blood and lymph node mononuclear cells (PBMC/LNMC) and gut-derived lamina propria lymphocytes (LPL).

The following **Tables 6-8** depict the relevant demographic and clinical data from the patients and healthy subjects who participated in the studies.

Table 6: Summarized clinical data from patients with HIV infection and healthy subjects who participated in the CD32 study. Values are medians (ranges). *Level of quantification: 50 copies/mL. PBMC peripheral blood mononuclear cells; LNMC lymph node mononuclear cells.

Classification (type of sample)	N	Age	M/F (% M)	Viral load (Copies/mL)*	CD4 ⁺ T-cell count (Cells/μL)
Healthy subjects (PBMC)	14	26 (22-70)	8/6 (57)	Not applicable	Not applicable
HIV patients on ART (PBMC)	13	45 (34-69)	13/0 (100)	Below level of detection	534 (131–1030)
Viremic HIV patients (PBMC)	23	41 (25-62)	16/7 (70)	75,500 (41,500–22,500)	263 (1–829)
LN of uninfected individuals (LNMC)	5	53 (28-70)	4/1 (80)	Not applicable	Not applicable
LN of HIV patients on ART (LNMC)	4	41 (26-57)	3/1 (75)	2.5 (2-5)	181 (106–803)
LN of viremic HIV patients (LNMC)	4	29 (26-35)	3/1 (75)	55,337.5 (49,000–71,000)	389 (254–546)

Table 7: Clinical details of patients with UC who participated in the $\alpha 4\beta 7$ study. Baseline refers to Vedolizumab-naïve patients, follow-up refers to patients that have received Vedolizumab. PBMC peripheral blood mononuclear cells; LPL lamina propria lymphocytes; VDZ Vedolizumab; PSC primary sclerosing cholangitis; LTX liver transplantation; n.a. information not available. *Prednisolone, Tacrolimus, Mycophenolat, UDC.

ID	PBMC/LPL	Sample	Initial UC diagnosis	Medication	Clinical response to UC therapy	Severity of UC	Duration of VDZ therapy (weeks)	Calprotectin ($\mu\text{g/g}$)	CRP (mg/L)	Clinical comment
UC 1	PBMC	baseline	1978	Prednisolone, Mesalazine	n.a.	intermediate	0	1880	17	no response to initial therapy, pancreatitis
	PBMC	follow-up	n.a.	Prednisolone, Vedolizumab	no	intermediate-severe	19	2730	7	switch to TNF-a
UC 2	PBMC	baseline	2013	Prednisolone	n.a.	mild-intermediate	0	n.a.	< 5	patient initiated treatment stop
	PBMC	follow-up	n.a.	Vedolizumab	partial	mild	47	n.a.	< 5	
UC 3	PBMC	baseline	2009	Budesonide	partial	mild-intermediate	0	n.a.	< 5	
UC 4	PBMC	baseline	2009	Azathioprine, Valganciclovir, Mesalazine, UDC	n.a.	severe	0	n.a.	34	st. p. CMV colitis, PSC
	PBMC	follow-up	n.a.	Azathioprine, UDC, Mesalazine, Vedolizumab	no	severe	57	n.a.	31	worsening of symptoms
UC 5	PBMC	follow-up	1997	Vedolizumab	yes	in remission	16	54,3	< 5	stricture
UC 6	PBMC	baseline	2016	5-ASA, Infliximab, Valganciclovir	n.a.	intermediate	0	416	< 5	st. p. CMV colitis
UC 7	PBMC	baseline	2012	Azathioprine, Adalimumab	n.a.	mild-intermediate	0	149	< 5	PSC, colectomy 2014
UC 8	PBMC	baseline	2016	5-ASA, Budesonide,*	n.a.	mild-intermediate	0	87,3	< 5	PSC, post-LTX*
	PBMC	follow-up	n.a.	Vedolizumab,*	yes	mild-intermediate	20		< 5	
UC 9	PBMC	baseline	2013	Azathioprine, Prednisolone	n.a.	intermediate-severe	0	290	< 5	
	PBMC	follow-up	n.a.	Mesalazine, Vedolizumab	yes	complete remission	39	19,8	< 5	

Table 7: Clinical details of patients with UC who participated in the $\alpha 4\beta 7$ study (continued).

ID	PBMC/ LPL	Sample	Initial UC diagnosis	Medication	Clinical response to UC therapy	Severity of UC	Duration of VDZ therapy (weeks)	Calprotectin ($\mu\text{g/g}$)	CRP (mg/L)	Clinical comment
UC 10	LPL	not applicable	2018	Prednisolone, Mesalazine	n.a.	mild	n.a.	n.a.	< 5	
UC 11	LPL	not applicable	2018	None	n.a.	mild	n.a.	n.a.	< 5	
UC 12	LPL	not applicable	2018	None	n.a.	complete remission	n.a.	n.a.	< 5	PSC
UC 13	LPL	not applicable	2018	Mesalazine, Budesonide	n.a.	mild	n.a.	n.a.	6	PSC
UC 14	LPL	not applicable	2018	Adalimumab, Mesalazine	n.a.	mild	n.a.	n.a.	n.a.	Budd–Chiari syndrome
UC 15	LPL	not applicable	2018	Ustekinumab	n.a.	mild	n.a.	n.a.	< 5	

Table 8: Clinical details of patients with HIV infection who participated in the $\alpha 4\beta 7$ study. All samples were PBMC. LoD limit of detection; n.a. data not available. EFV Efavirenz; TDF Tenofovir disoproxil; FTC Emtricitabine; RPV Rilpivirine; DTG Dolutegravir; ABC abacavir; 3TC Lamivudine; ATV Atazanavir; RTV Ritonavir; LPV Lopinavir; RAL Raltegravir; NVP Nevirapine.

Patient ID	Viral load (Copies/mL)	Age /Sex	CD4 ⁺ count (Cells/ μ L)	Nadir (Cells/ μ L)	Initial Diagnosis	CDC stage	Therapy
ART 1	< LoD	56 m	724	n.a.	n.a.	n.a.	n.a.
ART 2	< LoD	62 f	318	183	2003	A2	EFV/TDF/FTC
ART 3	< LoD	53 m	385	371	2003	n.a.	EFV/TDF/FTC
ART 4	< LoD	39 m	613	43	1999	C3	RPV/TDF/FTC
ART 5	< LoD	52 m	243	n.a.	n.a.	n.a.	n.a.
ART 6	< LoD	62 m	1030	520	2003	A1	DTG/TDF/FTC
ART 7	< LoD	38 m	945	n.a.	n.a.	n.a.	n.a.
ART 8	< LoD	45 m	629	n.a.	n.a.	n.a.	n.a.
ART 9	< LoD	44 m	365	70	1989	B3	EFV/TDF/FTC
ART 10	< LoD	58 m	717	203	1998	C2	EFV/TDF/FTC
ART 11	< LoD	47 m	680	n.a.	n.a.	n.a.	n.a.
ART 12	< LoD	38 m	414	9	2001	C3	EFV/ABC/3TC
ART 13	< LoD	71 m	858	n.a.	2000	B2	EFV/ABC/3TC
ART 14	< LoD	45 m	109	n.a.	n.a.	n.a.	EFV/ABC/3TC
ART 15	< LoD	29 m	609	327	2002	B2	ATV/RTV/TDF/FTC
ART 16	< LoD	46 f	355	n.a.	n.a.	n.a.	n.a.
ART 17	< LoD	67 m	191	n.a.	n.a.	n.a.	n.a.
ART 18	< LoD	47 f	226	n.a.	1997	n.a.	LPV/RTV/TDF/FTC
ART 19	< LoD	36 m	388	8	2007	B3	EFV/TDF/FTC
ART 20	< LoD	56 m	387	60	1986	C3	FTC/ABC/LPV/RTV/RAL
ART 21	< LoD	41 m	366	n.a.	n.a.	n.a.	n.a.
ART 22	< LoD	38 m	386	n.a.	n.a.	n.a.	n.a.
ART 23	< LoD	44 m	561	254	1998	n.a.	NVP/TDF/FTC
VIREMIC 1	50300	30 m	34	n.a.	n.a.	n.a.	not applicable
VIREMIC 2	58700	20 f	465	n.a.	n.a.	n.a.	not applicable
VIREMIC 3	93500	54 f	306	306	1999	B2	not applicable
VIREMIC 4	5300000	43 m	6	6	2004	C3	not applicable
VIREMIC 5	77400	43 m	329	251	2000	n.a.	not applicable
VIREMIC 6	157050	33 m	381	n.a.	n.a.	n.a.	not applicable
VIREMIC 7	75500	33 m	467	n.a.	n.a.	n.a.	not applicable
VIREMIC 8	225000	54 m	829	520	2003	A1	not applicable
VIREMIC 9	398700	52 f	472	472	1989	A2	not applicable
VIREMIC 10	41500	48 m	321	203	1998	C2	not applicable
VIREMIC 11	55000	42 m	456	n.a.	n.a.	n.a.	not applicable
VIREMIC 12	190000	35 f	110	n.a.	n.a.	n.a.	not applicable
VIREMIC 13	190000	62 m	374	321	2008	A2	not applicable
VIREMIC 14	1500000	32 m	113	113	2012	n.a.	not applicable
VIREMIC 15	370000	51 f	45	34	2012	C3	not applicable
VIREMIC 16	166000	67 m	546	n.a.	2000	B2	not applicable
VIREMIC 17	119000	62 m	470	317	n.a.	n.a.	not applicable
VIREMIC 18	117000	37 m	311	n.a.	n.a.	n.a.	not applicable
VIREMIC 19	500000	48 m	52	n.a.	n.a.	n.a.	not applicable
VIREMIC 20	294500	53 m	67	n.a.	n.a.	n.a.	not applicable
VIREMIC 21	661600	36 m	205	n.a.	n.a.	n.a.	not applicable
VIREMIC 22	130000	41 m	515	438	2005	A1	not applicable
VIREMIC 23	425000	37 m	263	n.a.	n.a.	n.a.	not applicable
VIREMIC 24	690000	42 m	107	107	2003	C3	not applicable
ELITEctrl 1	< LoD	21 m	1154	n.a.	n.a.	n.a.	n.a.
ELITEctrl 2	< LoD	36 f	899	n.a.	n.a.	n.a.	n.a.
ELITEctrl 3	< LoD	71 f	375	n.a.	n.a.	n.a.	n.a.
ELITEctrl 4	< LoD	37 f	1219	529	2008	A1	n.a.
ELITEctrl 5	< LoD	52 f	994	n.a.	n.a.	n.a.	n.a.

Table 9 summarizes the demographic and clinical data from HIV-infected and uninfected individuals who participated in the $\alpha 4\beta 7$ study.

Table 9: Summarized clinical data from patients with HIV infection and uninfected controls. Values are medians (ranges). *Level of quantification: 50 copies/mL. PBMC peripheral blood mononuclear cells; LNMC lymph node mononuclear cells.

Classification (type of sample)	n	Age	M/F (% M)	Viral load (Copies/mL)*	CD4 ⁺ T-cell count (Cells/ μ L)
Healthy subjects (PBMC)	15	28 (19-43)	7/8 (47%)	n.a.	n.a.
HIV patients on ART (PBMC)	23	29 (46-71)	20/3 (87%)	n.a.	388 (109-1030)
Viremic HIV patients (PBMC)	24	43 (20-67)	19/5 (79%)	178 000 (41 500 -5 300 000)	316 (6-829)
HIV elite controllers (PBMC)	5	37 (21-71)	4/1 (20%)	n.a.	994 (375-1219)
LN of HIV-infected patients (LNMC)	3	38 (37-38)	3/0 (100%)	379 288 (8576 -750 000)	465 (265-665)
LN of uninfected individuals (LNMC)	3	48 (28-53)	2/1 (67%)	n.a.	n.a.

2.3 Methods

2.3.1 Acquisition and cryopreservation of PBMC and isolation of LNMC

PBMC of patients with HIV infection or UC were obtained at the Outpatient Center of the University Medical Center Hamburg-Eppendorf after informed and written consent. Blood samples were drawn directly in vacutainers containing a gel matrix and sodium heparin as anti-coagulant and then spun down. Afterwards, the top fraction containing lymphocytes and monocytes was decanted, washed once with PBS and then resuspended in freezing medium. Cells were aliquoted and stored in liquid nitrogen until experiments were conducted.

Biopsied lymph nodes were isolated by the General, Visceral and Thoracic Surgery Department of the University Medical Center Hamburg-Eppendorf after informed and written consent from patients with HIV and uninfected individuals. Pieces of the lymph nodes were drawn in sterile PBS and disintegrated with a scalpel. LNMC were isolated from the tissue by careful squeezing and flushing with medium and were then cryopreserved as described above.

2.3.2 Acquisition of gut biopsies and preparation of lamina propria lymphocytes

Gut biopsies of patients with UC or healthy individuals were obtained during check-up or screening colonoscopies at the Clinic and Polyclinic for Interdisciplinary Endoscopy of the University Medical Center Hamburg-Eppendorf after informed and written consent.

Five double biopsies from the sigmoid colon mucosa were taken with a standard biopsy forceps and drawn into sterile PBS.

Samples were processed directly according to a protocol by Morón-López *et al.* with minimal adaptations¹⁹⁶. First, samples were centrifuged for 10 min at 400 x g at RT after which the PBS was decanted. The biopsies were then resuspended in HBSS containing 1 mM DTT and 1 mM EDTA to disintegrate the tissue. The sample tubes were placed on a rocker-shaker for 25 min followed by centrifugation (7 min, 500 x g, RT). After that, the medium was decanted and samples were incubated in 6-well, low-binding plates in HBSS supplemented with 10 % FCS, antibiotics and antifungals overnight (1 mg/mL Piperacillin/Tazobactam and 1,25 µg/mL Amphotericin B). The next day, the remaining tissue was disrupted by pipetting, and mononuclear cells (lamina propria lymphocytes, LPL) were collected from the supernatant and stained and measured directly.

2.3.3 Surface staining for flow cytometry

Vials containing frozen cells were carefully swayed in the water bath for approx. 30 sec. After that, 500 μ L of medium at room temperature was added. After careful resuspension, the cells were transferred to a Falcon tube containing 30 mL of medium and centrifuged (7 min, 500 x g, RT). The pellet was resuspended in PBS and cells were manually counted using Trypan blue and a Neubauer counting chamber. All centrifugation steps were carried out at 7 min, 500 x g, RT unless stated otherwise.

The compositions of the different panels and the respective quantities of antibody used can be found in the appendix (**Suppl. Tables 1-3**). The desired number of cells ($1-2 \times 10^6$) was placed into a FACS tube, 2 mL of PBS was added before cells were spun down and the supernatant was discarded. The pellet was then resuspended in 100 μ L live/dead dye (diluted 1:1000). After 15 min incubation, cells were washed with FACS buffer (2 mL with subsequent centrifugation and decantation of the buffer). Tubes were decanted, which left a residual volume of about 50 μ L of FACS buffer. Antibodies were added as a master mix in a total volume of 50 μ L FACS buffer and samples were incubated for 20 min at RT in the dark. After that, samples were washed once more with FACS buffer. Cells were then fixed with 500 μ L PFA (1 % v/v) for 30 min at RT in the dark. After another washing step with FACS buffer, cells were stored in the fridge until the time of the measurement.

Samples stained with anti- α 4 and anti- β 7 required three staining steps, as the α 4-specific antibody was unconjugated. After incubation with the unconjugated primary antibody and following the washing step, a secondary, conjugated antibody was added (20 min at RT each). After another washing step, 5 μ L Fc block per sample was added and incubated for 5 min at RT before the master mix was added without prior washing and incubated for 20 min at RT. After washing, cells were fixed and stored as described above.

2.3.4 Flow Cytometry

The technique of flow cytometry is based on the detection of fluorescently labelled antibodies that bind to the antigen of interest either on the surface of cells or within them.

Inside the flow cell of the flow cytometer, the cells pass a laser beam one by one which excites the fluorophore and causes a light signal which is amplified by a photomultiplier and then interpreted by the software. The signals are translated into so-called dot plots or histograms. Depending on the configuration of the machine, up to 16 parameters can be analysed. In addition, cellular properties such as size and granularity of the cells can be studied. Recently, a method that enables the labelling and detection of antibodies coupled to stable isotopes has been developed. Instead of fluorescence, the time of flight is analysed by a mass spectrometer (CyTOF).

The samples studied in the framework of this thesis were run on an LSR Fortessa. Before the actual samples were run, compensation controls were recorded to minimize spectral spill over. This phenomenon is caused by the usage of fluorophores whose emission spectra are in close proximity (e.g. BUV 510 and BUV 605). Thus, beads that bind antibodies non-specifically were single-stained with the antibodies of the respective panel and measured.

2.3.5 *In vitro* experiments

Stimulation of PBMC to examine possible up-regulation of CD32

PBMC from three healthy donors were thawed, washed once with PBS, and counted. Cells were then transferred to RPMI supplemented with 10 % FCS and 1 % Penicillin/Streptomycin and rested overnight. The next day, cells were stimulated with either magnetic bead-bound CD3/CD28 antibodies (ThermoFisher Scientific, Waltham, USA, bead:cell ratio 1:1) or PMA/ionomycin (Sigma-Aldrich, 5 ng/mL / 500 ng/mL, respectively) plus 20 U/mL IL-2 (Miltenyi, Bergisch Gladbach, Germany). PMA/ionomycin was removed after 1 day of stimulation. As a control, unstimulated PBMC (medium supplemented with and without IL-2) were cultivated in parallel. The beads were removed with a magnet before the staining. Cells were stained after 1 day, 3 days and after 5 days of stimulation and analysed by flow cytometry. To evaluate immediate effects of the stimulation, CD69 (a marker of early activation) was added to the antibody panel.

Stimulation of PBMC to examine possible up-regulation of $\alpha 4\beta 7$

PBMC from three healthy donors were prepared and stimulated as described in the section above. As a control, unstimulated PBMC (medium supplemented with and without IL-2) were cultivated in parallel. The medium was changed at days 4 and 5.

Cells were stained with Act1 as described above (section 2.3.3) and analysed by flow cytometry after 6 h, 3 days and 7 days. Again, the panel included CD69. Before staining, the beads were removed with a magnet.

Stimulation of PBMC with *all-trans* retinoic acid

Cells were prepared and stimulated as described above. To assess the effect of all-trans retinoic acid (RA) on the frequency of $\alpha 4\beta 7^+$ T cells, 100 nM RA (Enzo Life Sciences GmbH, Lörrach, Germany) in combination with bead-bound CD3/CD28 antibodies (ratio 1:1) were added to the cells. Cells were stained after 6 h, 3 days as well as after 7 days of stimulation and analysed by flow cytometry.

***In vitro* blockade with Vedolizumab**

PBMC from healthy donors were thawed, washed once with PBS, and counted. Cells were then transferred to RPMI supplemented with 10 % FCS and 1 % Penicillin/Streptomycin and rested in an incubator overnight. The next day, 1×10^6 cells each were incubated with the therapeutic $\alpha 4\beta 7$ -specific antibody (Vedolizumab) at different concentrations (0,0001 $\mu\text{g}/\text{mL}$ – 10 $\mu\text{g}/\text{mL}$) for 90 min, washed twice and then stained with the anti- $\alpha 4\beta 7$ antibody (clone Act1) or the anti- $\alpha 4$ antibody (clone 7.2R) in combination with a $\beta 7$ -specific antibody (clone FIB504).

2.4 Data analysis

2.4.1 Analysis of cytometric data

Cytometric data was analysed using FlowJo version 10.5.2 for Mac OS X (FlowJo, BD). Gates of poorly defined populations were set according to fluorescence minus one (FMO) controls. These indicate the background fluorescence of the remaining antibodies of the panel. Other possibilities include isotype controls which can be used to determine non-specific binding of the antibody isotype class itself (e.g. IgG2a) or cells that do not express the antigen of interest (e.g. from knock outs).

2.4.2 Statistical analysis

The data generated was analysed statistically and converted into graphs using GraphPad Prism version 7.0c for Mac OS X (GraphPad Software, Inc., La Jolla, CA, USA). For analysis, non-Gaussian distributions were assumed. Kruskal-Wallis and Dunn's post-test with an alpha value of 0.05 were performed for multiple comparisons. All reported p-values were multiplicity adjusted according to Dunn. To compare ranks, Wilcoxon matched-pairs signed rank tests were computed. Pearson's correlation and Spearman's rank correlation coefficient were applied for bivariate correlation analysis. Data in this thesis is expressed as means +/- standard deviation and frequencies in this thesis are described as means unless stated otherwise. A p-value of less than 0.05 was considered significant. P-values were translated into asterisks as follows: *p < 0.05, **p < 0.01, ***p < 0.001, ****p < 0.0001. Not significant: ns ≥ 0.05.

3 Results

In this thesis, samples from a cohort of 96 patients with HIV infection, 15 patients with UC and 37 healthy subjects used as controls were analysed phenotypically *ex vivo* using flow cytometry.

The first part of the results section covers findings regarding the expression pattern of the Fc receptor CD32(a) which has been proposed as a marker of latently infected CD4⁺ T cells. The second part focusses on the integrin $\alpha4\beta7$ which facilitates homing of T cells to the gut and poses a potential target for interventions acting against HIV reservoir formation in the GALT. Data on both topics has been partly published^{197,198}.

3.1 Phenotypic characterization of peripheral blood and lymph nodal CD32⁺ CD4⁺ T cells from healthy individuals and HIV-infected patients

3.1.1 Frequency of CD32⁺ T cells in the peripheral CD4⁺ and CD8⁺ memory T-cell compartment

First, the general distribution of CD32⁺ cells within the CD4⁺ and CD8⁺ T-cell compartment was examined to find out whether CD32 was mainly present one compartment, e.g. the memory compartment, or differed between cohort groups within the same compartment (**Figure 13**). The following figures show data from PBMC samples from HIV-infected subjects with detectable plasma viremia (termed “viremic”), undetectable plasma viral load (“ART”) and uninfected individuals (“healthy”). The populations are defined as follows: Tnaïve (CD45RA⁺/CCR7⁺), TCM (CD45RA⁻/CCR7⁺), TEM (CD45RA⁻/CCR7⁻/CD27⁺) and TTM (CD45RA⁻/CCR7⁻/CD27⁻). Since the frequency of CD32⁺ (CD4⁺) T cells is relatively low, the data is represented logarithmically.

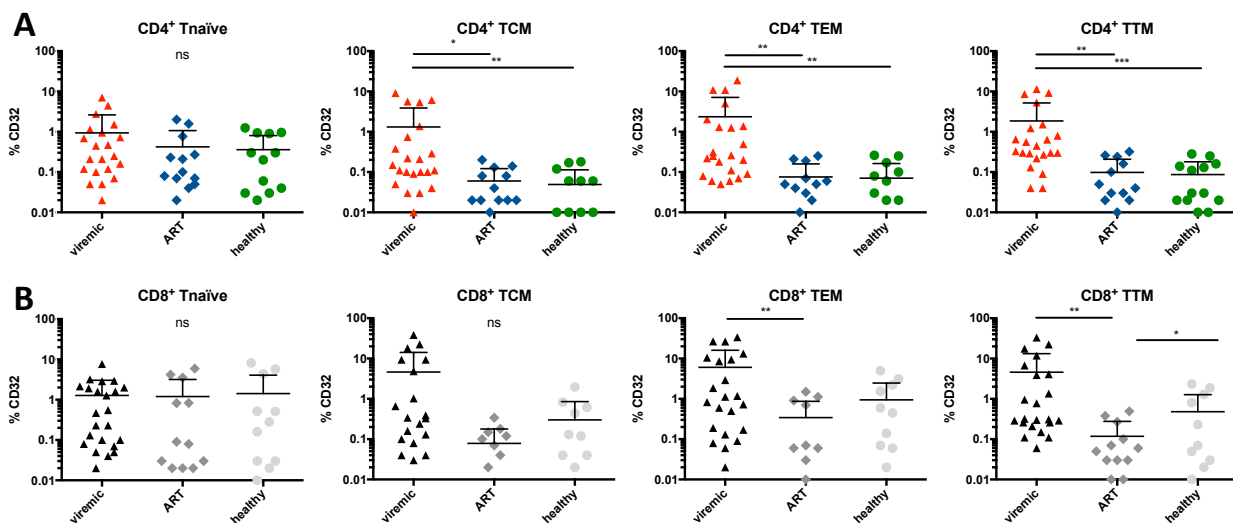


Figure 13: Frequency of CD32⁺ T cells in the CD4⁺ and CD8⁺ compartment. Frequencies of CD32⁺ CD4⁺ T cells (**A**) and CD32⁺ CD8⁺ T cells (**B**). CD32⁺ and CD32⁻ CD4⁺ and CD8⁺ T cells isolated from blood of HIV-infected patients with detectable viral load (viremic, red/black), with HIV-infected patients with undetectable viral load (ART, blue/dark grey) and healthy individuals (green/light grey). Cryopreserved samples were thawed and directly stained. Data from 23 HIV-infected patients with detectable viral load, 13 HIV-infected patients with undetectable viral load and 14 healthy individuals presented as means plus standard deviation. *Ns* ≥ 0.05 , **p* < 0.05, ***p* < 0.01, ****p* < 0.001, *****p* < 0.0001, as calculated by Kruskal-Wallis test. *Ns* on top of graph indicates that none of the comparisons reached significance.

There was no significant difference between the patient groups in either the CD4⁺ (**Figure 13A**) or CD8⁺ T-cell compartment (**Figure 13B**) regarding the frequency of CD32⁺ naïve T cells. Interestingly, the frequency of naïve CD32⁺ T cells was comparable between the CD4⁺ and CD8⁺ T-cell compartments but was higher in the CD8⁺ memory T-cell compartment (TCM, TEM, TTM) than in the respective CD4⁺ memory T-cell population.

In the CD4⁺ T-cell memory compartment, TCM, TEM and TTM cells of viremic HIV patients had a significantly higher expression of CD32 than the respective memory subsets in ART-treated patients or healthy controls (mean values TCM: viremic: 1,32 %, ART: 0,06 %, healthy: 0,05 %; TEM; viremic: 2,35 %, ART: 0,08 %, healthy: 0,07 %; TTM: viremic: 1,86 %, ART: 0,1 %, healthy: 0,09 %).

3.1.2 Expression of the HIV co-receptors on CD4⁺ CD32⁺ versus CD4⁺ CD32⁻ T cells

In addition to the CD4 molecule, either the chemokine receptor CXCR4 (used by T-tropic virus isolates or X4 viruses¹⁴) or CCR5 (used by M-tropic strains, also called R5 viruses^{15,16}) is needed to infect a target cell with HIV. To clarify whether CD32⁺ CD4⁺ T cells would be preferentially infected due to their relatively higher expression of either CXCR4 and/or CCR5, these markers were included in the analysis. The frequency of CCR5⁺ and CXCR4⁺ cells in CD32⁺ and CD32⁻ cells was compared (**Figure 14**).

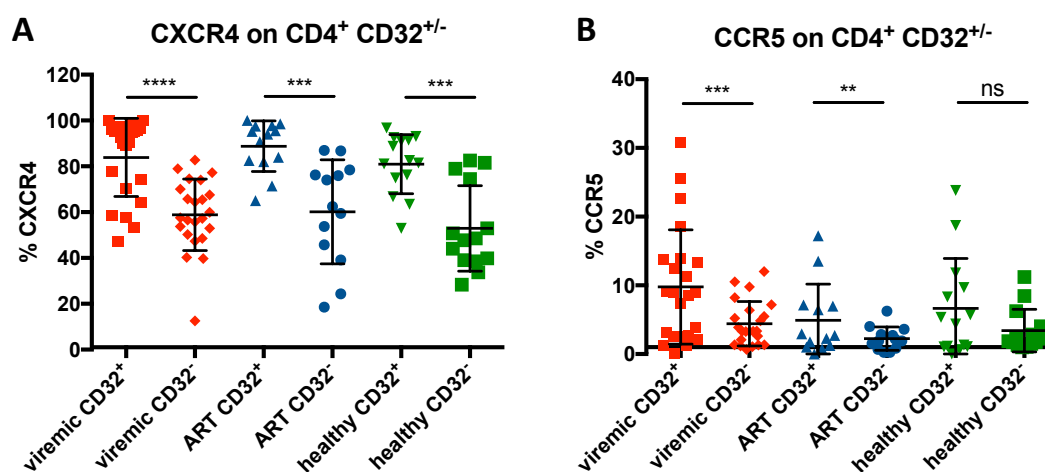


Figure 14: Expression of the HIV co-receptors CXCR4 and CCR5 on CD32⁺ versus CD32⁻ cells. Frequencies of CXCR4 (A) and CCR5 (B) CD32⁺ and CD32⁻ CD4⁺ T cells isolated from blood of HIV-infected patients with detectable viral load (viremic, red), with HIV-infected patients with undetectable viral load (ART, blue) and healthy individuals (green). Cryopreserved samples were thawed and directly stained. Data from 23 HIV-infected patients with detectable viral load, 13 HIV-infected patients with undetectable viral load and 14 healthy individuals presented as means +/- standard deviation. Ns \geq 0.05, * p < 0.05, ** p < 0.01, *** p < 0.001, **** p < 0.0001, as calculated by Wilcoxon matched-pairs signed rank test.

A significantly higher frequency of CD32⁺ CCR5⁺ and CXCR4⁺ CD4⁺ T cells was found in nearly all groups regardless of the disease status. In healthy controls, the difference between CD32⁺ and CD32⁻ CCR5⁺ cells did not reach significance. For CXCR4, the difference between CD32⁺ and CD32⁻ CD4⁺ T cells was most pronounced in samples from viremic patients (CD32⁺: 83,89 % versus CD32⁻: 58,83 %, p < 0,0001; **Figure 14A**). Also, the frequency of CCR5⁺ cells differed most between CD32⁺ and CD32⁻ CD4⁺ T cells from viremic patients (CD32⁺: 9,77 % versus CD32⁻: 4,42 %, $p=0,0002$; **Figure 14B**).

3.1.3 Immune activation was associated with the frequency of CD32⁺ CD4⁺ T cells and CD32⁺ CD4⁺ T cells were more activated than CD32⁻ CD4⁺ T cells

In the initial study by Descours *et al.*, only resting T cells were examined. This was done with the rationale that reservoir cells are mostly in a resting state⁶.

Here, correlations between activation and CD32 frequency were made to exclude that CD32 was rather an activation than a reservoir marker, and that CD32⁺ cells were enriched in proviral DNA solely because they can be preferentially infected. **Figure 15** shows the frequency of CD8⁺ HLA-DR⁺ T cells, which represent general activation, plotted against CD32⁺ CD4⁺ TTM from viremic individuals. This subset was chosen for analysis since the biggest differences in terms of frequency compared to healthy controls could be determined in TTM (Figure 13).

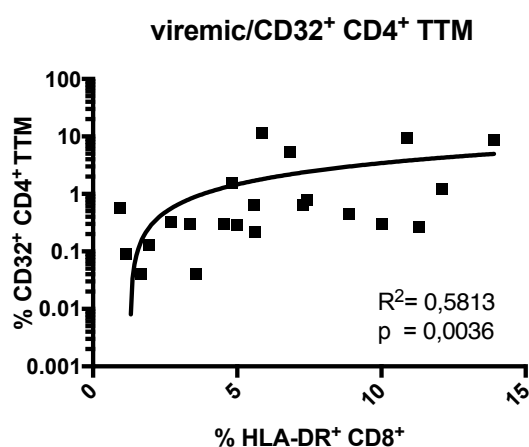


Figure 15: Correlation between frequencies of activated HLA-DR⁺ CD8⁺ T cells and CD32⁺ CD4⁺ T cells. Cryopreserved PBMC were thawed and directly stained. Data from 23 HIV-infected patients with detectable viral load; one data point is missing because its value was zero. Pearson correlation and Spearman rank correlation coefficient were applied for bivariate correlation analysis. R^2 denotes the nonparametric Spearman correlation coefficient.

Here, a significant correlation between the frequency of activated HLA-DR⁺ CD8⁺ T cells and frequency of CD32⁺ CD4⁺ TTM cells was detected ($R^2=0,5813$; $p=0,0036$).

Since a correlation between activation status (indicated by the frequency of HLA-DR⁺ CD8⁺ T cells) and the frequency of CD32⁺ CD4⁺ T cells could be shown, the frequency of HLA-DR⁺ cells was compared between CD32⁺ and CD32⁻ PBMC and LNMC (**Figure 16**).

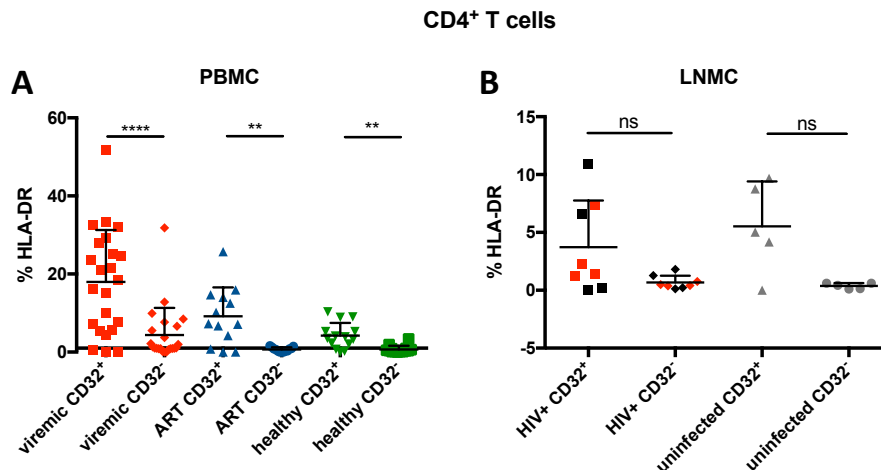


Figure 16: Frequency of HLA-DR⁺ CD4⁺ CD32⁺ and CD32⁻ T cells. (A) CD32⁺ and CD32⁻ CD4⁺ T cells isolated from blood of HIV-infected patients with detectable viral load (viremic, red), from HIV-infected patients with undetectable viral load (ART, blue) and healthy individuals (green). (B) CD32⁺ and CD32⁻ CD4⁺ T cells isolated from lymph nodes of HIV-infected patients (HIV+) and uninfected controls (uninfected). Viremic patients are indicated by red symbols. Cryopreserved samples were thawed and directly stained. PBMC data from 23 HIV-infected patients with detectable viral load, 13 HIV-infected patients with undetectable viral load and 14 healthy individuals presented as means plus standard deviation. LNMC data from 8 HIV-infected patients (4 of whom had viremia) and 5 uninfected controls. *Ns* ≥ 0.05 , **p* < 0.05, ***p* < 0.01, ****p* < 0.001, *****p* < 0.0001, as calculated by Kruskal-Wallis test.

The frequency of HLA-DR⁺ cells was indeed significantly higher in peripheral CD32⁺ CD4⁺ T cells than in the respective CD32⁻ group regardless of disease status (viremic: 17,95 % versus 4,37%, *p* < 0,0001; ART: 9,16 % versus 0,66 %, *p*=0,0012 and healthy: 4,22 % versus 0,70 %, *p*=0,0031; **Figure 16A**). In LNMC, a similar trend was evident but did not reach significance (HIV+ *p*=0,0547, uninfected *p*=0,1250; **Figure 16B**).

3.1.4 The copy number of integrated HIV-DNA in peripheral CD4⁺ T cells of patients with primary infection did not correlate with the frequency of CD32⁺ CD4⁺ T cells

A significant enrichment of inducible replication-competent provirus has been described in CD32a⁺ as compared to total CD4⁺ T cells, supporting the hypothesis of CD32(a) as marker of latently infected cells⁶.

Hence, a post-hoc analysis of PBMC where total, cellular HIV-DNA had already been determined by real-time PCR was carried out (see **Suppl. Table 5** for cohort statistics). Total HIV-DNA, also called cell-associated HIV-DNA, comprises all forms of HIV-DNA including stably integrated proviruses and unintegrated forms¹⁹⁹. The correlated frequencies of CD32⁺ CD4⁺ T cells and copies of total HIV-DNA in CD4⁺ T cells of HIV patients with primary infection are depicted in **Figure 17**.

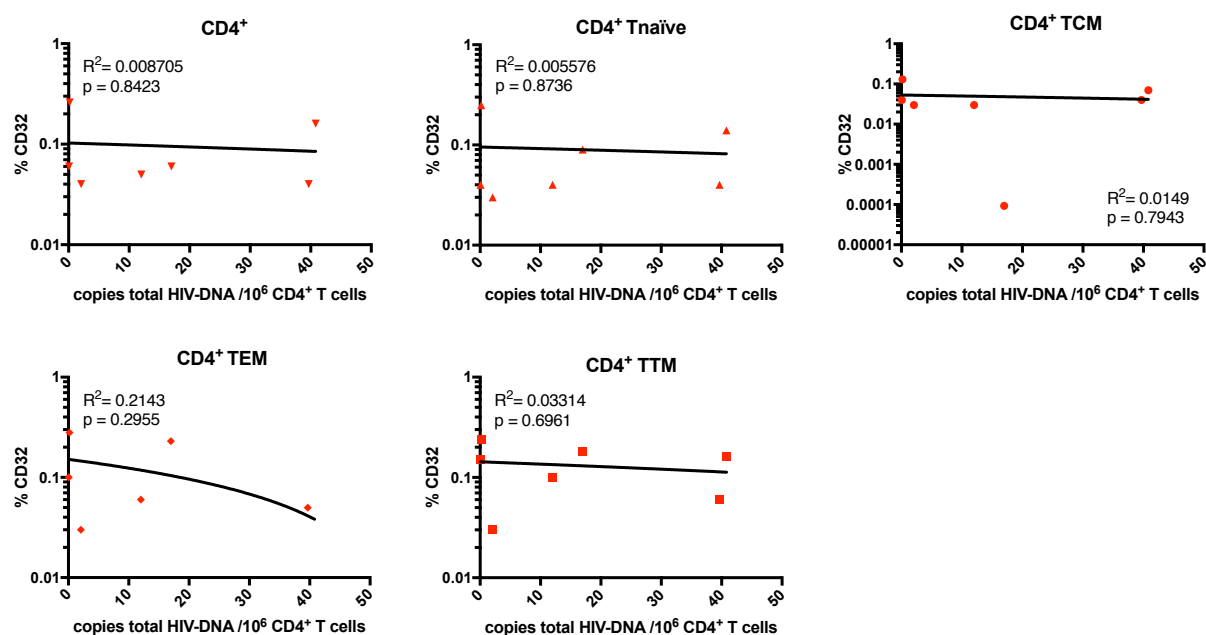


Figure 17: Frequency of peripheral CD4⁺ CD32⁺ T cells versus total HIV-DNA in CD4⁺ T cells in patients with primary HIV infection. Cryopreserved samples with pre-determined copies of total HIV-DNA were thawed and directly stained. Total HIV-DNA was determined via quantitative real-time PCR (Generic HIV-DNA Cell, Biocentric, Bandol, France) and normalized to CD4⁺ T-cell counts. PBMC data from 7 HIV patients with primary infection. In the CD4⁺ TEM graph, one data point is missing because its value was zero. Pearson correlation and Spearman rank correlation coefficient were applied for bivariate correlation analysis. R² denotes the nonparametric Spearman correlation coefficient. Figure generated in cooperation with G. Dunay²⁰⁰.

No correlation between the copies of integrated HIV-DNA in total CD4⁺ T cells and the frequency of CD32⁺ cells could be determined in the naïve or memory CD4⁺ T-cell subsets studied.

3.1.5 Higher frequency of PD-1⁺ and TIGIT⁺ cells among CD32⁺ CD4⁺ T cells from HIV-infected individuals

To investigate whether CD32⁺ CD4⁺ T cells had a more exhausted status than CD32⁻ cells, the frequency of PD-1⁺ and T cell immunoreceptor with Ig and ITIM domains (TIGIT⁺) CD32^{+/-} CD4⁺ T cells was compared in a small number of viremic HIV-infected individuals as well as patients on ART (n=5 each). The results are shown in **Figure 18**. It has been demonstrated previously that cells which express high levels of PD-1 are a critical source of replication competent HI virus in patients on ART³. Thus, PD-1⁺/CD32⁺ LNMC have been proposed to contribute to the latent reservoir²⁰¹. TIGIT is a negative checkpoint receptor, modulates T-cell activation and enhances the production of IL-10 by dendritic cells, thus acting in an inhibitory manner²⁰². Furthermore, it marks exhausted cells and has been shown to correlate with disease progression in HIV²⁰³.

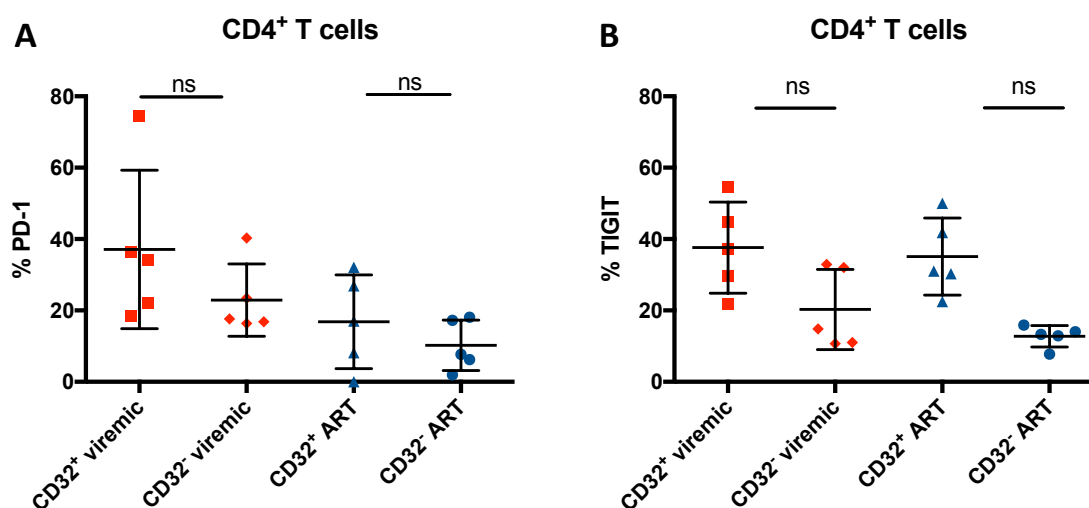


Figure 18: Frequency of PD-1⁺ (A) and TIGIT⁺ (B) CD4⁺ CD32⁺ and CD32⁻ T cells. Cells were isolated from blood of HIV-infected patients with detectable viral load (viremic, red) and from HIV-infected patients with undetectable viral load (ART, blue). Cryopreserved samples were thawed and directly stained. PBMC data from 5 HIV-infected patients with detectable and 5 HIV-infected patients with undetectable viral load presented as means +/- standard deviation. Ns \geq 0.05 as calculated by Kruskal-Wallis test.

Elevated frequencies of PD-1⁺ and TIGIT⁺ cells were found among CD32⁺ compared to CD32⁻ CD4⁺ T cells in samples from both viremic individuals and patients on ART. In samples from viremic patients, 37,08 % of CD4⁺ CD32⁺ T cells were PD-1⁺, whereas only 22,9 % of the corresponding

CD32⁻ were PD-1⁺ (**Figure 18A**). In patients on ART, 16,84 % (CD32⁺) versus 10,25 % (CD32⁻) CD4⁺ T cells were PD-1⁺. It is possible that due to the small sample number, the differences did not reach statistical significance.

The frequencies of TIGIT⁺ CD32^{+/-} T cells were comparable to the PD-1⁺ cells: 37,6 % (CD32⁺) versus 20,28 % (CD32⁻) in samples from viremic patients and 35,12 % (CD32⁺) versus 12,78 % (CD32⁻) CD4⁺ T cells in samples from patients on ART (**Figure 18B**). These differences did also not reach statistical significance ($p \geq 0.05$).

3.2 Comparison of the integrin $\alpha 4\beta 7$ expression pattern of memory T-cell subsets during HIV infection and in patients with ulcerative colitis

Another molecule that defines a subset of cells that play a significant role in HIV transmission and pathogenesis is the integrin $\alpha 4\beta 7$ ²⁰⁴. To this end, the surface expression of $\alpha 4\beta 7$ as well as the pattern of activation, homing and exhaustion markers of T cells were assessed in PBMC from HIV-infected patients and patients diagnosed with UC in comparison to healthy controls. Additionally, lymph nodal cells, gut-derived cells and longitudinal PBMC samples from an HIV patient with concomitant UC were studied. The following results have already been published¹⁹⁸.

First, preliminary experiments to achieve reliable measurements are described, in addition to *in vitro* experiments. In the second part, PBMC data from HIV-infected patients and UC patients is presented, detailing on the frequency of $\alpha 4\beta 7^+$ in total CD8⁺ T cells and CD4⁺ T cells including analysis of naïve and memory T-cell populations.

Subsequently, the analysis of tissue samples from the lymph nodes of uninfected and HIV-infected patients and samples from the gut mucosa from healthy controls and patients with UC will be described. In the last part of this thesis, a descriptive study of longitudinal samples from an HIV-infected patient with concomitant UC who was initiated on Vedolizumab therapy is presented.

3.2.1 Vedolizumab blocked the binding site of the $\alpha4\beta7$ -specific antibody clone Act1

In order to understand the *in vivo* situation better, the saturation kinetics of Vedolizumab were determined *in vitro* and a robust staining using two separate antibodies ($\alpha4$ -specific, clone 7.2R and $\beta7$ -specific, clone FIB504) was established, since a staining with the commonly used clone Act1 was not feasible.

Figure 19 shows the results of immunofluorescent PBMC stainings with the commonly used $\alpha4\beta7$ -specific antibody (clone Act1). The samples were obtained from a Vedolizumab-naïve patient (**Figure 19A**) and from a patient who had received a Vedolizumab infusion (**Figure 19B**).

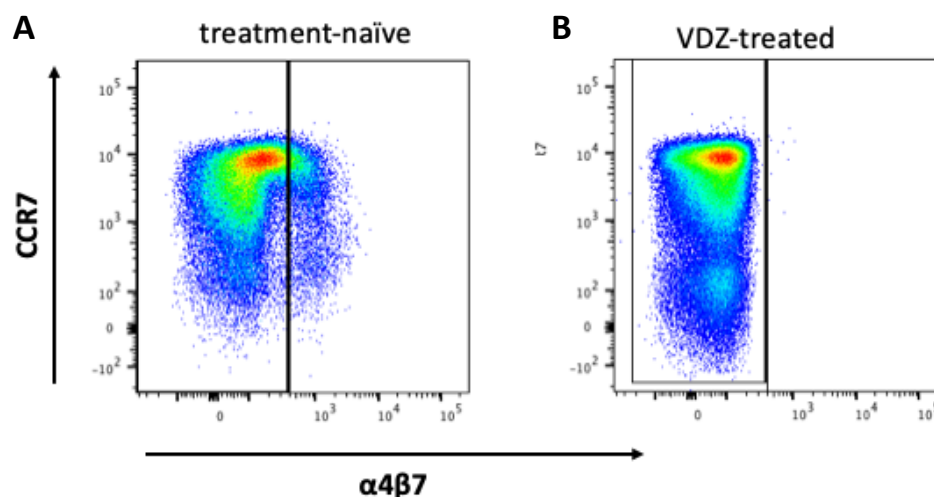


Figure 19: Vedolizumab blocks binding of the $\alpha4\beta7$ -specific antibody clone Act1 in *ex vivo* samples from UC patients. (A) *Ex vivo* PBMC staining from a treatment-naïve patient stained with anti- $\alpha4\beta7$ antibody (clone Act1). (B) *Ex vivo* PBMC staining from a Vedolizumab-treated patient stained with anti- $\alpha4\beta7$ antibody (clone Act1). Gating strategy: -Dump (live/dead dye, CD14, CD19), single cells, lymphocytes, CD3⁺, CD4⁺ T cells.

As illustrated in **Figure 19**, prior administration of Vedolizumab interfered with detection of $\alpha4\beta7$ in the patient's PBMC via the $\alpha4\beta7$ -specific antibody clone Act1 (**Figure 19B**), while staining samples from treatment-naïve patients with the same antibody resulted in a robust signal (**Figure 19A**).

After several follow-up samples did not show any positive signal for $\alpha 4\beta 7$, *in vitro* experiments were conducted to determine the lowest concentration of Vedolizumab that would allow for a robust staining with the $\alpha 4\beta 7$ -specific antibody. **Figure 20** illustrates the detectable frequency of $\alpha 4\beta 7^+$ CD4⁺ T cells after *in vitro* incubation with Vedolizumab.

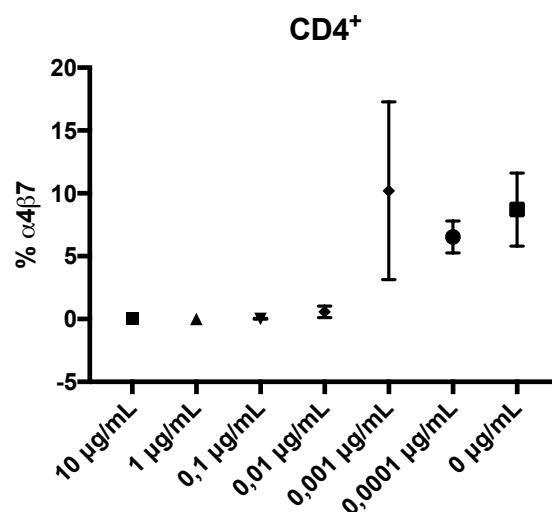


Figure 20: Percentage of $\alpha 4\beta 7$ expressing CD4⁺ T cells after *in vitro* incubation with Vedolizumab. Data from 3 healthy individuals. Samples were incubated with the therapeutic antibody for 90 min, washed twice and then stained with the $\alpha 4\beta 7$ -specific antibody Act1.

A dose-dependent signal from the antibody staining was only achieved at concentrations of Vedolizumab of 0,001 $\mu\text{g}/\text{mL}$ or lower (**Figure 20**). During clinical treatment of inflammatory bowel diseases, a dose of 300 mg antibody is administered. This amounts to 4 mg per kg, assuming a bodyweight of 75 kg.

The collected *in vitro* data is further supported by pharmacokinetic studies of Vedolizumab which report a saturation of the $\alpha 4\beta 7$ integrin molecule in peripheral blood T cells of greater than 95 % between 2 and 10 mg antibody per kg bodyweight²⁰⁵. Since 4 mg of antibody per kg was administered, it is assumed that practically all receptors were saturated with the therapeutic antibody which could lead to a steric hindrance.

Since the commonly used $\alpha 4\beta 7$ -specific antibody was not suitable for usage with samples from Vedolizumab-treated patients, a different staining approach was tested and validated. An $\alpha 4$ -specific antibody (clone 7.2R) was tested for immunostaining in combination with a $\beta 7$ -specific (clone FIB504) one. Although it has been stated that $> 99\%$ of $\beta 7^{\text{high}}$ cells in the blood are also $\alpha 4\beta 7$, an attempt was made to stain both $\alpha 4^+$ and $\beta 7^+$ double-positive cells^{181,206}.

Ten frozen PBMC samples from healthy volunteers were thawed and either stained with clone Act1 alone or with the combination of the two separately binding antibodies (**Figure 21**).

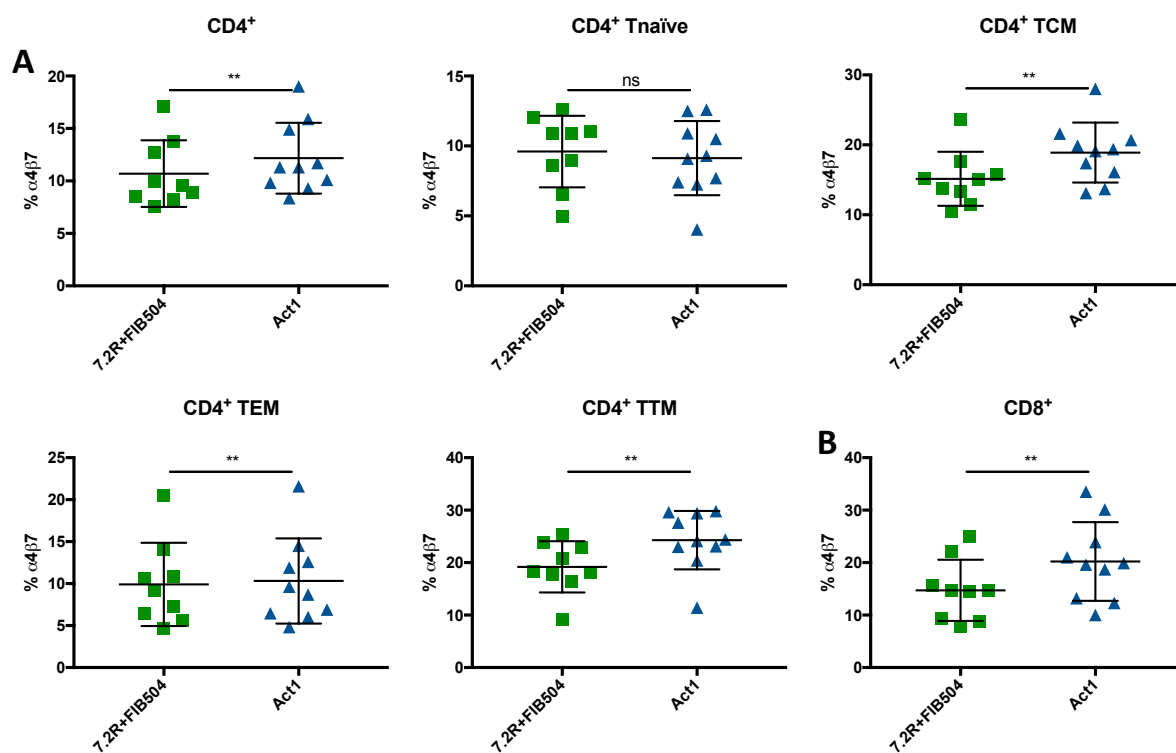


Figure 21: Comparison of the $\alpha 4\beta 7$ -specific clone Act1 and the $\alpha 4$ -specific clone 7.2R in combination with a separate $\beta 7$ -specific antibody. (A) Frequency of $\alpha 4\beta 7^+$ total $CD4^+$ T cells as well as naïve and memory subsets. (B) Frequency of total $\alpha 4\beta 7^+$ $CD8^+$ T cells. PBMC from 10 healthy controls were stained with either an $\alpha 4$ -specific antibody (clone 7.2R) in combination with a $\beta 7$ -specific antibody (clone FIB504) (left, green) or with the $\alpha 4\beta 7$ -specific antibody, clone Act1 (right, blue). Results were analysed using the Wilcoxon matched-pairs signed rank test, nonparametric test of paired samples. One sample stained with the $\alpha 4\beta 7$ -specific antibody had to be excluded as the staining did not work. Ns ≥ 0.05 , ** $p < 0.01$.

The direct comparison showed that, except for naïve CD4⁺ T cells, the frequencies of α4β7⁺ T cells detected were significantly higher in samples stained with the antibody that recognizes both subunits of α4β7 (clone Act1).

Next, a check was carried out to see whether the frequencies detected with the two staining approaches correlated with each other, since using the clone Act1 was still not feasible and the major aim of the study was to compare frequencies rather than to determine absolute numbers (Figure 22).

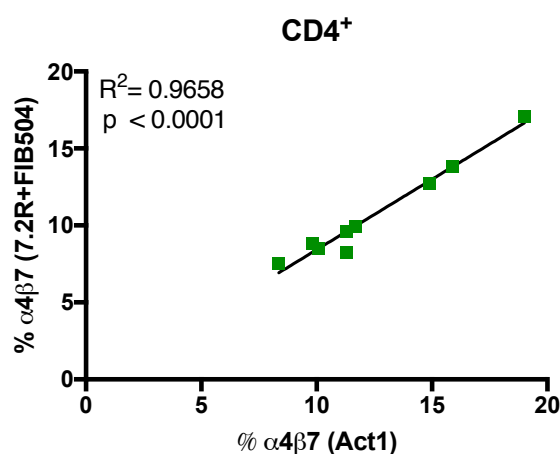


Figure 22: Correlation of the α4β7 frequencies detected with the α4β7-specific clone Act1 and the α4-specific clone 7.2R in combination with a separate β7-specific antibody. Data from PBMC from 10 healthy controls. Pearson correlation and Spearman rank correlation coefficient were applied for bivariate correlation analysis. R² denotes the nonparametric Spearman correlation coefficient.

Indeed, the data resulting from the two approaches was highly correlated (R²=0,97; p<0,0001), so it was decided to proceed with the combinatory staining for the samples from patients with UC. At that time, most of the samples from HIV-infected patients had already been stained with the clone Act1. There, robust stainings could be achieved because patients had not been treated with the therapeutic antibody (Vedolizumab) and the binding site of the analytic antibody was not blocked by Vedolizumab. Since no direct comparison between the two cohort groups in terms of frequency or MFI was needed, one part of the cohort was stained with the clone Act1 (HIV) and the other part with the combination of the two separate antibodies (7.2R and FIB504; **Suppl. Table 4**).

3.2.2 Definition of $\alpha 4\beta 7^+$ T-cell populations

In previously published literature by Sivro *et al.*, $\alpha 4\beta 7^+$ cells were divided into “intermediate” and “high” populations¹⁷⁸. This gating strategy has been applied to the samples measured within this work (Figure 23).

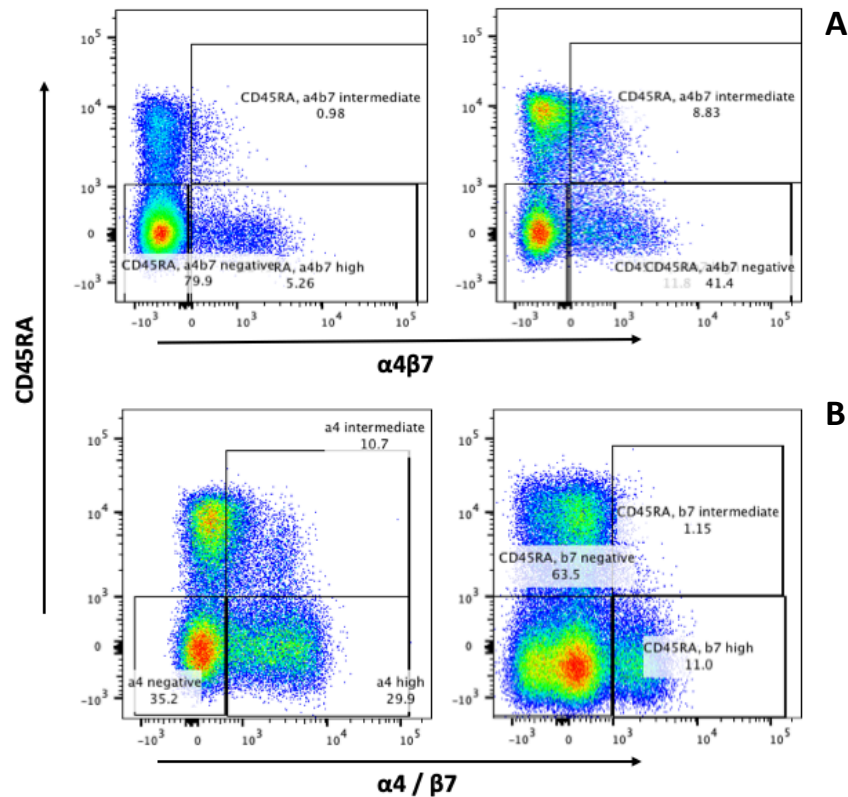


Figure 23: Exemplary plots of $\alpha 4\beta 7^{\text{intermediate}}$ and $\alpha 4\beta 7^{\text{high}}$ cells as well as $\alpha 4^{\text{intermediate}}/\alpha 4^{\text{high}}$ and $\beta 7^{\text{intermediate}}/\beta 7^{\text{high}}$ cells. (A) Cryopreserved samples from HIV-infected patients on ART were stained with the $\alpha 4\beta 7$ -specific antibody clone Act1. (B) Samples from healthy patients were stained with antibodies against $\alpha 4$ (clone 7.2R) and $\beta 7$ (clone FIB504). Gating strategy: -Dump (live/dead dye, CD14, CD19), single cells, lymphocytes, CD3⁺, CD4⁺ T cells.

Figure 23 shows that few intermediate positive cells were detected using this approach.

Therefore, it was decided to gate and analyse the entity of $\alpha 4\beta 7^+$ cells as shown in **Figure 24A**. Cells were plotted against CCR7 to be able to distinguish between naïve ($CCR7^+$) and memory cells ($CCR7^-$). This strategy was also supported by the work of Perciani *et al.*, who noted that it was incorrect to assume that all $\beta 7^+$ cells in the gut were also $\alpha 4\beta 7^+$ ²⁰⁷.

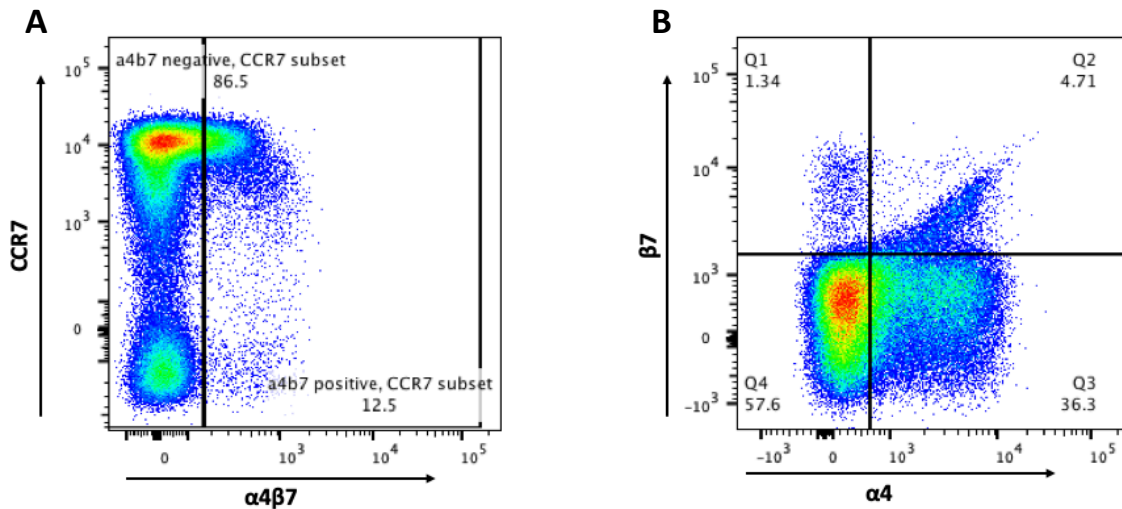


Figure 24: Gating of samples from an HIV-infected patient (A) and a patient with UC (B). The entity of $\alpha 4\beta 7^+$ plotted against CCR7 was gated in samples from HIV-infected patients. In patients with UC, double-positive cells were used for further analysis. Gating strategy: -Dump (live/dead dye, CD14, CD19), single cells, lymphocytes, CD3⁺, CD4⁺.

Samples from patients with UC were analysed using a combination of two antibodies (**Figure 24B**). Since $\alpha 4$ and $\beta 7$ form a heterodimer, their expression is directly correlated and the double-positive population in Q2 forms a diagonal.

3.2.3 Frequency of $\alpha 4\beta 7^+$ CD4⁺ T effector memory populations differed in HIV-infected versus healthy individuals

Studies in both humans and nonhuman primates have demonstrated that $\alpha 4\beta 7^{\text{high}}$ CD4⁺ T cells are highly susceptible to HIV/SIV infection and are quickly depleted during the acute phase of the disease^{179,181}.

For this reason, the relative frequencies of peripheral $\alpha 4\beta 7^+$ CD4⁺ T cells were compared in healthy volunteers and HIV patients (**Figure 25**). The following figures present data from HIV-infected subjects with detectable plasma viremia (termed “viremic”), undetectable plasma viral load (“ART”) and HIV-infected people that are able to control viremia and maintain stable CD4⁺ T-cell counts without medication (“elite ctrl”).

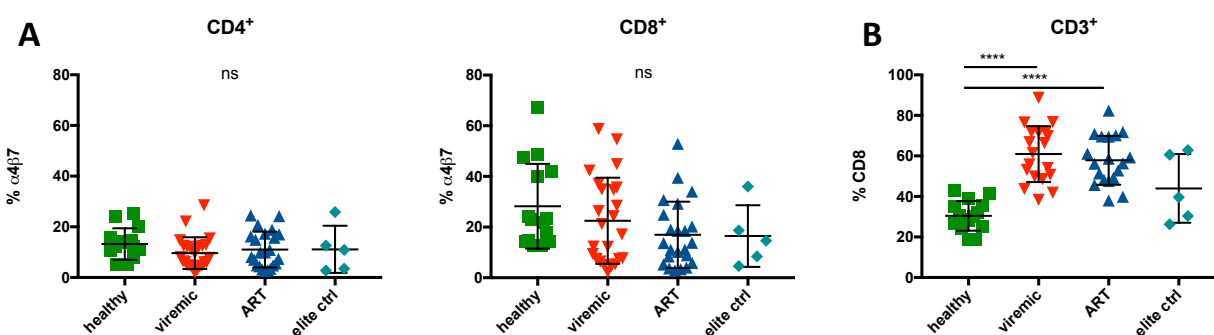


Figure 25: Frequency of $\alpha 4\beta 7^+$ cells does not differ in total CD4⁺ or CD8⁺ T cells from PBMC of HIV-infected patients compared to healthy individuals. (A) Frequencies of $\alpha 4\beta 7^+$ CD4⁺ and CD8⁺ T cells isolated from blood of healthy individuals (green), viremic HIV patients (red), HIV patients with undetectable viral load (ART, blue) and aviremic patients who did not receive ART (elite ctrl, light blue). (B) Frequencies of CD3⁺ CD8⁺ T cells in peripheral blood. Cryopreserved samples were thawed and directly stained with an $\alpha 4\beta 7$ -specific antibody (clone Act1). Data from 15 healthy controls, 24 viremic HIV patients, 23 HIV patients on ART and 5 elite controllers presented as means \pm standard deviation. Ns \geq 0.05, **** p < 0.0001, as calculated by Kruskal-Wallis test and adjusted for multiple comparisons by Dunn’s test. Ns on top of graph indicates that none of the comparisons reached significance.

There were no differences in the frequency of $\alpha 4\beta 7^+$ cells in the total CD4⁺ T-cell compartment when healthy individuals, viremic and HIV patients on ART and HIV elite controllers were compared (**Figure 25A**). In the CD8⁺ T-cell compartment, the frequencies of $\alpha 4\beta 7^+$ T cells were generally higher than in the CD4⁺ T-cell compartment (e.g. healthy: 28,23 % CD8⁺ $\alpha 4\beta 7^+$ versus 13,22 % CD4⁺ $\alpha 4\beta 7^+$, $p=0,0646$), but frequencies of $\alpha 4\beta 7^+$ CD8⁺ T cells did not differ significantly

between the cohort groups (**Figure 25A**). The frequencies of $\alpha 4\beta 7^+$ CD8⁺ T cells were slightly lower in samples from all HIV-infected patients and lowest in elite controllers compared to healthy controls, but the differences remained non-significant (**Figure 25A**). At the same time, the percentage of total CD8⁺ T cells was significantly increased in samples from viremic and ART-treated HIV patients compared to healthy controls (**Figure 25B**).

Additionally, an analysis was carried out to establish whether there were any differences in the naïve and memory CD4⁺ T-cell subsets, which were defined as follows according to their expression of the markers CD45RA and CCR7^{208,209}:

Tnaïve (CD45RA⁺/CCR7⁺), central memory T cells: TCM (CD45RA⁻/CCR7⁺), effector memory T cells: TEM (CD45RA⁻/CCR7⁻/CD27⁻), transitional memory T cells: TTM (CD45RA⁻/CCR7⁻/CD27⁺) and CD45RA-expressing TEM cells: TEMRA (CD45RA⁺/CCR7⁻). Results are shown in **Figure 26**.

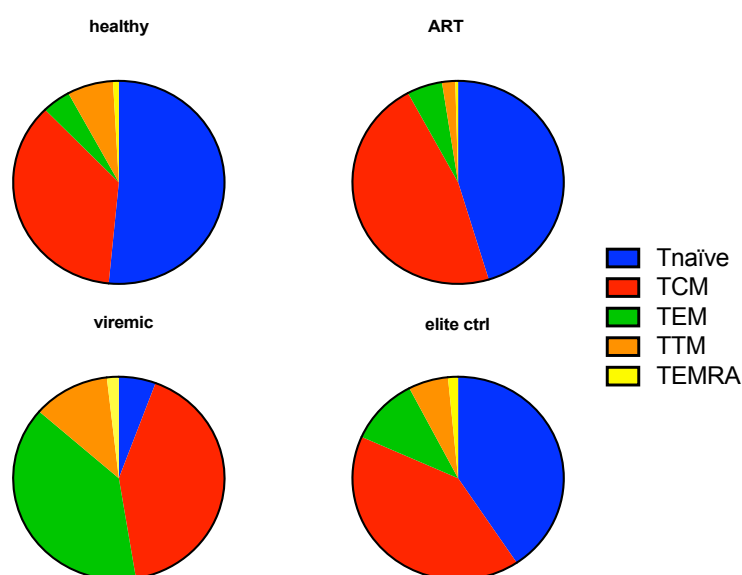


Figure 26: Distribution of CD4⁺ T-cell subsets in different cohort groups. Tnaïve (CD45RA⁺/CCR7⁺), central memory T cells: TCM (CD45RA⁻/CCR7⁺), effector memory T cells: TEM (CD45RA⁻/CCR7⁻/CD27⁻), transitional memory T cells: TTM (CD45RA⁻/CCR7⁻/CD27⁺) and CD45RA-expressing TEM cells: TEMRA (CD45RA⁺/CCR7⁻). Data from 15 healthy controls, 24 viremic HIV patients, 23 HIV patients on ART and 5 elite controllers.

The relative frequency of naïve T cells (blue) was markedly decreased in CD4⁺ T cells from viremic patients (lower left) and the frequency of CD4⁺ TEM in this group of patients was strongly increased compared to the healthy controls, ART-treated individuals and elite controllers. Next, the frequencies of $\alpha 4\beta 7^+$ cells were examined in these CD4⁺ T-cell subsets (**Figure 27**).

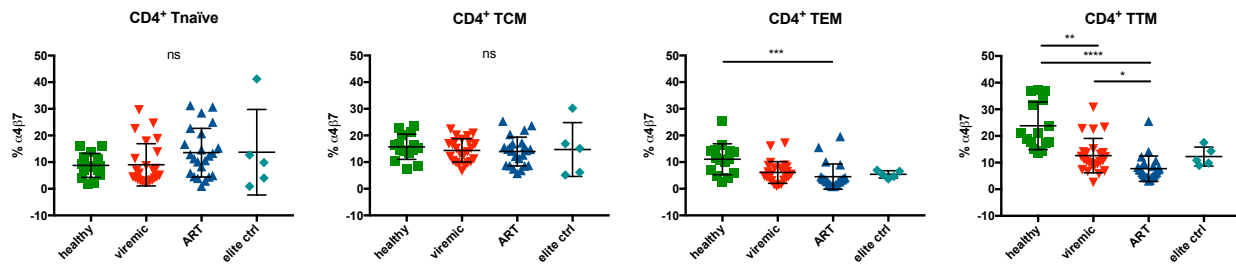


Figure 27: Frequency of $\alpha 4\beta 7^+$ cells differs in different effector memory CD4⁺ T-cell populations in PBMC from HIV-infected patients compared to healthy individuals. Frequencies of $\alpha 4\beta 7^+$ CD4⁺ T cells isolated from blood of healthy individuals (green), viremic HIV patients (red), HIV patients with undetectable viral load (ART, blue) and aviremic patients who did not receive ART (elite ctrl, light blue). Cryopreserved samples were thawed and directly stained with an $\alpha 4\beta 7$ -specific antibody (clone Act1). Data from 15 healthy controls, 24 viremic HIV patients, 23 HIV patients on ART and 5 elite controllers presented as means +/- standard deviation. *Ns* ≥ 0.05 , **p* < 0.05, ***p* < 0.01, ****p* < 0.001, *****p* < 0.0001, as calculated by Kruskal-Wallis test and adjusted for multiple comparisons by Dunn's test. *Ns* on top of graph indicates that none of the comparisons reached significance.

There was no significant difference in the frequency of $\alpha 4\beta 7^+$ naïve and central memory CD4⁺ T cells in HIV patients with different clinical courses of disease and healthy individuals. TEM and TTM cells of HIV patients, in particular ART-treated HIV patients, expressed $\alpha 4\beta 7$ at a significantly lower frequency than the respective memory subset of healthy controls did, with the exception of HIV elite controllers (TEM: healthy 11,08 %, ART 4,53 %, viremic 6,12 %, elite ctrl. 5,42 %; healthy versus ART *p*=0,0001 - TTM: healthy 23,81 %, ART 7,71 %, viremic 12,61 %, elite ctrl. 12,28 %; healthy versus viremic *p*=0,0053, healthy versus ART *p*<0,0001, ART versus viremic *p*=0,0216).

3.2.4 The frequency of $\alpha 4\beta 7^+$ CD4⁺ T cells was upregulated after *in vitro* stimulation with bead bound anti-CD3/CD28

To determine whether the *in vivo* frequency of $\alpha 4\beta 7^+$ T cells is associated with the activation status of the T cells, PBMC from healthy donors were stimulated *in vitro* with bead bound CD3/CD28 or PMA/ionomycin for 7 days (**Figure 28A-C**). Retinoic acid (RA) produced by gut-associated dendritic cells has been described as a modulator of $\alpha 4\beta 7$ expression in mesenteric lymph nodes and Peyer's patches *in vivo*^{167,210}. Thus, RA was used as an additional control (**Figure 28D**).

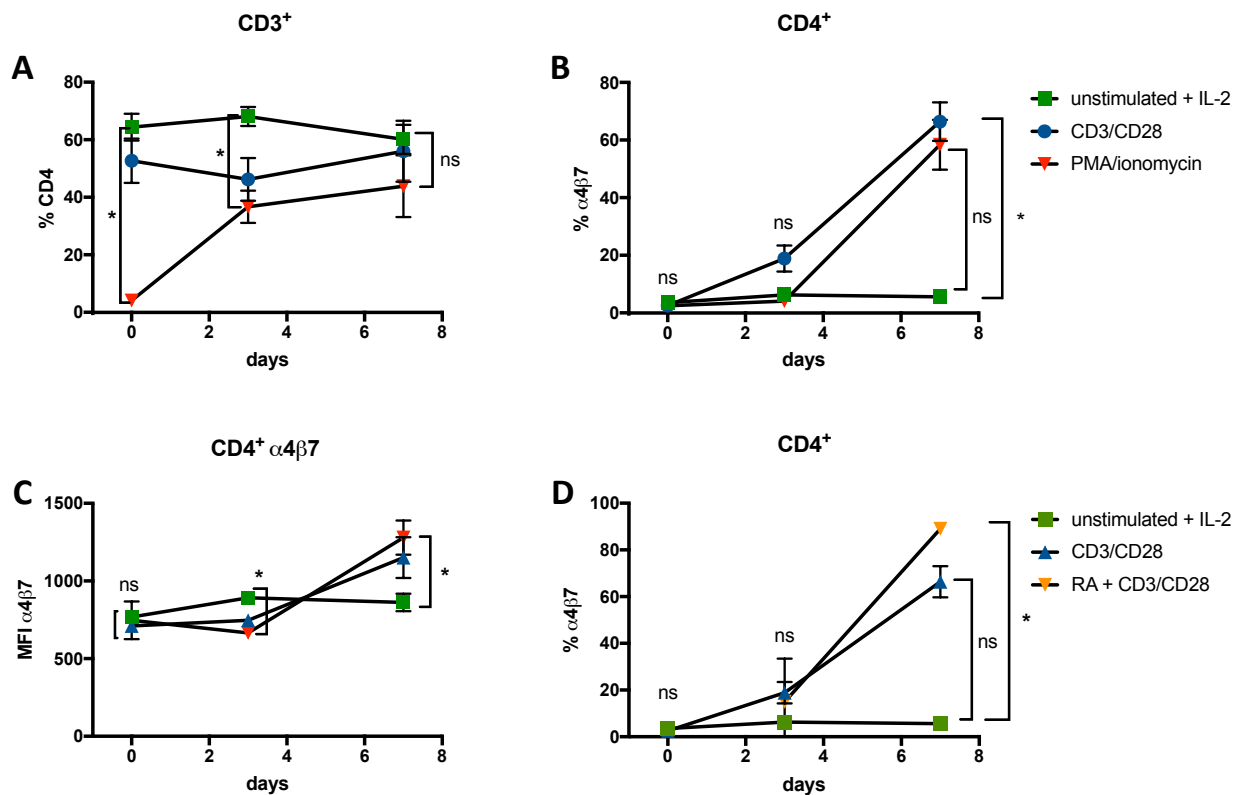


Figure 28: Upregulation of $\alpha 4\beta 7^+$ CD4⁺ T cells after *in vitro* stimulation with bead-bound anti-CD3/CD28. (A) Percentage of CD4⁺ T cells. (B) Percentage of $\alpha 4\beta 7$ -expressing CD4⁺ T cells. (C) Mean fluorescence intensity (MFI) of $\alpha 4\beta 7$ -expressing CD4⁺ T cells. (D) Percentage of $\alpha 4\beta 7$ -expressing CD4⁺ T cells after stimulation with 100 nM all-trans retinoic acid (RA) and bead-bound CD3/CD28. Cryopreserved samples from 3 healthy donors were thawed and used for culture. Day 0 depicts the status of the cells after 6 hours of stimulation. Friedmann tests for multiple comparisons were performed. Ns ≥ 0.05 , *p < 0.05.

After seven days of stimulation with bead-bound CD3/CD28 or PMA/ionomycin, the frequency of CD4⁺ T cells was similar to unstimulated samples (**Figure 28A**), whereas the frequency of $\alpha 4\beta 7^+$ CD4⁺ T cells stimulated with bead-bound CD3/CD28 was significantly increased compared to unstimulated controls (66,37 % versus 5,59 %, $p=0,0286$; **Figure 28B**). After six hours of stimulation (day 0) and at day 3, no significant difference between the groups could be observed. The density of $\alpha 4\beta 7$ on CD4⁺ T cells as measured by the mean fluorescence intensity (MFI) was lower on day 3 in samples stimulated with PMA/ionomycin than in the unstimulated controls (666 versus 891, $p=0,0286$; **Figure 28C**). After stimulation of the cells for seven days, a significant increase in the MFI in samples stimulated with PMA/ionomycin was observed (862 versus 1279, $p=0,0286$). After stimulation with RA for seven days, the frequency of $\alpha 4\beta 7^+$ CD4⁺ T cells was significantly higher than in the unstimulated controls (89 % versus 5,59 %, $p=0,0286$; **Figure 28D**).

In summary, *in vitro* stimulation of PBMC with bead-bound CD3/CD28 and retinoic acid was observed to be associated with an activation- and retinoic-acid dependent upregulation of $\alpha 4\beta 7^+$ CD4⁺ T cells.

3.2.5 Evaluation of the HLA-DR⁺ frequency as marker for activated cells

Since an activation-dependent upregulation of $\alpha 4\beta 7$ was observed *in vitro*, an analysis was conducted to see whether there was a higher frequency of HLA-DR⁺ $\alpha 4\beta 7^+$ than HLA-DR⁺ $\alpha 4\beta 7^-$ CD4⁺ T cells in PBMC from HIV and UC patients (**Figure 29**).

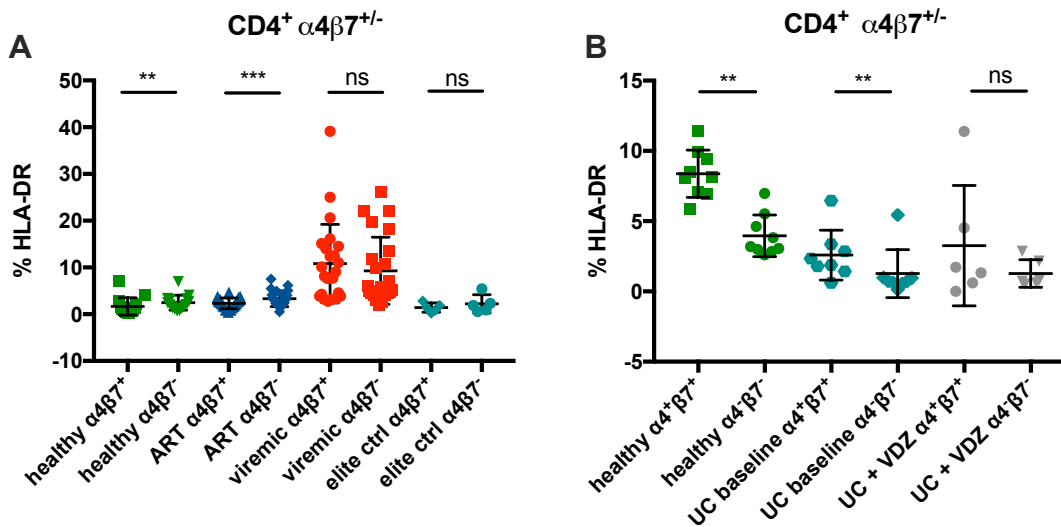


Figure 29: Comparative analysis of HLA-DR on $\alpha 4\beta 7^+$ and $\alpha 4\beta 7^-$ cells of healthy controls, patients with UC and HIV-infected individuals. Frequencies of HLA-DR⁺ $\alpha 4\beta 7^+$ and $\alpha 4\beta 7^-$ CD4⁺ T cells isolated from blood of healthy individuals (green), (A) viremic HIV patients (red), HIV patients with undetectable viral load (ART, blue) and aviremic patients who did not receive ART (elite ctrl, light blue). Cryopreserved samples were thawed and directly stained with an $\alpha 4\beta 7$ -specific antibody (clone Act1). Data from 15 healthy subjects, 24 viremic HIV patients, 23 HIV patients on ART and 5 elite controllers. (B) Vedolizumab-naïve patients with ulcerative colitis (UC baseline, light blue) and patients with ulcerative colitis treated with Vedolizumab (UC + VDZ, grey). Cryopreserved samples were thawed and directly stained with an $\alpha 4$ -specific antibody (clone 7.2R) plus a $\beta 7$ -specific antibody (clone FIB504). Data from 9 healthy subjects, 8 Vedolizumab-naïve patients with UC and 6 patients with UC treated with Vedolizumab. Data presented as means +/- standard deviation. Ns ≥ 0.05 , * $p < 0.05$, ** $p < 0.01$, *** $p < 0.001$, **** $p < 0.0001$, as calculated by Wilcoxon matched-pairs signed rank test.

In patients on ART, the frequency of HLA-DR⁺ CD4⁺ T cells was significantly lower in $\alpha 4\beta 7^+$ T cells than in $\alpha 4\beta 7^-$ T cells (**Figure 29A**). Also noteworthy are the conflicting results obtained from the healthy controls: while the samples stained with clone Act1 showed a significant increase in the frequency of HLA-DR⁺ in $\alpha 4\beta 7^+$ versus $\alpha 4\beta 7^-$ CD4⁺ T cells (1,68 % in $\alpha 4\beta 7^+$ versus 2,48 % in $\alpha 4\beta 7^-$, $p=0,0084$) the samples stained with a combination of 7.2R and FIB504 showed a significant

decrease (8,37 % in $\alpha 4\beta 7^+$ versus 3,96 % in $\alpha 4\beta 7^-$, $p=0,0039$). This discrepancy is reviewed in the discussion section.

The data obtained from patients with UC look different: The frequency of HLA-DR⁺ CD4⁺ T cells was significantly increased in $\alpha 4\beta 7^+$ T cells from healthy individuals (8,37 % in $\alpha 4\beta 7^+$ versus 3,96 % in $\alpha 4\beta 7^-$, $p=0,0039$) and untreated patients with UC (2,59 % in $\alpha 4\beta 7^+$ versus 1,27 % in $\alpha 4\beta 7^-$, $p=0,0078$; **Figure 29B**). A similar trend was evident in Vedolizumab-treated UC patients, but did not reach statistical significance.

3.2.6 Frequency of PD-1⁺ cells was higher among $\alpha 4\beta 7^{+}$ T cells of HIV-infected individuals

To evaluate whether there was also a difference in the frequency of PD-1⁺ cells between $\alpha 4\beta 7^{+}$ and $\alpha 4\beta 7^{-}$ CD4⁺ T cells, PBMC from HIV-infected patients, healthy individuals and patients with UC were measured (**Figure 30**).

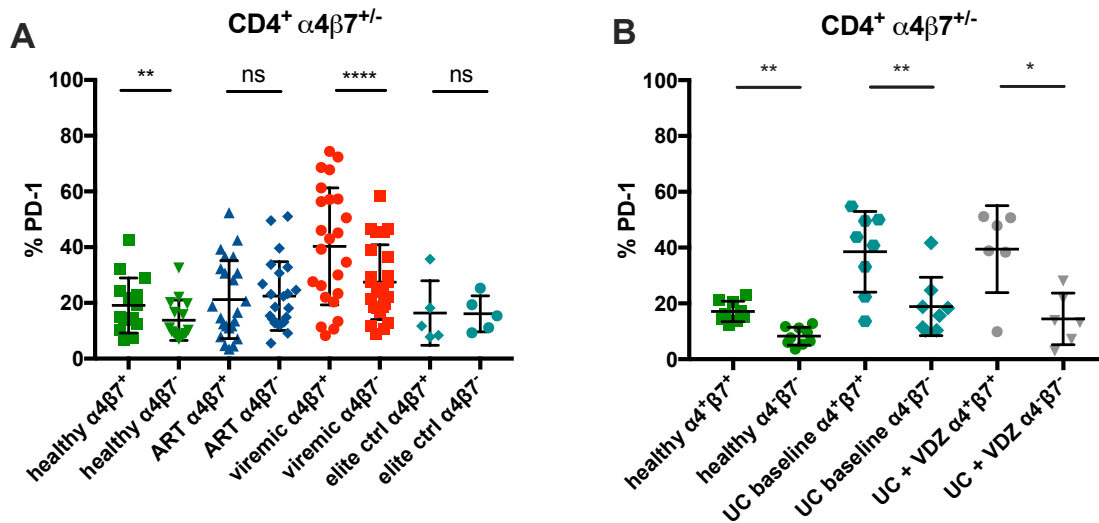


Figure 30: Comparative analysis of PD-1 on $\alpha 4\beta 7^{+}$ and $\alpha 4\beta 7^{-}$ cells from healthy controls, HIV-infected individuals and patients with UC. Frequencies of HLA-DR⁺ $\alpha 4\beta 7^{+}$ and $\alpha 4\beta 7^{-}$ CD4⁺ T cells isolated from blood of healthy individuals (green), (A) viremic HIV patients (red), HIV patients with undetectable viral load (ART, blue) and aviremic patients who did not receive ART (elite ctrl, light blue). Cryopreserved samples were thawed and directly stained with an $\alpha 4\beta 7$ -specific antibody (clone Act1). Data from 15 healthy subjects, 24 viremic HIV patients, 23 HIV patients on ART and 5 elite controllers. (B) Vedolizumab-naïve patients with ulcerative colitis (UC baseline, light blue) and patients with ulcerative colitis treated with Vedolizumab (UC + VDZ, grey). Cryopreserved samples were thawed and directly stained with an $\alpha 4$ -specific antibody (clone 7.2R) plus a $\beta 7$ -specific antibody (clone FIB504). Data from 9 healthy subjects, 8 Vedolizumab-naïve patients with UC and 6 patients with UC treated with Vedolizumab. Data presented as means +/- standard deviation. Ns ≥ 0.05 , * $p < 0.05$, ** $p < 0.01$, *** $p < 0.001$, **** $p < 0.0001$, as calculated by Wilcoxon matched-pairs signed rank test.

The frequency of PD-1⁺ cells was significantly higher in $\alpha 4\beta 7^{+}$ compared to $\alpha 4\beta 7^{-}$ CD4⁺ T cells from healthy donors (17,11 % in $\alpha 4\beta 7^{+}$ versus 8,27 % in $\alpha 4\beta 7^{-}$, $p = 0,0039$; **Figure 30A**). The same pattern of elevated PD-1 frequency in $\alpha 4\beta 7^{+}$ compared to $\alpha 4\beta 7^{-}$ cells could be seen in samples from viremic HIV patients (viremic: 40,29 % versus 27,48 %, $p < 0,0001$; **Figure 30A**), untreated patients with UC (38,5 % in $\alpha 4\beta 7^{+}$ versus 18,91 % in $\alpha 4\beta 7^{-}$, $p = 0,0078$) and patients with UC after Vedolizumab treatment (39,47 % in $\alpha 4\beta 7^{+}$ versus 14,46 % in $\alpha 4\beta 7^{-}$, $p = 0,0312$; **Figure 30B**).

3.2.7 Expression of the HIV co-receptor CCR5 on $\alpha 4\beta 7^+$ and $\alpha 4\beta 7^-$ CD4⁺ T cells

One possible reason for the susceptibility of $\alpha 4\beta 7^+$ cells to HIV infection is their high expression of the HIV co-receptor CCR5. The frequencies of CCR5⁺ CD4⁺ T cells were compared in $\alpha 4\beta 7^+$ and $\alpha 4\beta 7^-$ T cells from HIV-infected patients, healthy individuals and patients with UC (**Figure 31**).

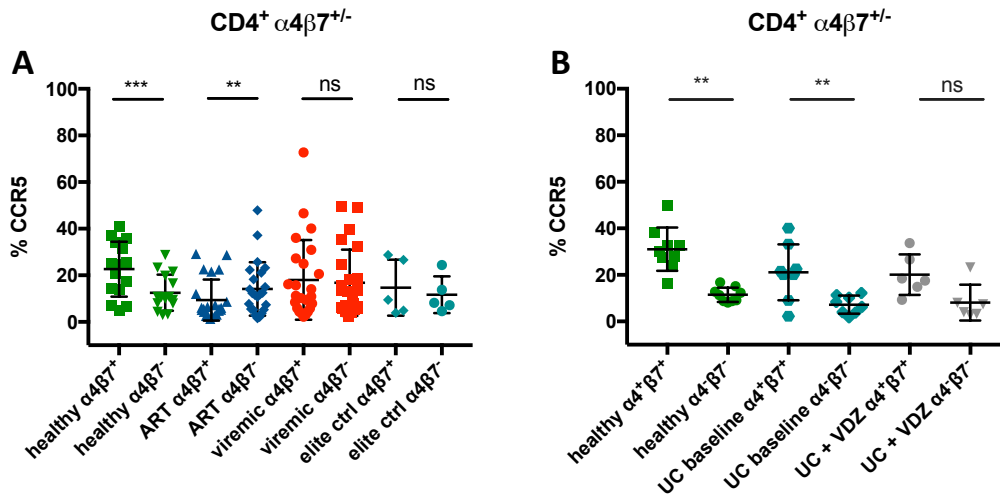


Figure 31: Comparative analysis of CCR5 on $\alpha 4\beta 7^+$ and $\alpha 4\beta 7^-$ CD4⁺ T cells from healthy controls, patients with UC and HIV-infected individuals. Frequencies of HLA-DR⁺ $\alpha 4\beta 7^+$ and $\alpha 4\beta 7^-$ CD4⁺ T cells isolated from blood of healthy individuals (green), (A) viremic HIV patients (red), HIV patients with undetectable viral load (ART, blue) and aviremic patients who did not receive ART (elite ctrl, light blue). Cryopreserved samples were thawed and directly stained with an $\alpha 4\beta 7$ -specific antibody (clone Act1). Data from 15 healthy subjects, 24 viremic HIV patients, 23 HIV patients on ART and 5 elite controllers. (B) Vedolizumab-naïve patients with ulcerative colitis (UC baseline, light blue) and patients with ulcerative colitis treated with Vedolizumab (UC + VDZ, grey). Cryopreserved samples were thawed and directly stained with an $\alpha 4$ -specific antibody (clone 7.2R) plus a $\beta 7$ -specific antibody (clone FIB504). Data from 9 healthy subjects, 8 Vedolizumab-naïve patients with UC and 6 patients with UC treated with Vedolizumab. Data presented as means +/- standard deviation. Ns ≥ 0.05 , * $p < 0.05$, ** $p < 0.01$, *** $p < 0.001$, **** $p < 0.0001$, as calculated by Wilcoxon matched-pairs signed rank test.

Indeed, the frequency of CCR5⁺ cells was higher in $\alpha 4\beta 7^+$ CD4⁺ T cells in samples from healthy donors (22,65 % versus 12,53 %, $p = 0,0009$). In contrast, a decreased frequency of CCR5⁺ cells was measured in samples from ART-treated patients ($\alpha 4\beta 7^+$: 9,41 % versus $\alpha 4\beta 7^-$: 14,14 %, $p = 0,0082$; **Figure 31A**). In patients with UC, the levels were generally lower than in the healthy controls but the pattern of higher frequencies of $\alpha 4\beta 7^+$ remained (healthy: $\alpha 4\beta 7^+$: 31,04 % versus $\alpha 4\beta 7^-$: 11,45 %, $p = 0,0078$; untreated patients with UC: $\alpha 4\beta 7^+$: 21,12 % versus $\alpha 4\beta 7^-$: 7,23 %, $p = 0,0078$; **Figure 31B**). The differences in patients with UC after Vedolizumab treatment did not reach significance.

3.2.8 The frequency of $\alpha 4\beta 7^+$ CD4⁺ T cells was decreased in the naïve CD4⁺ T-cell compartment of patients with UC after treatment with Vedolizumab

In order to get a better understanding of the T-cell expression pattern in patients with inflammation of the gut (and the effect of Vedolizumab treatment on this), cells from patients with UC were analysed, some of whom were receiving this treatment.

PBMC samples were obtained at baseline (before Vedolizumab treatment initiation) and right before the administration of the follow-up infusions (week 0-2-6, followed by infusions every 8 weeks). The graph shows the data at week 0 (“baseline”) and the last available timepoint of the infusions (“+VDZ”) (Figure 32).

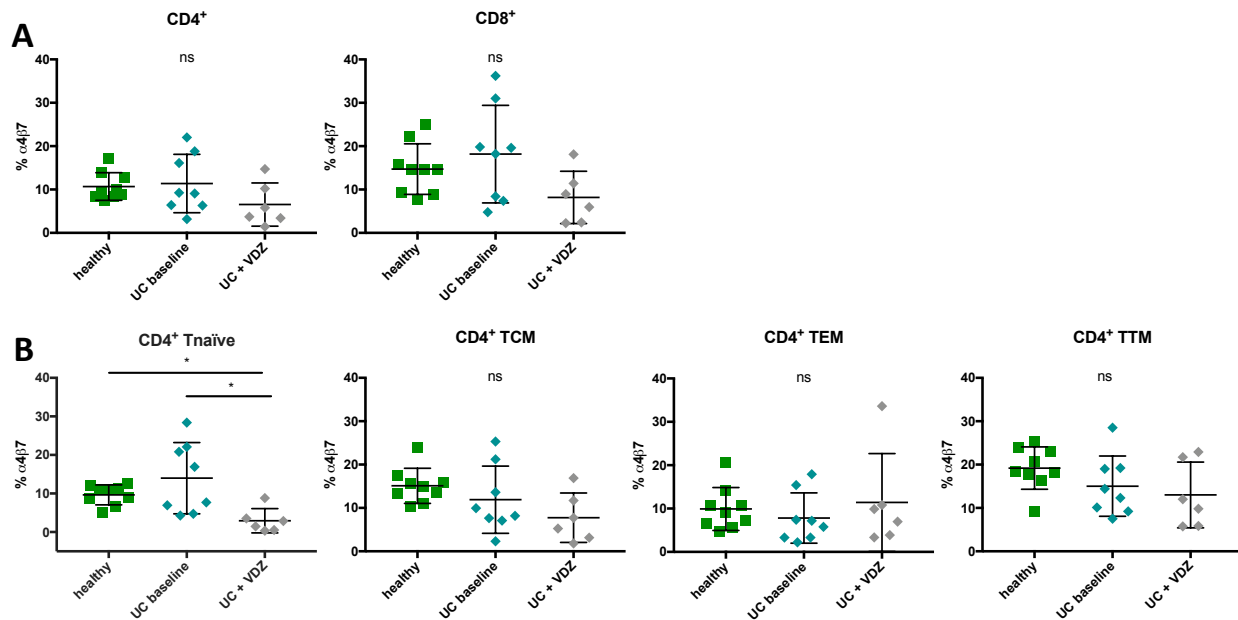


Figure 32: Frequency of $\alpha 4\beta 7^+$ cells is significantly decreased on naïve CD4⁺ T cells from patients with UC treated with Vedolizumab compared to untreated patients. Frequencies of $\alpha 4\beta 7^+$ CD4⁺ T cells isolated from blood of healthy individuals (green), Vedolizumab-naïve patients with ulcerative colitis (UC baseline, light blue) and patients with ulcerative colitis treated with Vedolizumab (UC + VDZ, grey). (A) Frequency of total $\alpha 4\beta 7^+$ CD4⁺ and CD8⁺ T cells. (B) Frequency of $\alpha 4\beta 7^+$ within CD4⁺ naïve and memory T cells. Cryopreserved samples were thawed and directly stained with an $\alpha 4$ -specific antibody (clone 7.2R) plus a $\beta 7$ -specific antibody (clone FIB504). Data from 9 healthy subjects, 8 Vedolizumab-naïve patients with UC and 6 patients with UC treated with Vedolizumab presented as means +/- standard deviation. Ns ≥ 0.05 , * $p < 0.05$, ** $p < 0.01$, *** $p < 0.001$, **** $p < 0.0001$, as calculated by Kruskal-Wallis test and adjusted for multiple comparisons by Dunn's test. Ns on top of graph indicates that none of the comparisons reached significance.

No significant differences regarding the frequency of $\alpha 4\beta 7^+$ cells were found in total CD4⁺ or total CD8⁺ T cells between the different cohort groups (**Figure 32A**). Still, there was a trend towards a decreased frequency of CD4⁺ and CD8⁺ $\alpha 4\beta 7^+$ T cells in samples from Vedolizumab-treated versus untreated patients (CD4: 6,54 % versus 11,39 %, $p=0,49$; CD8: 8,18 % versus 18,17 %, $p=0,1592$).

In contrast to HIV-infected patients, where differences in the $\alpha 4\beta 7$ -frequency within the memory T-cell compartment of healthy versus HIV-infected individuals were detectable, the frequencies in the PBMC compartment of UC patients were generally comparable to samples from healthy volunteers (**Figure 32B**). However, there was a significant decrease in the frequency of $\alpha 4\beta 7^+$ naïve CD4⁺ T cells when comparing the following patient groups: baseline samples from patients with UC versus samples after treatment with Vedolizumab (UC untreated 13,98 %, UC + VDZ 2,93 %, $p=0,0144$) and samples from healthy controls versus samples after treatment with Vedolizumab (healthy: 9,65 %, UC + VDZ 2,93 %, $p=0,0225$).

The suggested mode of action of Vedolizumab is that it prevents $\alpha 4\beta 7^+$ T cells from migrating to GIT by inhibiting the required binding of T cells to MAdCAM-1. A recent report has also demonstrated an attenuation of lymphoid aggregates in the terminal ileum after Vedolizumab therapy²¹¹. Since only minor differences were detected in PBMC samples from patients treated with Vedolizumab, mononuclear cells from the sigmoid colon (lamina propria lymphocytes, LPL) were also examined. Samples were taken during routine colonoscopies and directly processed as described in section 2.3.2. **Figure 33** shows the frequency of $\alpha 4\beta 7^+$ T cells within total CD4⁺ and CD8⁺ T cells as well as within CD4⁺ naïve and memory T cells.

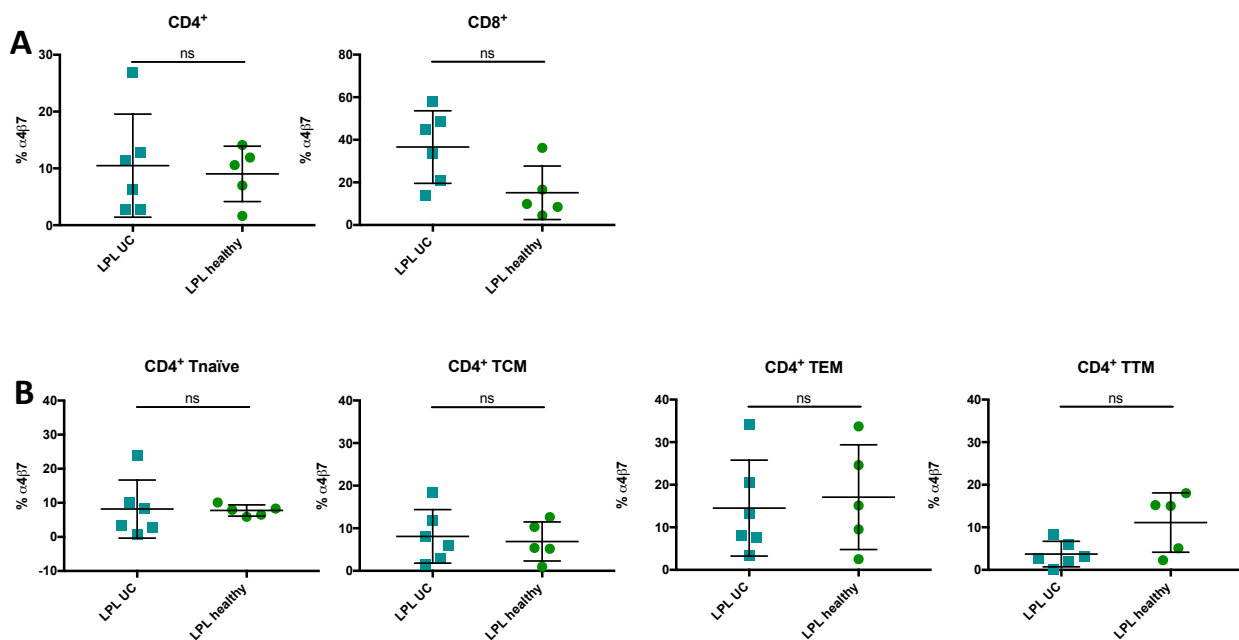


Figure 33: Frequency of $\alpha 4\beta 7^+$ cells does not differ between naïve and memory CD4⁺ T-cell populations of gut derived lymphocytes of healthy individuals and patients with UC. Frequencies of $\alpha 4\beta 7^+$ CD4⁺ T cells isolated from the sigmoid colon lamina propria of patients with ulcerative colitis (LPL UC, light blue) and healthy individuals (LPL healthy, green). **(A)** Frequency of total $\alpha 4\beta 7^+$ CD4⁺ and CD8⁺ T cells. **(B)** Frequency of $\alpha 4\beta 7^+$ within CD4⁺ naïve and memory T cells. LPL were isolated from gut biopsies overnight and stained directly. Samples were stained with an $\alpha 4$ -specific antibody (clone 7.2R) plus a $\beta 7$ -specific antibody (clone FIB504). Data from 6 patients with UC and 5 healthy individuals presented as means +/- standard deviation. Ns ≥ 0.05 as calculated by Mann-Whitney test.

The highest frequency of $\alpha 4\beta 7^+$ cells was detected in total CD8⁺ T cells in samples from patients with UC (36,62 %; **Figure 33A**). In total CD4⁺ T cells, the frequency of $\alpha 4\beta 7^+$ was 10,49 % (LPL UC) and 9,05 % (LPL healthy). The frequency of $\alpha 4\beta 7^+$ cells within different LPL CD4⁺ T-cell subsets was

similar when comparing samples from patients with UC and healthy individuals, whereas the highest frequency was detected in the CD4⁺ TEM subset regardless of the disease status (**Figure 33B**). There were comparable frequencies of $\alpha 4\beta 7^+$ in naïve T cells (LPL UC: 8,17 %, LPL healthy: 7,75 %), TCM (LPL UC: 8,09 %, LPL healthy: 6,89 %), TEM (LPL UC: 14,51 %, LPL healthy: 17,08 %) and TTM (LPL UC: 3,72 %, LPL healthy: 11,11 %).

The same analysis was conducted with samples from lymph nodes (lymph node mononuclear cells, LNMC). The expected frequencies were rather low compared to GIT, since $\alpha 4\beta 7$ does not mediate homing to lymph nodes. Results are shown in **Figure 34**.

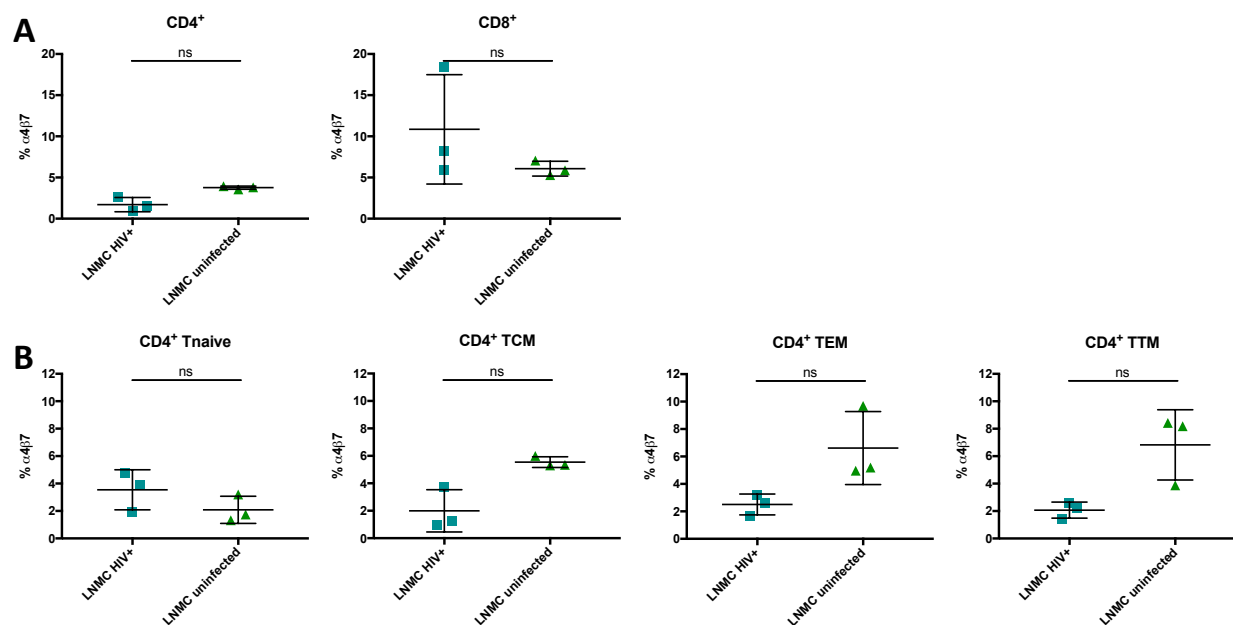


Figure 34: Frequency of $\alpha 4\beta 7^+$ cells does not differ between naïve and memory CD4⁺ T-cell populations of lymph node mononuclear cells from HIV-infected and uninfected individuals. Frequencies of $\alpha 4\beta 7^+$ CD4⁺ T cells isolated from lymph nodes of HIV-infected (LNMC HIV+, black) and HIV negative (LNMC uninfected, grey) individuals. **(A)** Frequency of total $\alpha 4\beta 7^+$ CD4⁺ and CD8⁺ T cells. **(B)** Frequency of $\alpha 4\beta 7^+$ within CD4⁺ naïve and memory T cells. Cryopreserved samples were thawed and directly stained with an $\alpha 4$ -specific antibody (clone 7.2R) plus a $\beta 7$ -specific antibody (clone FIB504). Data from 3 HIV-infected patients and 3 HIV negative individuals presented as means +/- standard deviation. $Ns \geq 0.05$ as calculated by Mann-Whitney test.

The frequency of $\alpha 4\beta 7^+$ cells was generally lower on LNMC than on LPL for all subsets studied regardless of the infection status. Of the CD4⁺ LNMC from HIV-negative controls, 3,77 % were $\alpha 4\beta 7^+$ (HIV-infected: 1,71 %; **Figure 34A**). Similarly to LPL, the frequency of $\alpha 4\beta 7^+$ in the CD8⁺ T-cell compartment was higher overall than it was in the CD4⁺ T-cell compartment (HIV negative: 6,07 %, HIV-infected: 10,85 %). In LNMC from uninfected individuals, the following frequencies of CD4⁺ $\alpha 4\beta 7^+$ cells were measured: 2,09 % in naïve T cells, 5,54 % in TCM, 6,61 % in TEM and 6,83 % in TTM (HIV: 3,54 % $\alpha 4\beta 7$ in naïve T cells, 1,99 % in TCM, 2,5 % in TEM and 2,07 % in TTM; **Figure 34B**).

In sum, the frequencies of $\alpha 4\beta 7$ in the tissues studied (lymph nodes, gut) were comparable to those measured in peripheral blood. No significant differences were found between samples from patients with UC versus healthy individuals or HIV-infected patients versus HIV-negative people. The last step was to evaluate possible correlations between $\alpha 4\beta 7$ expression and the following classic markers of HIV infection: systemic activation, depletion of CD4⁺ T cells and plasma viral load.

The expression of high levels of $\beta 7$ on CD4⁺ T cells has been linked to a greater susceptibility to HIV infection and a faster disease progression¹⁷⁸. For this reason, the frequency of $\alpha 4\beta 7^+$ CD4⁺ T cells was plotted against the frequency of activated CD8⁺ T cells, CD4⁺ T-cell counts and plasma viral load (**Figure 35**).

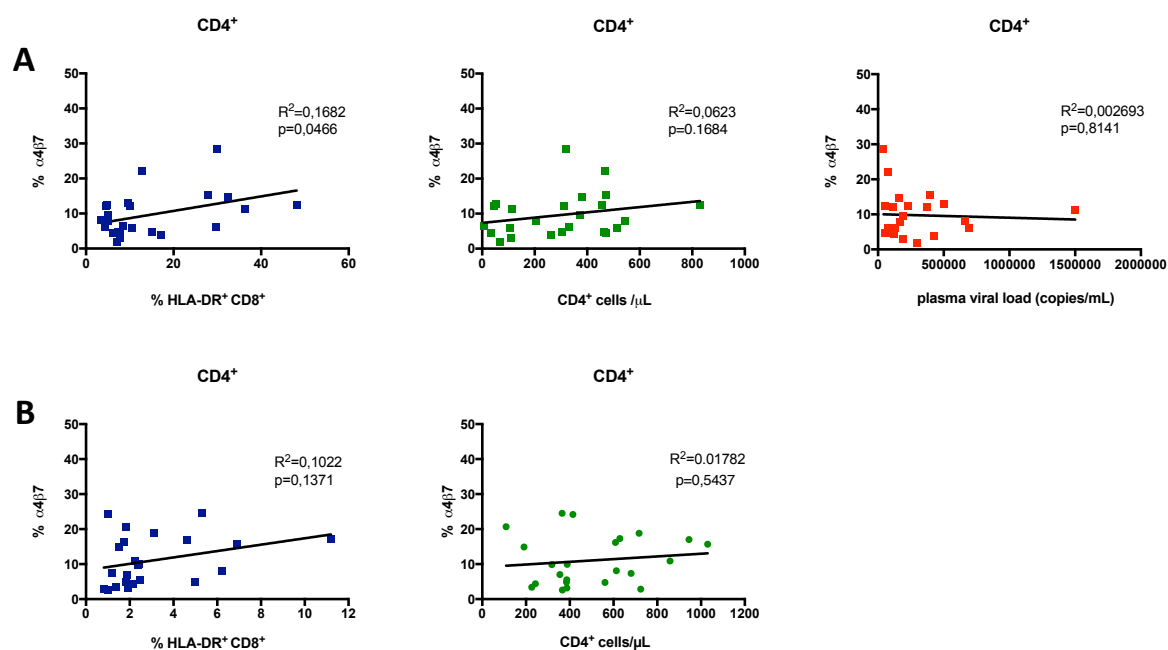


Figure 35: $\alpha 4\beta 7$ is not correlated with activation, CD4⁺ T-cell count or plasma viral load in HIV. General activation is represented by HLA-DR⁺ CD8⁺ T cells. Representative plots are shown which depict total CD4⁺ T cells. (A) viremic patients, (B) patients on ART. Data from 24 viremic individuals and 23 patients on ART. Pearson correlation and Spearman rank correlation coefficient were applied for bivariate correlation analysis. R^2 denotes the nonparametric Spearman correlation coefficient.

Although previous studies have shown that HIV preferentially infects and deletes $\alpha 4\beta 7^+$ CD4⁺ T cells, no correlation between the plasma viral load and the frequency of $\alpha 4\beta 7^+$ CD4⁺ T cells was observed in samples from viremic patients (**Figure 35A**) or patients on ART (**Figure 35B**), possibly due to the limited sample size.

3.2.9 Longitudinal study of $\alpha 4\beta 7$ expression by CD4⁺ T cells from an HIV-infected patient with UC treated with Vedolizumab

An HIV-infected patient diagnosed with UC who had been on ART for 17 years was seen at the UKE outpatient centre for inflammatory bowel disease. HIV infection and IBD share common features: T_H17 cells in the gut that are critical for the maintenance of gut barrier functions are depleted in both diseases, leading to an increased permeability of the gut mucosa^{212,213}. As a consequence of this impaired barrier, microbial components from the gut lumen such as LPS can enter the bloodstream and trigger systemic inflammation (“leaky gut” phenomenon)²¹⁴. Another factor is microbial dysbiosis in the intestine, which further intensifies immune activation and inflammation^{215,216}. Although gastrointestinal disorders such as diarrhoea and abdominal pain are common symptoms experienced by HIV-infected patients, the coexistence of both HIV infection and IBD is rare²¹⁷.

Management of IBD in patients with concurrent HIV Infection is more difficult than in patients without comorbidity. For example, certain anti-inflammatory drugs that target interleukins must be used with restraint, since decreased levels of certain interleukins have been shown to contribute to HIV disease progression and susceptibility to opportunistic infections²¹⁸. To date, few studies have described the effect of Vedolizumab treatment in patients with IBD and concomitant HIV infection with regard to $\alpha 4\beta 7$ kinetics in peripheral blood.

The patient seen at the UKE was on a regimen of Tenofovir Alafenamid/Emtricitabin and Dolutegravir, resulting in well-controlled HIV viremia. PBMC samples before and during treatment with Vedolizumab (at weeks 4, 14, 32, 48, 72 and 80 after treatment initiation) were collected and analysed.

The viral load remained below the detectable threshold and CD4⁺ T-cell counts ranged from 749 - 1239 cells/ μ L throughout the study. Vedolizumab was administered safely and without any serious adverse events and the patient reported an amelioration of symptoms during therapy which could be related both to clinical parameters (e.g. CRP values) and macroscopic and microscopic findings from the endoscopic examination.

Figure 36 shows the frequency of $\alpha 4\beta 7$ in the $CD4^+$ and $CD8^+$ T-cell compartment over the course of the study.

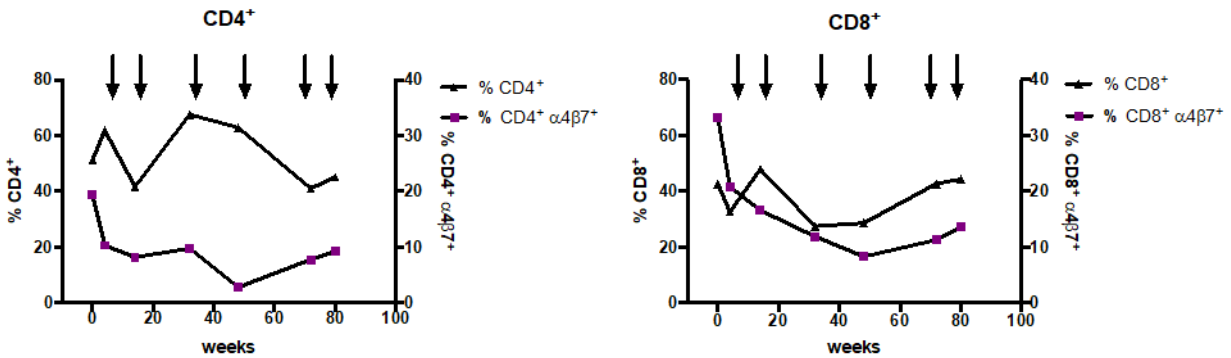


Figure 36: Longitudinal study of the frequencies of $\alpha 4\beta 7^+$ $CD4^+$ and $CD8^+$ T cells from an HIV patient with concomitant UC. Percentages of the respective population are plotted on the left Y-axis, the frequency of $\alpha 4\beta 7^+$ cells within the respective population is plotted on the right Y-axis. Cryopreserved samples were thawed and directly stained with an $\alpha 4$ -specific antibody (clone 7.2R) plus a $\beta 7$ -specific antibody (clone FIB504). Arrows indicate the times at which Vedolizumab was infused.

The frequencies of both $CD4^+$ and $CD8^+$ T cells fluctuated over time. Nevertheless, a steady decrease was observed in the frequency of both $CD4^+$ and $CD8^+$ $\alpha 4\beta 7^+$ T cells until week 48 in both compartments ($CD4^+$: 19,3 % at baseline to 2,82 % (week 48); $CD8^+$: 33,2 % at baseline to 8,33 % (week 48)). Notably, levels of $CD8^+$ $\alpha 4\beta 7^+$ T cells were generally higher than frequencies of $CD4^+$ $\alpha 4\beta 7^+$ T cells (mean of all timepoints 16,53 % of $CD8^+$ versus 9,63 % of $CD4^+$).

Next, frequencies of naïve and memory $\alpha 4\beta 7^+$ CD4⁺ T cells over the course of therapy were examined (**Figure 37**).

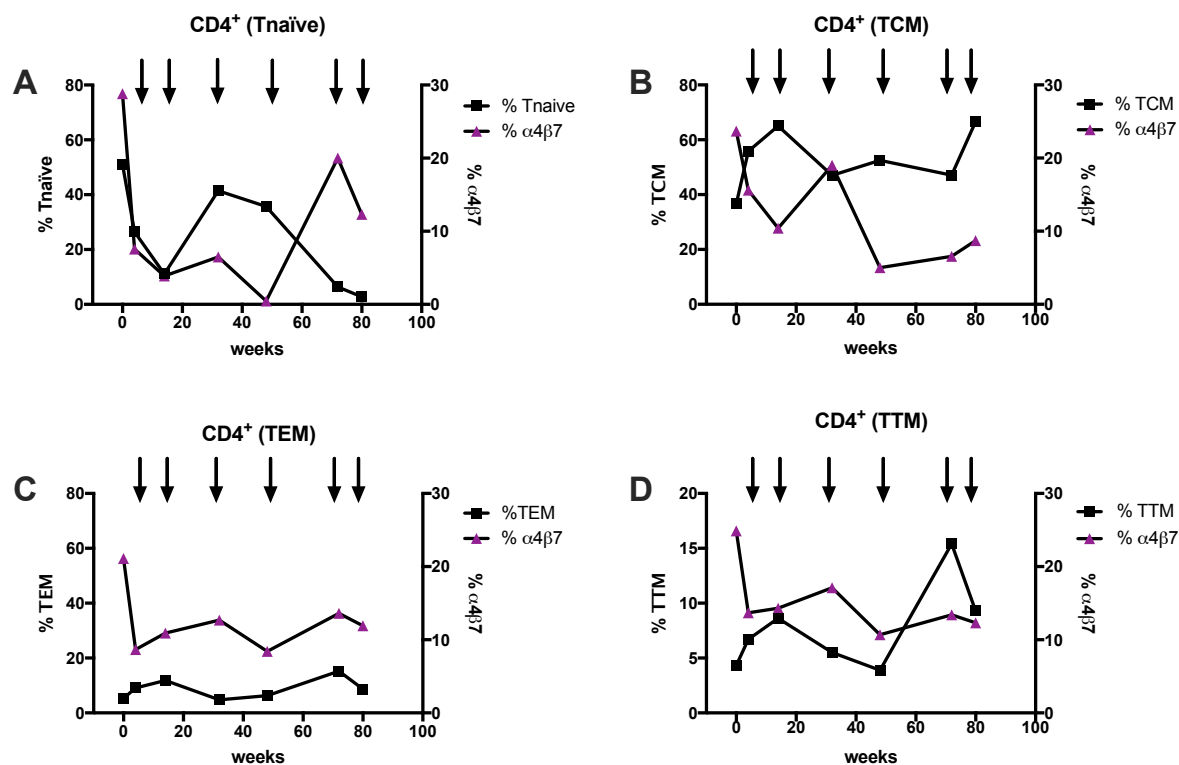


Figure 37: Frequencies of $\alpha 4\beta 7^+$ CD4⁺ T cells within different CD4⁺ T-cell compartments over the course of therapy. Percentages of the respective population are plotted on the left Y-axis, the frequency of $\alpha 4\beta 7^+$ cells within the respective population is plotted on the right Y-axis. Cryopreserved samples were thawed and directly stained with an $\alpha 4$ -specific antibody (clone 7.2R) plus a $\beta 7$ -specific antibody (clone FIB504). Arrows indicate the times at which Vedolizumab was infused.

Similar to the results from samples from HIV-uninfected UC patients, the frequency of $\alpha 4\beta 7^+$ naïve CD4⁺ T cells decreased under Vedolizumab therapy until week 48.

The frequency of naïve CD4⁺ T cells decreased initially (weeks 0-14), increased temporarily (weeks 14-72) and drastically decreased again thereafter (from 35,7 % (week 48) to 6,34 % (week 72) and 2,78 % (week 80); **Figure 37A**). The same trend was observed in the frequency of $\alpha 4\beta 7^+$ naïve CD4⁺ T cells, whose frequency increased from 0,45 % to 20 % and then decreased to 12,3 % (week 80). It was hypothesized that the patient could have developed endogenous antibodies against Vedolizumab (see also Discussion).

The frequency of CD4⁺ TCM remained relatively stable during treatment (**Figure 37B**). The frequency of $\alpha 4\beta 7^+$ TCM cells steadily decreased except for one peak at week 32, where it rose from 10,4 % to 19 %. The frequencies of TEM and $\alpha 4\beta 7^+$ TEM proceeded analogously during the follow-up. Disregarding a drop from 21,1 % to 8,66 % initially, and another from 12,7 % to 8,4 % at week 48, the frequencies of TEM and $\alpha 4\beta 7^+$ TEM remained comparable (**Figure 37C**). The frequency of $\alpha 4\beta 7^+$ TTM cells was generally lower (mean 7,68 %) than the other subsets and remained low after an initial drop, whereas the frequency of TTM showed a sharp increase between week 48 (3,89 %) and week 72 (15,4 %), where it peaked (**Figure 37D**).

The chemokine receptor CCR9 also mediates leukocyte trafficking to the GIT via binding to the C-C motif chemokine ligand 25 (CCL25)²¹⁹. For this reason, an analysis was conducted to see whether the frequency of CCR9⁺ CD4⁺ T cells would increase during therapy to counteract for the lack of functional $\alpha 4\beta 7^+$ CD4⁺ T cells (**Figure 38**).

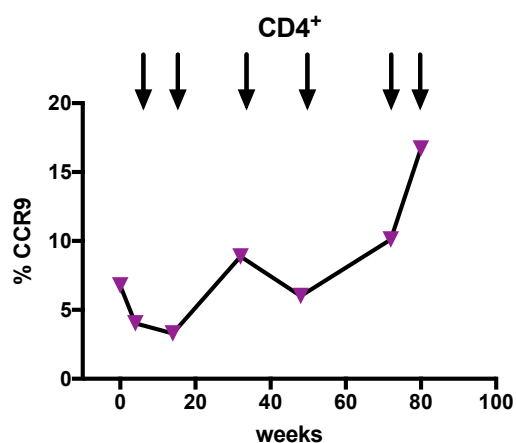


Figure 38: Changes in the frequency of CCR9⁺ CD4⁺ T cells during Vedolizumab therapy. Cryopreserved samples were thawed and directly stained with an $\alpha 4$ -specific antibody (clone 7.2R) plus a $\beta 7$ -specific antibody (clone FIB504). Arrows indicate the times at which Vedolizumab was infused.

As shown, the frequency of CCR9⁺ CD4⁺ T cells did indeed increase continuously during therapy (from 4,02 % at week 4 to 16,7 % at week 80).

Next, an analysis of HLA-DR⁺ T-cell frequencies was carried out. The reasons for this were twofold: Firstly, HIV infection coincides with a general activation of the immune system. Secondly, the formation of endogenous antibodies towards the end of the follow-up period was suspected, which could have also resulted in activation (**Figure 39**).

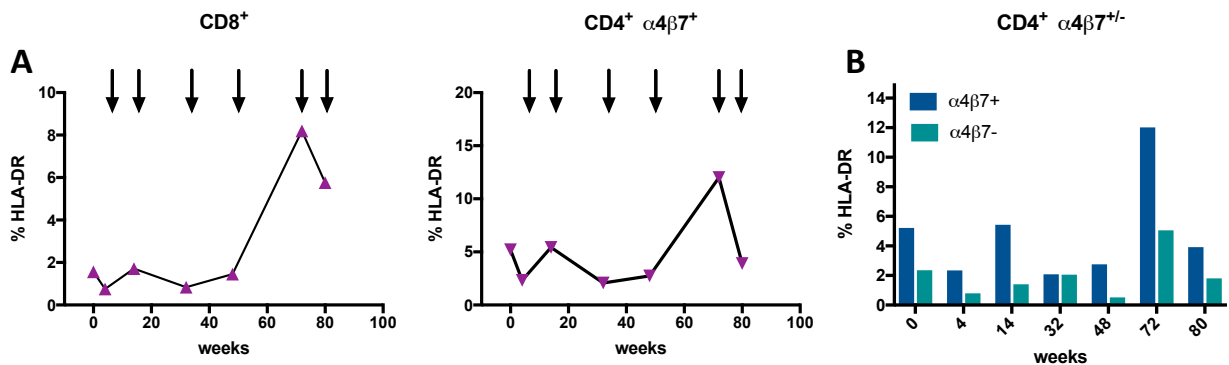


Figure 39: Activation as indicated by HLA-DR expression of CD8⁺ and CD4⁺ α4β7^{+/-} T cells. (A) Systemic activation indicated by HLA-DR⁺ CD8⁺ T cells. **(B)** Activation status of CD4⁺ α4β7⁺ T cells. **(C)** Activation of CD4⁺ α4β7⁺ versus α4β7⁻ T cells. Cryopreserved samples were thawed and directly stained with an α4-specific antibody (clone 7.2R) plus a β7-specific antibody (clone FIB504). Arrows indicate the times at which Vedolizumab was infused.

A clear peak could be measured at week 72 both in the CD8⁺ T-cell compartment and amongst CD4⁺ α4β7⁺ T cells (8,2 % and 12 %, respectively; **Figure 39A**). Interestingly, the mean frequency of HLA-DR⁺ α4β7⁺ CD4⁺ T cells was higher (4,8 %) than the mean frequency of HLA-DR⁺ CD8⁺ T cells (2,9 %). When comparing α4β7⁺ versus α4β7⁻ CD4⁺ T cells, a higher proportion of α4β7⁺ cells were activated (about a two-fold increase) than their α4β7⁻ counterparts at all measured timepoints except week 32, where the frequencies of HLA-DR⁺ α4β7⁺ and HLA-DR⁺ α4β7⁻ were equal (**Figure 39B**).

Another marker for short term activation, but also exhaustion, is PD-1. Changes in the frequency of this subset of cells can be seen in **Figure 40**.

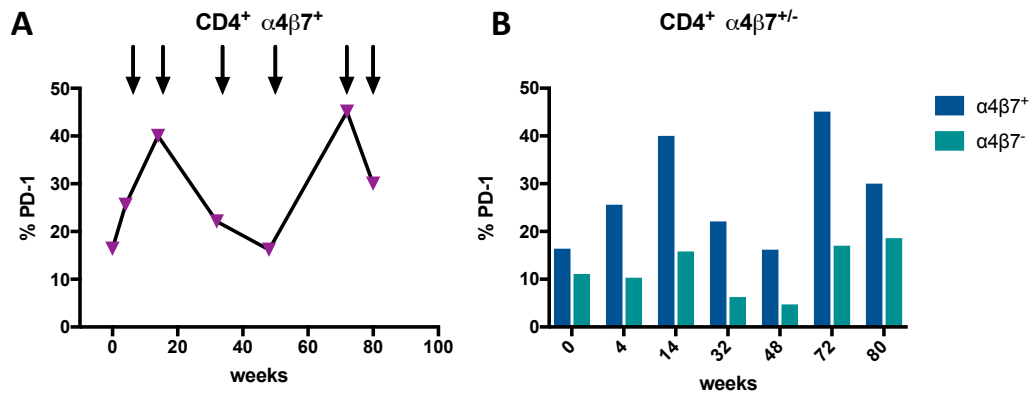


Figure 40: Activation/exhaustion of CD4⁺ α4β7⁺ T cells as indicated by PD-1 expression. (A) Frequency of PD-1⁺ CD4⁺ α4β7⁺ T cells. **(B)** Frequency of PD-1⁺ CD4⁺ α4β7⁺ versus α4β7⁻ T cells. Cryopreserved samples were thawed and directly stained with an α4-specific antibody (clone 7.2R) plus a β7-specific antibody (clone FIB504). Arrows indicate the times at which Vedolizumab was infused.

Similarly to the frequency of HLA-DR⁺ CD4⁺ α4β7⁺ T cells, there was a peak in the frequency of PD-1⁺ CD4⁺ α4β7⁺ T cells at week 72 (45,1 %) and also at week 14 (40 %; **Figure40A**). When compared to α4β7⁻ CD4⁺ T cells, the frequency of PD-1⁺ cells was higher in the α4β7⁺ fraction at all measured timepoints (**Figure40B**).

4 Discussion

To date, the lack of a methodology to reliably and completely trace all latently HIV-infected cells in the blood and various tissues of people infected with HIV has stood in the way of finding a cure. Whilst actively infected cells can be cleared by the immune system or die due to cytopathic effects, latently infected cells persist over long periods. However, there is no sole marker or a set of markers that can distinguish infected from non-infected cells with high sensitivity and specificity. Moreover, eradication efforts are hampered by the fact that relevant viral reservoirs are located in particularly secluded immunological niches.

Therefore, new ways to reliably trace latently HIV-infected cells in the blood and different tissues are currently being sought. Additionally, different approaches that trigger viral replication in latently infected cells that can be subsequently recognized by the immune system have been tried (shock and kill approach), but have so far led to limited success in patients^{151–153}. Another strategy that has recently been taken to clinical trials in humans is to intervene early to minimize the initial formation of the latent reservoir in the GALT during primary infection. This is achieved by blocking integrin-mediated homing of peripheral effector T cells or to effectively clamp down continuous infection of newly gut-homed CD4⁺ T cells.

In this thesis, the expression patterns of the two following molecules have been examined: **CD32** which is an Fc γ receptor and suggested marker of resting, latently infected CD4⁺ T cells and integrin **$\alpha 4\beta 7$** on T cells which facilitates gut homing. The main findings are as follows:

Contrary to data published by the initial study by Descours *et al.*, data generated in this thesis and other studies show that expression of CD32 does not exclusively mark resting CD4⁺ T cells and is dependent on the activation status of the cell regardless of patients' disease status⁶. In particular, the data generated here showed no correlation between total HIV-DNA and frequency of CD32⁺ CD4⁺ T cells¹⁹⁷. Also, no correlation between CD32⁺ T cells and CD4⁺ T-cell count or HIV plasma viral load could be seen. However, the previously reported increased susceptibility to HIV infection due to a higher frequency of cells expressing the HIV co-receptors CXCR4 and CCR5 among CD32⁺ versus CD32⁻ CD4⁺ T cells was indirectly confirmed in this thesis (see section 3.2.7).

In the experiments conducted for this thesis, only minor variations in the frequency of $\alpha 4\beta 7^+$ among total $CD4^+$ T cells were detected in peripheral blood and the tissues studied. This was the case irrespective of disease or treatment (Vedolizumab) status¹⁹⁸. Vedolizumab is an antibody used in the treatment of inflammatory bowel disease, but has been proposed as a concomitant drug during primary HIV infection because of its potential to limit the generation of latently infected cells by impeding the homing of T cells to the gut. The administration of Vedolizumab caused only minor changes in the frequency of peripheral $\alpha 4\beta 7^+$ $CD4^+$ memory T cells but caused marked alterations in the frequency of naïve $CD4^+$ T cells in patients with UC (see section 3.2.8). In contrast, a loss of $\alpha 4\beta 7^+$ memory T cells was detected in samples from HIV-infected individuals which did not recover under ART. Peripheral $\alpha 4\beta 7^+$ $CD4^+$ T cells of healthy individuals and patients with UC were more activated and were more frequently $CCR5^+$ than their $\alpha 4\beta 7^-$ counterparts. The measured frequencies of $\alpha 4\beta 7^+$ T cells in the gut did not significantly differ between patients with UC and healthy individuals.

The following discussion is separated into two sections: The first section focuses on the Fc γ receptor CD32, the second part discusses the findings made in the context of integrin $\alpha 4\beta 7$.

CD32, a new potential reservoir marker

In the last few years, markers that distinguish latently HIV-infected cells from productively infected and uninfected cells have been investigated intensively²²⁰. Descours *et al.* reported that the Fc γ receptor CD32a marked resting CD4⁺ T cells that were highly enriched in replication-competent virus⁶. The group studied the gene expression signature of resting, latently infected cells that contained a viral reporter construct, followed by an *in vitro* screening of the respective surface markers. Finally, samples from HIV-infected patients on ART were examined to confirm results. From their results, the researchers proposed CD32a as a marker of latently infected, resting cells with undetectable expression on bystander cells⁶.

Contrary to the results of the aforementioned study⁶, the data collected in this thesis imply a strong link between cellular activation and CD32 expression on T cells¹⁹⁷. This finding is in line with other publications^{221,222}. Possible reasons for this discrepancy are given in the following discussion. Regardless of disease status, the frequency of HLA-DR⁺ cells was higher in the CD32⁺ than the CD32⁻ CD4⁺ T-cell population. Also, the frequency of CD32⁺ CD4⁺ T cells correlated with general immune activation (frequency of HLA-DR⁺ CD8⁺ T cells). However, the frequency of CD32⁺ CD4⁺ T cells did not directly correlate with the frequency of HLA-DR⁺ in the same subset (i.e. there was no correlation between the frequencies of HLA-DR⁺ TEM and CD32⁺ TEM). This suggests that CD32 is not a marker of T-cell activation in the classical sense.

Notably, the frequency of CD32⁺ cells was significantly higher in all memory subpopulations in samples from viremic compared to aviremic patients on ART. This observation strongly suggests that actively infected cells can also be CD32⁺ or that under ART, latently infected cells migrate to tissue sites and can no longer be detected in PBMC.

Both HIV co-receptors CXCR4 and CCR5 were significantly up-regulated among CD32⁺ CD4⁺ T cells compared to CD32⁻ CD4⁺ T cells in all groups studied, indicating a greater susceptibility to HIV infection. These results are in line with those from previous publications^{201,222}. The higher activation status of CD32⁺ CD4⁺ T versus their CD32⁻ counterparts may be a contributory factor to this vulnerability.

In this thesis, cells from a small patient cohort with primary HIV infection were analysed with respect to their total HIV-DNA (i.e. all forms of cellular HIV-DNA including stably integrated proviruses and unintegrated forms; not to be confused with the plasma viral load) in addition to phenotypical analyses. No significant correlation between total HIV-DNA and frequency of CD32⁺ CD4⁺ T cells was detected. Furthermore, no correlation between the frequency of CD32⁺ cells in any CD4⁺ T-cell population and the CD4⁺ T-cell count or HIV plasma viral load could be defined. These findings are in line with results from Thornhill *et al.* who found that HIV-DNA was enriched in CD32⁺ versus CD32⁻ CD4⁺ T cells but did not detect a direct correlation between integrated HIV-DNA or cell-associated HIV-RNA in CD4⁺ T cells and percentage of CD32⁺ CD4⁺ T cells in ART-treated or therapy naïve patients²²³. Finally, in this thesis, a significant number of CD32⁺ CD4⁺ T cells were measured in samples from healthy individuals, which conflicts with the statement by Descours and colleagues that CD32(a) was not expressed on uninfected bystander cells. Several other groups aimed to verify the results of the initial study by Descours *et al.* Since the original publication in March 2017, various publications have dealt with the potential role of CD32(a) as a marker of latently infected cells in HIV infection. The results of these studies are summarized in **Table 10**.

Table 10: Overview of the literature on CD32(a). The outcomes summarised focus on data obtained from the study cohort(s), leaving out some results generated *in vitro*. The landmark study is marked in bold.

Evidence in favour of CD32(a) as a reservoir marker

Publication Author, year	Cohort; type of sample	Results/Conclusion
Iglesias-Ussel M <i>et al.</i> , 2013. ²²⁴	6 HIV-infected aviremic patients on ART; PBMC	CD32 gene transcripts were upregulated in latently infected versus uninfected CD4 ⁺ T cells generated <i>in vitro</i>
Descours B <i>et al.</i>, 2017.⁶	12 HIV-infected aviremic patients on ART; PBMC	CD32 ⁺ CD4 ⁺ T cells were highly enriched in inducible replication-competent proviruses
Noto A <i>et al.</i> , 2018. ²⁰¹	19 HIV-infected aviremic patients on ART, 9 untreated, viremic patients; LNMC	CD32 ⁺ PD-1 ⁺ CD4 ⁺ T cells were significantly enriched in cell-associated HIV-RNA compared to CD32 ⁻ PD-1 ⁻ CD4 ⁺ T cells
Vásquez JJ <i>et al.</i> , 2019. ²²⁵	4 HIV-infected patients on ART, 1 untreated, viremic patient, 1 aviremic HIV controller; rectal and/or ileal biopsies	Higher proportion of HIV-RNA ⁺ cells co-expressed CD32 ⁻ RNA in ART-suppressed individuals than in those with viremia
Darcis G <i>et al.</i> , 2020. ²²⁶	55 HIV-infected aviremic patients on ART; PBMC	-Frequencies of CD32 ⁺ CD4 ⁺ T cells correlated with HIV-DNA loads in PBMC -High enrichment for HIV-DNA in purified CD32 ⁺ CD4 ⁺ T cells from ART-treated patients

Table 10: Overview of the literature on CD32(a).**Evidence against a role of CD32(a) as reservoir marker**

Publication Author, year	Cohort; type of sample	Results/Conclusion
Grau-Expósito J <i>et al.</i> , 2017. ²²⁷	23 HIV-infected aviremic patients on ART, 18 untreated, viremic patients; PBMC	Ex vivo infection of unstimulated PBMC upregulated expression of CD32 indicating that productive HIV infection upregulates the expression of CD32
Abdel-Mohsen M <i>et al.</i> , 2018. ²²⁸	50 HIV-infected aviremic patients on ART, 20 viremic patients (6 on ART, 14 untreated); PBMC, LNMC, tonsil-derived cells	-CD32 ⁺ HIV-infected T cells had an activated phenotype and contained HIV-RNA, indicating active HIV transcription -The majority of HIV-DNA resided in CD32 ⁻ cells
Martin GE <i>et al.</i> , 2018. ²²²	39 HIV-infected aviremic patients on ART; PBMC	-CD32 expression on CD4 ⁺ T cells did not correlate with HIV-DNA or cell-associated HIV-RNA -CD32 might identify a population of HIV enriched cells but is not a dominant biomarker for HIV persistence
Badia R <i>et al.</i> , 2018. ²²¹	23 HIV-infected aviremic patients on ART; PBMC	-Majority of CD32 ⁺ /CD4 ⁺ T cells from HIV-infected individuals under antiretroviral treatment were HLA-DR ⁺ indicating CD32 is a marker of CD4 ⁺ T cell activation in HIV-infected individuals -No difference in provirus integration or replication-competent inducible latent HIV between CD32 ⁺ and CD32 ⁻ CD4 ⁺ T cells

Table 10: Overview of the literature on CD32(a).**Evidence against a role of CD32(a) as reservoir marker (continued)**

Publication Author, year	Cohort; type of sample	Results/Conclusion
Bertagnolli LN <i>et al.</i> , 2018. ²²⁹	20 HIV-infected aviremic patients on ART; PBMC	CD32 ⁺ CD4 ⁺ T cells did not contain the majority of intact proviruses
Pérez L <i>et al.</i> , 2018. ²³⁰	10 “individuals with chronic HIV infection” on ART (no information about viremia); PBMC	-No enrichment for HIV-DNA in CD32 ⁺ CD4 ⁺ T cells -CD32 expression associated previously with CD4 ⁺ T cells from adherent non-T-cells or cellular material bearing this marker
García M <i>et al.</i> , 2018. ²³¹	10 HIV-infected aviremic patients on ART, 10 untreated, viremic patients, 10 elite controllers; PBMC	-No significant correlation between the level of total HIV-DNA and the level of CD32 expression in resting memory CD4 ⁺ T cells and peripheral T _{FH} cells -Total HIV-DNA level was correlated with the expression of CD127 and CCR6
Dhummakupt A <i>et al.</i> , 2019. ²³²	5 perinatally HIV-infected adolescent aviremic patients on ART; PBMC	-60-fold enrichment in the absolute number of infected cells in the CD32 ⁻ population compared with CD32 ^{hi} cells -Exponential HIV replication occurred exclusively in CD32 ⁻ CD4 ⁺ T cells indicating that latent HIV reservoir resides mainly in CD32 ⁻ CD4 ⁺ T cells in virally suppressed, perinatally HIV-infected adolescents
Thornhill JP <i>et al.</i> , 2019. ²²³	18 HIV-infected aviremic patients on ART; rectal and ileal biopsies, PBMC	-In blood, CD32 ^{high} CD4 ⁺ T cells were mainly doublets of CD4 ⁺ T cells and B cells -GALT CD32 ^{high} doublets were primarily composed of T _{FH} cells; there was a significant correlation between rectal HIV-DNA levels and CD32 expression on T _{FH} cells (known to be preferentially infected by HIV)

Other researchers who tried to reproduce these experiments did not find an enrichment of HIV-DNA in the CD32^{high} or CD32^{intermediate} fraction of CD4⁺ T cells, leading them to suggest that the original results might have stemmed from formation of T cell–B cell or T cell–monocyte conjugates²³⁰.

Badia *et al.* and Abdel-Mohsen *et al.* concluded that, rather than marking latently infected cells, CD32(a) was associated with T-cell activation^{221,228}. There was no difference in CD32⁺ versus CD32⁻ CD4⁺ T cells regarding replication-competent inducible virus in aviremic individuals. Moreover, it was shown that CD32 on CD4⁺ T cells was upregulated upon stimulation *in vitro*²²¹. This is in line with earlier findings from Engelhard and colleagues who detected an activation-dependent expression of CD32 (and the Fcγ receptor CD16) on CD4⁺ and CD8⁺ T cells²³³.

There is a consensus that CD32⁺ CD4⁺ T cells can be infected with HIV, but that CD32 does not exclusively mark latently infected, quiescent cells but is mostly expressed on activated cells that contain transcriptionally active HIV^{222,228}. Abdel-Mohsen *et al.* detected HIV-RNA, indicating active HIV transcription²²⁸. The finding made in this thesis that CXCR4 and CCR5 were significantly upregulated in the CD32⁺ CD4⁺ T-cell population supports the hypothesis formed by Martin *et al.*, that preferential infection of these cells rather than an upregulation of the marker upon infection were the reason for the enrichment of HIV-DNA found in the CD32⁺ CD4⁺ T cells²²². In contrast, Grau-Expósito *et al.* described a two-fold upregulation of CD32 expression following infection of T cells with HIV *ex vivo*²²⁷. Hence, it can be assumed that CD32 is expressed on actively HIV-infected T cells as well, e.g. in the samples from viremic patients examined in this thesis.

Others have reported a potential role for CD32 in maintaining HIV infection. Together with PD-1, lymph node-derived CD32⁺ CD4⁺ T cells were shown to be enriched in HIV-DNA compared to PD-1⁻ CD32⁻ CD4⁺ T cells²⁰¹. Of note, CD32⁺ CD4⁺ T cells not expressing PD-1 were not enriched in proviral DNA/RNA. In the samples studied from viremic and patients on ART in this thesis, a trend towards a more exhausted phenotype (frequency of TIGIT⁺ and PD-1⁺ cells) of CD32⁺ versus CD32⁻ CD4⁺ T cells became evident, which is in line with other published data²²⁶. Possibly due to a small sample size, this trend did not reach statistical significance.

A link between HIV-DNA loads in PBMC and percentages of CD32⁺ CD4⁺ T cells was also demonstrated by Darcis and colleagues who applied a multi-step cell-sorting protocol to exclude T-B cell conjugates²²⁶. In addition, the group found that HIV-DNA (but not RNA) was highly enriched in purified CD32⁺ CD4⁺ T cells from patients on ART and that provirus in these purified cells could be activated *ex vivo* to produce virus. The researchers thus concluded that CD32⁺ CD4⁺ T cells were capable of supporting HIV transcriptional latency²²⁶.

Vásquez *et al.* reported a higher co-localization of HIV- and CD32-RNA in CD3⁺ gut-derived T cells from patients on ART than in samples from viremic patients and described a link between HIV transcriptional activity and the transcription of CD32-RNA²²⁵.

In 1997, McLain *et al.* described the expression of the Fcγ receptors CD64, CD32 and CD16 on a human cell line used in HIV research (C8166) and hypothesized that these were putative receptors for virus-IgG complexes²³⁴. These complexes are formed during the viremic phase of infection and are bound by Fcγ receptors on monocytes, macrophages and dendritic cells, eliciting an immune response^{189,235}. In this thesis, a higher frequency of CD8⁺ CD32⁺ than CD4⁺ CD32⁺ memory T cells from viremic HIV patients was measured (two- to three-fold increased). This could point towards CD32 having an antiviral role when expressed on T cells.

Later it was reported that polymorphisms in the Fcγ receptor genes are linked to the severity and susceptibility of certain infections and autoimmune diseases because they affect the binding affinity of the IgG Fc fragment¹⁹¹. HIV-infected men with the RR genotype for the gene encoding for CD32a were shown to have faster disease progression (e.g. to critical CD4⁺ T-cell counts) than those with an RH or HH genotype. Furthermore, an association between the His/His131 FcγRIIa genotype in infants and susceptibility to perinatal HIV infection was reported²³⁶.

Although it was assumed that the expression of CD32 was limited to myeloid and lymphoid B cells, Iglesias-Ussel and colleagues found an upregulation of CD32 in latently infected versus uninfected CD4⁺ T cells by using microarray analyses and confirmatory quantitative reverse transcriptase PCR as well as flow cytometry prior to the publication by Descours *et al.*²²⁴.

Viral DNA and RNA were not examined in this thesis; instead the focus was on a phenotypical analysis of the samples. Ideally, CD4⁺ CD32⁺ and CD4⁺ CD32⁻ T cells should have been sorted with a subsequent measurement of integrated viral DNA to assess their respective reservoir potential.

In this thesis, only a small patient cohort with primary HIV infection was analysed with respect to total HIV-DNA. In samples from HIV-infected patients with detectable viremia and aviremic patients on ART, no significant correlation between total HIV-DNA and frequency of CD32⁺ CD4⁺ T cells was detected.

A significant obstacle in studying latently HIV-infected cells in peripheral blood is their low frequency, making an analysis by flow cytometry difficult and imprecise. An analysis of CD32 on different, smaller CD4⁺ T cell subpopulations was not always feasible, since the number of events was too small. For example, only 0,28 % of total CD4⁺ T cells in samples from patients on ART were positive for CD32. To obtain higher numbers of CD4⁺ T cells, it is necessary to perform leukapheresis and subsequent enrichment of CD4⁺ T cells prior to analysis.

It should also be noted that the CD32-specific antibody used in the experiments in this thesis stains all three isoforms (CD32a, b and c). It could be the case that the background expression that was detected in samples from the healthy individuals had stemmed partly from other isoforms. This could explain the discrepancy between the results of this thesis and those reported in the original paper, which claimed that there was no expression of CD32 on uninfected bystander cells⁶.

In this thesis, cryopreserved cells were used in contrast to freshly isolated cells that were examined in the original study by Descours *et al.*. Since freeze-thawing does have a significant effect on some surface molecules, the effect on the frequency of CD32⁺ T cells was assessed in samples from healthy individuals. Although small differences were found, matched analysis showed no significant difference between the groups.

What is still largely unknown is the distribution and phenotype of CD32⁺ CD4⁺ T cells in tissues. Most research, including this thesis, has focussed on peripheral blood cells, but there is also the possibility that latently infected CD32⁺ CD4 T cells migrate to and reside in other tissues, such as the GALT. There is strong evidence that the vast majority of latently infected cells reside in lymphoid tissue, so higher frequencies of CD32⁺ CD4⁺ T cells were expected in LNMC than in PBMC^{87,237–239}. Surprisingly, the frequency of CD32⁺ T cells in LNMC was lower in total, and in all CD4⁺ T-cell subsets studied in this thesis, than in the respective fractions of PBMC. One reason for this might be that receptor signatures in circulating and tissue-resident cells differ. If that were

true, eradication of latently infected cells would be even more complex, since different strategies to target circulating and tissue-resident cells would be needed.

To conclude, there is proven evidence that CD32 on T cells is associated with HIV infection. Cells that are actively or latently HIV-infected have been shown to carry CD32(a) on their surface, either due to upregulation upon infection or increased susceptibility to infection. An obstacle to drug development which needs to be considered is that numerous other cells (such as monocytes and B cells) express CD32 as well. Furthermore, significant numbers of CD4⁺ T cells from healthy, uninfected donors express CD32. Nevertheless, this thesis along with findings made by other groups, has emphasised the expression of CD32(a) is strongly associated with cellular activation, independently of the disease status of the individual.

The integrin $\alpha 4\beta 7$ expression pattern of memory T-cell subsets in HIV infection and ulcerative colitis

One elusive goal of HIV treatment is to accomplish a sterilizing cure by targeting and eradicating all infected cells from the body. An alternative aim is to minimize the pool of latently infected cells that likely contributes to the continuous inflammation and associated comorbidities, thereby allowing viral suppression without the need of daily ART²⁴⁰. In order to achieve this, it would be necessary to disrupt the reservoir of infected T cells in the gastrointestinal tract and to prevent their replenishment by gut-homing memory CD4⁺ T target cells.

The integrin $\alpha 4\beta 7$ which facilitates gut homing appears like an optimal target molecule that has been extensively researched in the context of HIV. An overview of the associated literature is given in **Table 11**.

Table 11: Overview of the literature on $\alpha 4\beta 7$. The outcomes summarised focus on data obtained from the study cohort(s), leaving out some results generated *in vitro*. The landmark study is marked in bold.

Evidence in favour of $\alpha 4\beta 7$ as target for intervention

Publication Author, year	Cohort; type of sample	Results/Conclusion
Arthos J <i>et al.</i> , 2008. ¹⁸⁰	PBMC from healthy donors; Serum from 2 HIV viremic patients	-HIV envelope protein gp120 bound to an activated form of $\alpha 4\beta 7$, mediated by a tripeptide in the V2 loop of gp120 (mimics structures presented by the natural ligands of $\alpha 4\beta 7$) -On CD4 ⁺ T cells, engagement of $\alpha 4\beta 7$ by gp120 resulted in rapid activation of LFA-1, the central integrin involved in establishment of virological synapses, which facilitate cell-to-cell spreading of HIV
Kader M <i>et al.</i> , 2009. ¹⁷⁹	8 Mamu*A01 ^{neg} rhesus macaques (infected with SIVmac251), 8 uninfected Mamu*A01 ^{neg} rhesus macaques; PBMC	- $\alpha 4\beta 7^{\text{hi}}$ CD4 ⁺ T cells were found to harbour most T _H 17 cells that were significantly depleted during acute SIV infection -Resting memory $\alpha 4\beta 7^{\text{hi}}$ CD4 ⁺ T cells in the blood were preferentially infected and depleted during acute SIV infection
Soler D <i>et al.</i> , 2009. ²⁴¹	Normal human tissue (38 different types, 3 donors per type, e.g. lymphoid, GI-derived), Whole blood of healthy individuals, Human B cell lymphoma line (expressing $\alpha 4\beta 7$ stably)	-The highest level of Vedolizumab bound to a subset (ca. 25%) of human peripheral blood memory CD4 ⁺ T lymphocytes (including gut-homing T _H 17 cells), did not bind to majority (ca. 60 %) of memory CD4 ⁺ T lymphocytes -Vedolizumab bound exclusively to $\alpha 4\beta 7$, not $\alpha 4\beta 1$ or $\alpha E\beta 7$ and selectively inhibited adhesion of $\alpha 4\beta 7$ to MAdCAM-1
Cicala C <i>et al.</i> , 2009. ¹⁸¹	Healthy donors (exact number missing); cervical cytobrush samples from 8 female sex workers; PBMC, CD4 ⁺ T cells from ascending, transverse, descending, sigmoid colon and rectum	- $\alpha 4\beta 7^{\text{high}}$ CD4 ⁺ T cells (enriched with metabolically active CD4 ⁺ T cells) were more susceptible to productive infection than CD4 ⁺ T cells - $\alpha 4\beta 7^{\text{high}}$ CD4 ⁺ T cells are CCR5 ^{high} and CXCR4 ^{low} ; on these cells, $\alpha 4\beta 7$ appeared in a complex with CD4 -Specific affinity of gp120 for $\alpha 4\beta 7$ provides a mechanism for HIV to target activated cells

Table 11: Overview of the literature on $\alpha 4\beta 7$.Evidence in favour of $\alpha 4\beta 7$ as target for intervention (continued)

Publication Author, year	Cohort; type of sample	Results/Conclusion
Byrareddy SN <i>et al.</i> , 2016. ¹⁸³	18 rhesus macaques (infected with SIVmac239- <i>nef-stop</i>)	Monkeys treated with the $\alpha 4\beta 7$ -specific antibody maintained low to undetectable viral loads and normal CD4 ⁺ T-cell counts in plasma and gastrointestinal tissues for more than 9 months, even after all treatment was withdrawn.
Guzzo C <i>et al.</i> , 2017. ¹⁸²	12 HIV-1 isolates, 19 acutely HIV-infected individuals (infected < 6 months), 14 chronically HIV-infected individuals (infected > 6 months), no information about ART status, 11 rhesus macaques infected with SIVmac251; PBMC, blood plasma	- $\alpha 4\beta 7$ was efficiently incorporated into the envelope of HIV-1 virions -Functional $\alpha 4\beta 7$ was present in circulating virions from HIV-infected patients and SIV-infected macaques -Incorporated $\alpha 4\beta 7$ was functionally active as it bound to MAdCAM-1, promoting HIV capture by and infection of MAdCAM-1-expressing cells -Selective and specific uptake of $\alpha 4\beta 7^+$ HIV-1 virions by high endothelial venules in the intestinal mucosa
Sivro A <i>et al.</i> , 2018. ¹⁷⁸	PBMC from 59 "high-risk" women who got infected with HIV during the study, 106 women from the same cohort who remained uninfected, PBMC and gut tissue from rhesus macaques infected with SIVmac251	-Pre-HIV infection frequencies of $\alpha 4\beta 7^+$ peripheral blood CD4 ⁺ T cells, independent of other T cell phenotypes and genital inflammation, were associated with increased rates of HIV acquisition -Pre-HIV $\alpha 4\beta 7^+$ CD4 ⁺ T cells predicted a higher set-point viral load and a greater than twofold increase in the rate of CD4 ⁺ T-cell decline
Uzzan M <i>et al.</i> , 2018. ²¹¹	12 healthy volunteers, 10 patients with HIV infection, aviremic on ART, 5 patients with mild inflammatory bowel disease and concomitant HIV infection, aviremic or low viremia on ART; LPL (terminal ileum, left colon), PBMC	-Anti $\alpha 4\beta 7$ therapy led to a significant and unexpected attenuation of lymphoid aggregates, most notably in the terminal ileum

Table 11: Overview of the literature on $\alpha 4\beta 7$.Evidence against $\alpha 4\beta 7$ as target for intervention

Publication Author, year	Cohort; type of sample	Results/Conclusion
Wyant T <i>et al.</i> , 2013. ²⁴²	$\alpha 4\beta 7$ -stably expressing human B-cell lymphoma cell line RPMI8866, 3 healthy donors; PBMC	-Vedolizumab failed to elicit cytotoxicity, lymphocyte activation, and cytokine production from memory T lymphocytes and did not interfere with the suppressive ability of regulatory T cells -Vedolizumab induced internalization of $\alpha 4\beta 7$; rapid re-expression with full functionality after Vedolizumab withdrawal
Zeissig S <i>et al.</i> , 2018. ²⁴³	17 patients with Crohn's disease, 21 patients with UC; PBMC, intraepithelial leukocytes and LPL from sigmoid colon	-Vedolizumab only had minor effects on intestinal T cell abundance, instead affected innate immunity and particularly intestinal macrophage populations -Vedolizumab did not affect the mucosal T-cell repertoire or leucocyte trafficking <i>in vivo</i>
Ling L <i>et al.</i> , 2019. ²⁴⁴	$\alpha 4\beta 7$ -expressing 293T cells, NSG-human peripheral blood lymphocytes mice; PBMC, LPL from small intestine	Vedolizumab neither prevented nor controlled HIV-1 _{SF162} infection both <i>in vitro</i> and in humanized mice
Abbink P <i>et al.</i> , 2019. ²⁴⁵	SIVmac251-infected rhesus macaques that initiated ART during either early acute infection (n=36) or late chronic infection (n=14); PBMC, LNMC, colorectal-derived cells	-In animals who were initiated on ART during either acute or chronic infection, anti- $\alpha 4\beta 7$ antibody infusion had no detectable effect on the viral reservoir or viral rebound after ART discontinuation -Anti- $\alpha 4\beta 7$ antibody administration did not provide therapeutic efficacy in the model of pathogenic SIVmac251 infection of rhesus macaques

Table 11: Overview of the literature on $\alpha 4\beta 7$.Evidence against $\alpha 4\beta 7$ as target for intervention (continued)

Publication Author, year	Cohort; type of sample	Results/Conclusion
Di Mascio M <i>et al.</i> , 2019. ²⁴⁶	22 SIVmac239- <i>nef-stop</i> -infected rhesus macaques negative for Mamu-A001, -B008 and -B017 alleles; lymph node and rectal biopsies, PBMC	-Levels of plasma viremia before the first antibody infusion and pre-infection levels of $\alpha 4\beta 7^{\text{hi}}$ CD4 ⁺ T cells correlated with levels of viral replication upon discontinuation of all treatments, but treatment with $\alpha 4\beta 7$ -specific antibody did not -Follow-up plasma viremia, peripheral blood CD4 ⁺ T-cell counts, and lymph node and rectal tissue viral load were not significantly different between $\alpha 4\beta 7$ -specific and control monoclonal antibody groups
Iwamoto N <i>et al.</i> , 2019. ²⁴⁷	30 SIVmac239- <i>nef-stop</i> -infected rhesus macaques negative for Mamu-A001, -B008 and -B017 alleles; Rectum and jejunum biopsies, PBMC	-Decreases in the representation of $\alpha 4\beta 7$ -expressing CD4 ⁺ and CD8 ⁺ T cells from PBMC, and a selective increase in $\alpha 4\beta 7$ -expressing T _H 17 cells -Lack of effect of $\alpha 4\beta 7$ -specific antibody on post-treatment viremia -No differences between groups in cell-associated viral load from gut biopsies at any time point -No delay in rebound viremia after cessation of ART
Sneller MC <i>et al.</i> , 2019. ²⁴⁸	19 HIV-infected aviremic individuals on ART	-Vedolizumab resulted in down-regulation of surface $\alpha 4\beta 7$ expression on CD4 ⁺ T lymphocytes -Only a single subject in the trial experienced prolonged suppression of plasma viremia after interruption of ART -No measurable impact on the size of the HIV reservoir as measured by HIV-DNA and cell-associated HIV-RNA in peripheral blood CD4 ⁺ T cells

Early studies have reported that the HIV envelope protein gp120 binds to and signals through $\alpha 4\beta 7$ ¹⁸⁰. The integrin forms a complex with the CD4 molecule on the cell surface and makes these cells highly susceptible to infection¹⁸¹. Incorporated into new virions, $\alpha 4\beta 7$ even facilitates homing of viral particles to the intestine, where a vast number of target cells are available. Nawaz *et al.* observed that MAdCAM-1 co-stimulation through $\alpha 4\beta 7$ promotes HIV replication by upregulation of CCR5 and cellular proliferation²⁴⁹.

Based on this data, a study in rhesus macaques was conducted¹⁸³. After being infected with SIV, the monkeys were injected with a therapeutic $\alpha 4\beta 7$ -specific antibody, prior to ART and subsequently antibody treatment being withdrawn. The humanized form of this antibody that restricts gut homing of memory T cells is already in use for the treatment of IBD²⁴¹. Strikingly, in the rhesus macaque study, viremia was controlled for over 50 weeks after treatment interruption and blood CD4⁺ T-cell counts were maintained.

Within this thesis, a phenotypical analysis of the expression of $\alpha 4\beta 7$ on CD4⁺ T cells in different anatomical compartments of patients with HIV was conducted, since data on the expression pattern was largely missing. PBMC, LPL and LNMC were studied regarding their surface expression of $\alpha 4\beta 7$ and for markers of exhaustion and activation status. Overall, only small differences between the cohort groups and changes under Vedolizumab therapy were found. No significant differences in the frequency of bulk $\alpha 4\beta 7^+$ CD4⁺ or $\alpha 4\beta 7^+$ CD8⁺ T cells could be detected in PBMC from patients with HIV and different clinical course. Yet, there was a marked decrease in $\alpha 4\beta 7^+$ CD4⁺ effector memory T cells in samples from viremic patients which did not recover under ART. This observation is in line with previously published data¹⁷⁸. Effector memory T cells in general are more activated than central memory and naïve T cells and thus are preferentially infected by HIV and depleted.

Indeed, by comparing $\alpha 4\beta 7^+$ and $\alpha 4\beta 7^-$ CD4⁺ T cells in this thesis, the measured frequency of HLA-DR⁺ cells was higher among $\alpha 4\beta 7^+$ than $\alpha 4\beta 7^-$ CD4⁺ T cells in PBMC from healthy donors and Vedolizumab-naïve patients with UC. In samples from HIV patients on ART, however, the frequency of HLA-DR⁺ cells was higher among $\alpha 4\beta 7^-$ CD4⁺ T cells. In samples from viremic individuals, the frequency of HLA-DR⁺ cells was generally higher overall than in samples from other groups, but differences between $\alpha 4\beta 7^+$ and $\alpha 4\beta 7^-$ CD4⁺ T cells did not reach significance. It

may be that the general immune activation in HIV infection obscures the differences between $\alpha 4\beta 7^+$ and $\alpha 4\beta 7^- CD4^+$ T cells that were observed in healthy individuals. Alternatively, the staining procedures applied to samples from patients with HIV and UC could have had an impact when comparing both groups. Notably, the samples from healthy individuals showed inverse results: whereas the frequency of HLA-DR⁺ cells was higher within $\alpha 4\beta 7^+$ CD4⁺ T cells of healthy individuals stained with the $\alpha 4$ -specific clone 7.2R in combination with a $\beta 7$ -specific antibody, samples from healthy controls stained with the $\alpha 4\beta 7$ -specific clone Act1 showed a decreased frequency of HLA-DR⁺ $\alpha 4\beta 7^+$ CD4⁺ T cells compared to $\alpha 4\beta 7^- CD4^+$ T cells. This is one of the reasons why the results from the two staining approaches were not compared side by side, but within each group instead.

In PBMC from healthy individuals and patients with UC, there was a higher frequency of the HIV co-receptor CCR5⁺ cells amongst $\alpha 4\beta 7^+$ compared to $\alpha 4\beta 7^- CD4^+$ T cells. CCR5 has been reported to be up-regulated upon binding to MAdCAM, which results in a significantly higher frequency of CCR5⁺ $\alpha 4\beta 7^+$ CD4⁺ T cells in the GIT, providing further viral target cells¹⁵⁹. Indeed, in this thesis, a significantly higher frequency of CCR5⁺ $\alpha 4\beta 7^+$ CD4⁺ T cells was found in LPL compared to PBMC samples from healthy individuals and patients with UC. Taken together, the detected higher frequency of activated cells and cells expressing the HIV co-receptor CXCR4 or CCR5 underline the previously reported susceptibility of $\alpha 4\beta 7^+$ CD4⁺ T cells to HIV infection.

The frequency of cells expressing PD-1, a regulator of T cell exhaustion, was higher amongst $\alpha 4\beta 7^+$ compared to $\alpha 4\beta 7^- CD4^+$ T cells in PBMC from healthy individuals and patients with UC, regardless of Vedolizumab therapy²⁵⁰. In HIV infection, cells that express high levels of PD-1 have been reported as a source of replication-competent virus in patients on ART, thus forming part of the latent reservoir^{3,201}. In this thesis, the frequency of PD-1⁺ PBMC from viremic patients was markedly higher among $\alpha 4\beta 7^+$ than $\alpha 4\beta 7^- CD4^+$ T cells, but this trend was not observed in PBMC from patients on ART. In addition, the frequency of PD-1⁺ $\alpha 4\beta 7^{+/-}$ CD4⁺ T cells was lower in this group. It could be that the PD-1⁺ cells die over time or that these cells migrate to (lymphoid) tissues, becoming undetectable in the blood.

To determine the effect of Vedolizumab therapy on the migration of CD4⁺ T-cell subsets to the gut, samples (PBMC and LPL) from patients with UC receiving this therapeutic antibody were examined. Whereas the frequencies of the studied memory subsets remained unchanged, a decrease in peripheral naïve $\alpha 4\beta 7^+$ CD4⁺ T cells was observed in samples from patients under Vedolizumab therapy. It could be that naïve cells are more prone to modification: under regular physiological conditions, IL-7 modifies the expression of $\alpha 4\beta 7$ and triggers the transition to its activated form on naïve cells²⁵¹. Also, the turnover of central memory cells is rather slow, meaning that it could take some time for this population to be affected by treatment with the therapeutic antibody.

The downregulation of $\alpha 4\beta 7$ seems to occur independently from the saturation of $\alpha 4\beta 7$ with Vedolizumab. In this work, it was observed that the immunofluorescent staining of samples from Vedolizumab-treated patients with an $\alpha 4\beta 7$ -specific antibody was not possible, indicating that most of the CD4⁺ T cells were fully saturated with Vedolizumab.

If it is in fact mainly naïve CD4⁺ T cells that are affected by Vedolizumab treatment, this could cause a problem with the successful treatment of HIV infection. If memory T cells are not affected by the therapy, then they could migrate to the gut regardless and become infected. This is in line with an observation made in the macaque study by Byrareddy *et al.*, in which, contrary to what would have been expected, the GIT was found repopulated with CD4⁺ T cells in Vedolizumab-treated animals¹⁸³. Hence, it could be that there is either an alternative homing mechanism or a different way that Vedolizumab works. Lord *et al.* suggested that it may not be a decreased number of cells infiltrating the GIT, but rather a replacement of pro-inflammatory cells with Tregs and/or T_H2 cells that mitigates the inflammation in patients with IBD²⁵². In the data generated here, a higher frequency of CCR9⁺ CD4⁺ T cells on Vedolizumab therapy was found. This finding is surprising, as CCR9 usually facilitates homing to the small intestine and not the colon. However, the samples came from patients with UC, in which an upregulation of the CCR9 ligand CCL25 has been demonstrated²⁵³. Hence, it could be that CCR9-facilitated homing does partly compensate for the blocked $\alpha 4\beta 7$ -mediated pathway under Vedolizumab therapy.

The use of therapeutic antibodies as long-term medication also has general drawbacks, one of them being the formation of neutralizing host antibodies (anti-drug antibodies). For Vedolizumab, this is seen in roughly one in five patients during induction therapy and in less than 5 % during maintenance therapy²⁰⁵. The HIV patient with UC that was longitudinally studied within this thesis has presumably formed anti-drug antibodies. Since the frequency of naïve T cells strongly decreased markedly during therapy even though there was no rebound in viremia, plasma samples were sent to a diagnostic laboratory where the concentration of therapeutic antibody was determined. The serum concentrations of Vedolizumab measured in two samples (week 72 and week 80) were far below the expected value, so it is assumed that antibodies indeed had developed, which would explain the increase in frequency of naïve $\alpha 4\beta 7^+ CD4^+$ T cells. Naïve $\alpha 4\beta 7^+ CD4^+$ T cells that were already saturated with Vedolizumab could have been killed after binding of host anti-drug antibodies by antibody-dependent cellular cytotoxicity (ADCC). This would also explain the drop in the frequency of naïve $CD4^+$ T cells.

Nevertheless, Vedolizumab has been evaluated as concomitant therapy in HIV-infected individuals based on the findings made in the macaque study¹⁸³. Here, results were controversial: Uzzan *et al.* conducted a study in humans to investigate the HIV viral reservoir in the gut²¹¹. There, Vedolizumab was administered to patients with mild IBD and concomitant HIV infection which led to an attenuation of lymphoid aggregates in the terminal ileum, supporting the suggested beneficial effect of Vedolizumab in the context of HIV infection. A phase II study with 16 HIV-infected patients on ART receiving either 300 or 150 mg of Vedolizumab reported a dose-dependent effect of Vedolizumab on the following measures: peak rebound plasma viremia, viral load doubling time and rebound time²⁵⁴. Still, viral rebound was observed in all participants by week six following ART withdrawal.

Other studies also led to conflicting results: Sneller *et al.* conducted a study of 20 HIV-infected patients with ART-controlled viremia²⁴⁸. The study design resembled that of the macaque study: first Vedolizumab was administered in combination with ART, then ART was stopped and finally Vedolizumab infusions were also stopped. As expected, the frequency of $\beta 7^+ CD4^+$ T cells declined during Vedolizumab therapy but returned to baseline levels after therapy was stopped. Five patients suppressed viremia for 26 weeks and one of them did not have to restart ART until week 46 after treatment interruption. Nonetheless, the researchers concluded that Vedolizumab

treatment was insufficient to achieve sustained suppression of viremia without ART because the results of the parameters studied were akin to those of the placebo control group²⁴⁸. Thornhill *et al.* studied samples from a patient with Crohn's disease who got infected with HIV and received Vedolizumab starting approximately ten weeks after diagnosis²⁵⁵. Although a marked decrease in $\beta 7^+$ CD4⁺ T cells was measured, the authors stated that Vedolizumab was unlikely to induce sustained viral remission, as the HIV-DNA in PBMC from this patient was higher than for any of the patients in the control cohort. The viral load in lymphoid tissue and gut LPL was also comparable to that of the control cohort. Zeissig and colleagues reported changes in the innate rather than the adaptive immune system in the gut of IBD patients after administration of Vedolizumab, which could be a reason for its limited efficacy in the treatment of HIV infection²⁴³. It should be noted, however, that the Vedolizumab therapy in these studies was not started immediately after patients had been diagnosed with HIV. Since the reservoir is known to be established early in infection, it could be that it had already been established before the therapy was started²⁵⁶.

One criticism of the study published by Byrareddy *et al.* is that the virus used to infect the animals was not fully virulent and carried a stop codon in the *nef* gene²⁵⁷. Di Mascio and colleagues infected 22 rhesus macaques with SIV in an attempt to reproduce results from the original study²⁴⁶. Sequencing the viral stock, they found a mutation in the stop codon in the *nef* gene, resulting in a truncated protein and a *nef*-negative phenotype (SIVmac239-*nef*-stop instead of wild-type SIVmac239). Although this mutation is repaired during the course of infection, it could still have an impact on viral replication and the hosts' immune responses. No differences in terms of follow-up viremia, CD4⁺ T-cell counts or viral load in lymph nodal and rectal tissue between antibody-treated animals and those that received a control antibody were observed²⁴⁶.

The data generated in this work further characterized the $\alpha 4\beta 7$ expression in healthy and HIV-infected individuals as well as patients with UC. Furthermore, it adds to the information needed for future studies investigating Vedolizumab as possible HIV cure strategy, but also has certain limitations. The ideal cohort would have evidently consisted of patients that were treated with Vedolizumab during primary HIV infection. In this case, a virologic assessment in order to determine possible impacts of the Vedolizumab treatment on the reservoir should have been

conducted. Another detriment of this work is the missing examination of $\alpha 4\beta 7$ on different other lymphocyte populations, such as Tregs, T_H17 cells, $\gamma\delta$ T cells or MAIT cells that are also likely to be affected by the treatment with Vedolizumab.

The greatest constraint is the small number of gut biopsies that could be obtained and that no LPL from HIV-infected patients could be studied. The biopsies were not obtained at standardized time points, but as add-ons from a real-world patient cohort during routine examinations. Also, only material from the sigmoid colon was examined, whereas material from other interesting immunological sites such as the ileum was lacking.

In the available LPL samples, no significant differences in the frequencies of $CD4^+ \alpha 4\beta 7^+$ naïve and memory T cells were found between healthy individuals versus those with UC. One reason for this could be the heterogeneity of the sampled patients, who were on different anti-inflammatory drug regimens and had different concomitant medical conditions (two patients were diagnosed with primary sclerosing cholangitis and one has a liver transplant). Also, matched blood and gut samples from patients receiving Vedolizumab were not available in sufficient numbers. This only allows autonomous snapshots of the two compartments. Even if higher frequencies of $\alpha 4\beta 7^+ CD4^+$ T cells had been measured after Vedolizumab-mediated blockade of the integrin, this could have only allowed limited conclusions as to whether a smaller number of cells migrated to the gut.

Lastly, the gating strategy used in this work is different from that used in previous studies, where $\alpha 4\beta 7^+$ cells were divided into populations showing high, low and intermediate expression¹⁷⁸. While Kelley *et al.* and others detected $\alpha 4\beta 7$ frequencies ranging from 15 to 40 %, only an average of 10 to 25 % $CD4^+ \alpha 4\beta 7^+$ T cells was detected in this thesis^{178,258}. This number corresponds to previously reported frequencies of $\alpha 4\beta 7^{\text{high}} CD4^+$ T cells^{178,258}. It was nevertheless decided not to refer to these cells as “high”, because the populations were less well defined in this work, making it difficult to classify cells into intermediate and high. Another factor that could have contributed to the lower frequency of cells detected in this thesis could be the suboptimal brightness of the secondary antibody (PE used e.g. by Sivro *et al.* versus BUV395 used in this work).

Overall, although comparable frequencies were measured using the two staining approaches (clone Act1 versus the combination of $\alpha 4$ -specific clone 7.2R and $\beta 7$ -specific antibody clone FIB504), the gating strategy applied in this thesis might have led to a smaller resolution and could be one of the reasons why few differences were found between the groups.

To conclude, while it has been demonstrated in several studies that $\alpha 4\beta 7$ is involved in the pathogenesis of HIV and SIV infection, current studies have refuted initially promising results that suggested antibody-mediated blockade of the integrin could sustain viral control after cessation of ART¹⁸³. The results of this thesis, together with other recent studies, suggest that mechanisms other than the blockade of the $\alpha 4\beta 7$ -mediated homing of T cells are responsible for the amelioration of symptoms in patients with IBD and the beneficial effects of Vedolizumab with respect to viral control that were previously reported.

5 Conclusion and Outlook

In order to develop a sterilizing or functional cure for HIV, latently infected CD4⁺ T cells that persist during infection, are highly stable over time and contain replication-competent provirus need to be identified. Since there is little to no viral gene expression in these cells, it is difficult for the immune system to recognise and eliminate them. Certain T-cell subsets, such as central memory T cells, have been suggested to be crucial in the formation of the stable viral reservoir of latently infected T cells¹³⁹. Yet, robust markers that enable discrimination between latently infected and uninfected cells are largely missing. In the last couple of years, a number of novel marker molecules that help to identify latently HIV-infected cells have been proposed²⁻⁶.

The aim of this thesis was to comprehensively characterize the expression pattern and potential role of two molecules (CD32(a) and $\alpha 4\beta 7$) that may be involved in the formation of the reservoir in CD4⁺ T-cell memory subsets in a cohort of HIV-infected individuals with different disease outcomes. It became apparent that CD32 expression of CD4⁺ T cells is dependent on the activation status of the cells and does not seem to mark resting, latently infected CD4⁺ T cells exclusively. These findings are in line with data published by other research groups^{221,228}.

It has been suggested that the amelioration of symptoms in IBD following Vedolizumab (an $\alpha 4\beta 7$ -specific therapeutic antibody) treatment is most likely due to an effect on innate immune cells rather than altered homing of T cells to the GIT²⁴³. Indeed, only minor changes in the frequency of $\alpha 4\beta 7^+$ CD4⁺ T cells in PBMC and LPL samples from patients with UC on Vedolizumab could be measured in this work.

Besides the usual problems associated with descriptive studies of real-life cohorts (e.g. availability of appropriate participants and collection of samples at non-standardized time points), restraints included donor heterogeneity in terms of differing medication schemes and concomitant diseases and the lack of tissue samples from the sigmoid colon and ileum of patients with UC and HIV infection.

One major shortcoming of this thesis is that the cells expressing the respective marker of interest were not sorted and examined via ddPCR to determine their (integrated) viral DNA. In the CD32 study, the frequency of CD32⁺ CD4⁺ T cells was too low for direct analysis from PBMC samples.

Instead, it would have been necessary to carry out leukaphereses to obtain enough cells for CD4⁺ T-cell enrichment and subsequent sort of the CD32⁺ T cells. Still, the results obtained from phenotypical analysis in this work demonstrate that CD32 is not an optimal marker of latently infected cells since there is significant background expression of this marker by CD4⁺ T cells in samples from uninfected donors, and an association with immune activation.

The assessment of $\alpha 4\beta 7^+$ CD4⁺ T cells regarding the integrated HIV-DNA is not vital for establishing their role in the pathogenesis of HIV infection. Although $\alpha 4\beta 7$ aids in the formation of the latent reservoir by trafficking activated effector cells to the GALT, it cannot be considered as a marker of latently infected cells. While CD4⁺ $\alpha 4\beta 7^{\text{high}}$ T cells are preferentially infected with HIV, the expression of the integrin is rapidly downregulated after migration to the gut. In addition, expression of $\alpha 4\beta 7$ is not specific to (latently) infected cells; it is also expressed on uninfected, gut-homing T lymphocytes.

Future experiments regarding the role of CD32(a) as potential reservoir marker should include samples from patients with other chronic viral infections such as Hepatitis B virus, to find out whether CD32(a) expression is a response towards viral infection *per se*. Also, it would be worthwhile to study CD32(a) expression on peripheral CD4⁺ T cells longitudinally, to determine kinetics during primary HIV infection and to investigate whether there are different CD32 isoforms present (inhibitory: CD32b or activating: CD32a and CD32c). Another question that should be addressed is whether resting CD32⁺ CD4⁺ T cells are enriched in proviral DNA compared to activated CD32⁺ CD4⁺ T cells. In both this work and previous studies, the focus was a comparison of CD32⁺ and CD32⁻ CD4⁺ T cells. In addition, HIV-specific T-cell staining via MHC class I+II tetramers should be performed, to check for possible correlations between integrin expression and HIV-specific CD4⁺ and CD8⁺ T-cell populations.

Despite recent findings that challenge the beneficial effects of Vedolizumab therapy during primary HIV infection on the size of the reservoir and post-treatment control, a combination of ART and Vedolizumab is being tested in treatment-naïve individuals in an ongoing Phase I/II trial in Spain (ClinicalTrials.gov Identifier: NCT03577782). Previous studies only enrolled patients who had already been on ART. Furthermore, the antibody will be tested in a European multi-centre,

phase II study of HIV-infected patients on ART, who will be given Vedolizumab in combination with a therapeutic HIV vaccine (NCT04120415).

This will be the first time that Vedolizumab is tested in combination with another immune intervention, which might prove to be more successful than the therapeutic antibody alone. Latency reversal is another HIV cure strategy that is followed up: While early “shock and kill” approaches failed to significantly reverse latency *in vivo*, recent studies in SIV-infected rhesus macaques and HIV-transgenic mice were successful in robustly disrupting the latent reservoir^{151,153}.

To conclude, the results of this thesis suggest that CD32(a) does not seem to mark resting, latently infected CD4⁺ T cells exclusively. Instead, in this work, the frequency of CD32⁺ CD4⁺ T cells was found to correlate with immune activation. This suggests that a re-evaluation of CD32(a) as a potential reservoir marker is necessary.

Furthermore, this thesis has investigated the dynamics of $\alpha 4\beta 7$ expression pattern on T cells from patients with HIV and UC, including those on Vedolizumab therapy. The data obtained here showed that Vedolizumab mainly caused a decrease in the frequency of naïve $\alpha 4\beta 7^+$ CD4⁺ T cells in patients with UC, whereas in viremic and aviremic HIV-infected patients, a significant decrease of CD4⁺ T cell memory populations was observed. The results of this work contribute to the information required for ongoing and future trials that investigate Vedolizumab as a treatment strategy in primary HIV infection, with potential to achieve post-treatment control of viremia.

6 Appendix

Supplementary Table 1: Flow cytometric panel for the phenotypic analysis of CD32 expression of T cells.

Antigen	Fluorophore	Clone	Supplier	Cat. no.	[μ l]/staining
CCR5	BUV737	2D7	BD	565293	2
CCR7	BV421	G043H7	BioLegend	353208	0,5
CD19	BV510	HIB19	BioLegend	302242	1
CD127	BV605	A019D5	BioLegend	351334	1
CD45RA	BV650	HI100	BioLegend	304136	0,25
HLA-DR	BV711	L243	BioLegend	307644	0,25
CD8	BV785	RPA-T8	BioLegend	301046	0,2
CD27	FITC	M-T271	BD	555440	1
CD4	PerCP Cy5.5	SK3	BioLegend	344607	0,1
CCR6	PE-Cy7	G034E3	BioLegend	353418	1
CXCR4	PE-Dazzle 594	12G5	BioLegend	306525	1
CD25	PE	M-A251	BioLegend	356104	0,5
CD32	APC	FUN-2	BioLegend	303207	1
Live/Dead dye	APC-Cy7	-	BioLegend	423105	1:1000
CD14	APC-Cy7	M5E2	BioLegend	301819	0,25
CD3	Alexa Fluor 700	UCHT1	BioLegend	300424	2

Supplementary Table 2: Flow cytometric panel for the phenotypic analysis of $\alpha 4\beta 7$ expression of T cells (samples from HIV patients).

Antigen	Fluorophore	Clone	Supplier	Cat. no.	[μ l]/staining
alpha4beta7	unconjugated	Act1	NIH reagent program	11718	1:1000
rat anti-mouse	BUV395	X56	BD	742481	1:100
CCR5	BUV737	2D7	BD	565293	2
CCR7	BV421	G043H7	BioLegend	353208	2
CD4	BV510	SK3	BioLegend	344633	0,5
CD127	BV605	A019D5	BioLegend	351334	1
CD45RA	BV650	HI100	BioLegend	304136	0,2
HLA-DR	BV711	L243	BioLegend	307644	0,25
CD8	BV785	RPA-T8	BioLegend	301046	0,2
CD27	FITC	M-T271	BD	555440	1
CD57	PerCP Cy5.5	HNK-1	BioLegend	359622	1
CD39	PE Cy7	A1	BioLegend	328212	1
PD-1	PE-Dazzle 594	EH12.2H7	BioLegend	329939	0,5
CCR9	PE	L053E8	BioLegend	358904	1
CD32	APC	FUN-2	BioLegend	303207	1
CD19	APC-Cy7	H1B19	BioLegend	302218	0,25
CD14	APC-Cy7	M5E2	BioLegend	301819	0,25
Live/Dead dye	APC-Cy7	-	BioLegend	423105	1:1000
CD3	Alexa Fluor 700	UCHT1	BioLegend	300424	1

Supplementary Table 3: Flow cytometric panel for the phenotypic analysis of $\alpha 4\beta 7$ on T cells (samples from patients with UC).

Antigen	Fluorophore	Clone	Supplier	Cat. no.	[μ l]/staining
alpha4	unconjugated	7.2R	Novus Biologicals	MAB1354-100	6 μ L / 1x10 ⁶ cells
rat anti-mouse	BUV395	X56	BD	742481	1:100
CCR5	BUV737	2D7	BD	565293	2
CCR7	BV421	G043H7	BioLegend	353208	2
CD4	BV510	SK3	BioLegend	344633	0,5
CD127	BV605	A019D5	BioLegend	351334	1
CD45RA	BV650	HI100	BioLegend	304136	0,2
HLA-DR	BV711	L243	BioLegend	307644	0,25
CD8	BV785	RPA-T8	BioLegend	301046	0,2
CD27	FITC	M-T271	BD	555440	1
beta7	PerCP Cy5.5	FIB504	BioLegend	321220	2
CD39	PE Cy7	A1	BioLegend	328212	1
PD-1	PE-Dazzle 594	EH12.2H7	BioLegend	329939	0,5
CCR9	PE	L053E8	BioLegend	358904	1
CD32	APC	FUN-2	BioLegend	303207	1
CD19	APC-Cy7	H1B19	BioLegend	302218	0,25
CD14	APC-Cy7	M5E2	BioLegend	301819	0,25
Live/Dead dye	APC-Cy7	-	BioLegend	423105	1:1000
CD3	Alexa Fluor 700	UCHT1	BioLegend	300424	1

Supplementary Table 4: Overview of samples processed and experiments conducted to study $\alpha 4\beta 7^+$ T cells.

Samples	n	Kind	Antibody (combination)
Healthy subjects	15	PBMC	$\alpha 4\beta 7$ -specific (clone Act1)
HIV patients on ART	23	PBMC	$\alpha 4\beta 7$ -specific (clone Act1)
Viremic HIV patients	24	PBMC	$\alpha 4\beta 7$ -specific (clone Act1)
HIV elite controllers	5	PBMC	$\alpha 4\beta 7$ -specific (clone Act1)
Healthy subjects	9	PBMC	$\alpha 4$ -specific antibody (clone 7.2R) + $\beta 7$ -specific antibody (clone FIB504)
Ulcerative colitis baseline	8	PBMC	$\alpha 4$ -specific antibody (clone 7.2R) + $\beta 7$ -specific antibody (clone FIB504)
Ulcerative colitis + VDZ	6	PBMC	$\alpha 4$ -specific antibody (clone 7.2R) + $\beta 7$ -specific antibody (clone FIB504)
HIV + UC	1	PBMC	$\alpha 4$ -specific antibody (clone 7.2R) + $\beta 7$ -specific antibody (clone FIB504)
LN HIV+	3	LNMC	$\alpha 4$ -specific antibody (clone 7.2R) + $\beta 7$ -specific antibody (clone FIB504)
LN uninfected	3	LNMC	$\alpha 4$ -specific antibody (clone 7.2R) + $\beta 7$ -specific antibody (clone FIB504)
Gut biopsy healthy control	5	LPL	$\alpha 4$ -specific antibody (clone 7.2R) + $\beta 7$ -specific antibody (clone FIB504)
Gut biopsy ulcerative colitis	6	LPL	$\alpha 4$ -specific antibody (clone 7.2R) + $\beta 7$ -specific antibody (clone FIB504)

Supplementary Table 5: Detailed information about patients with acute HIV infection. *Level of quantification: 50 copies/mL.

	Age/sex	Viral load plasma (Copies/mL)*	Total DNA (Copies/1x10 ⁶ Cells)	CD4 ⁺ T-cell count (Cells/ μ L)	Total DNA normalized to CD4 ⁺ T cells (Total DNA/CD4 ⁺ T-cell count)
Acute 1	m/21	214599	11031,24	278	39,68
Acute 2	f/47	2700	3210,39	189	16,99
Acute 3	m/31	20	1240,6	600	2,07
Acute 4	m/32	3300000	8284,19	203	40,81
Acute 5	m/43	11000	54,8	647	0,08
Acute 6	m/41	6800000	27,68	157	0,18
Acute 7	m/53	6800000	6574,45	548	12,00

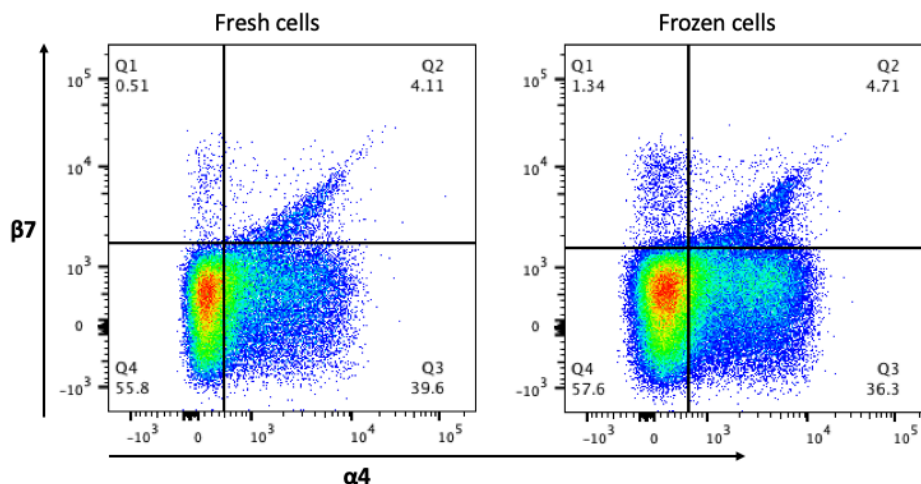
Comparison of freshly isolated and cryopreserved cells regarding their eligibility for phenotypical characterization

PBMC samples from patients were processed as described in “Material and Methods” (section 2.3.1) and stored in the vapour phase of LN₂ at -189 °C until analysis.

It has been demonstrated previously that certain proteins such as chemokine receptors (e.g. CCR5) are sensitive to freezing and thawing²⁵⁹. Thus, additional experiments were conducted to determine whether the markers of interest changed significantly during cryopreservation.

PBMC were collected and isolated as described in the “Material and Methods” section and then either stained directly or frozen down overnight at -80 °C and thawed and stained the next day.

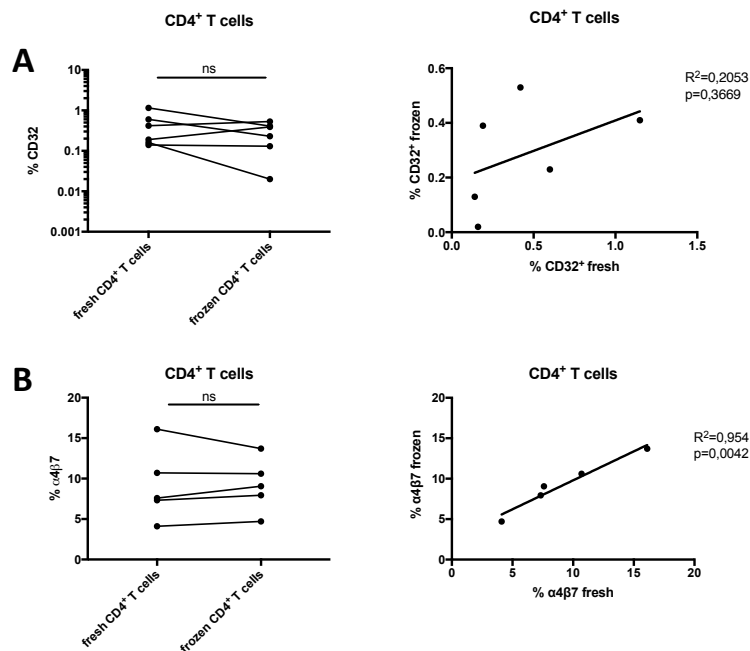
Supplementary Figure 1 shows raw data from fresh and frozen cells stained for the integrin $\alpha 4\beta 7$.



Supplementary Figure 1: Comparison of dot plots of fresh and frozen cells stained with the $\alpha 4$ -specific clone 7.2R in combination with $\beta 7$ -specific antibody (FIB504). PBMC were collected from healthy donors and stained directly. An aliquot of cells was frozen down at -80 °C overnight and stained the following day. Gating according to fluorescence minus one (FMO) controls.

Supplementary Figure 1 shows that the process of freezing and thawing before immunofluorescent staining did not interfere with the distribution of the $\alpha 4\beta 7$ -positive and $\alpha 4\beta 7$ -negative populations.

In addition, the frequency of and correlation between CD32⁺ and α 4 β 7⁺ CD4⁺ T cells that had either been directly stained or frozen down and stained after thawing, were determined (Supplementary Figure 2).

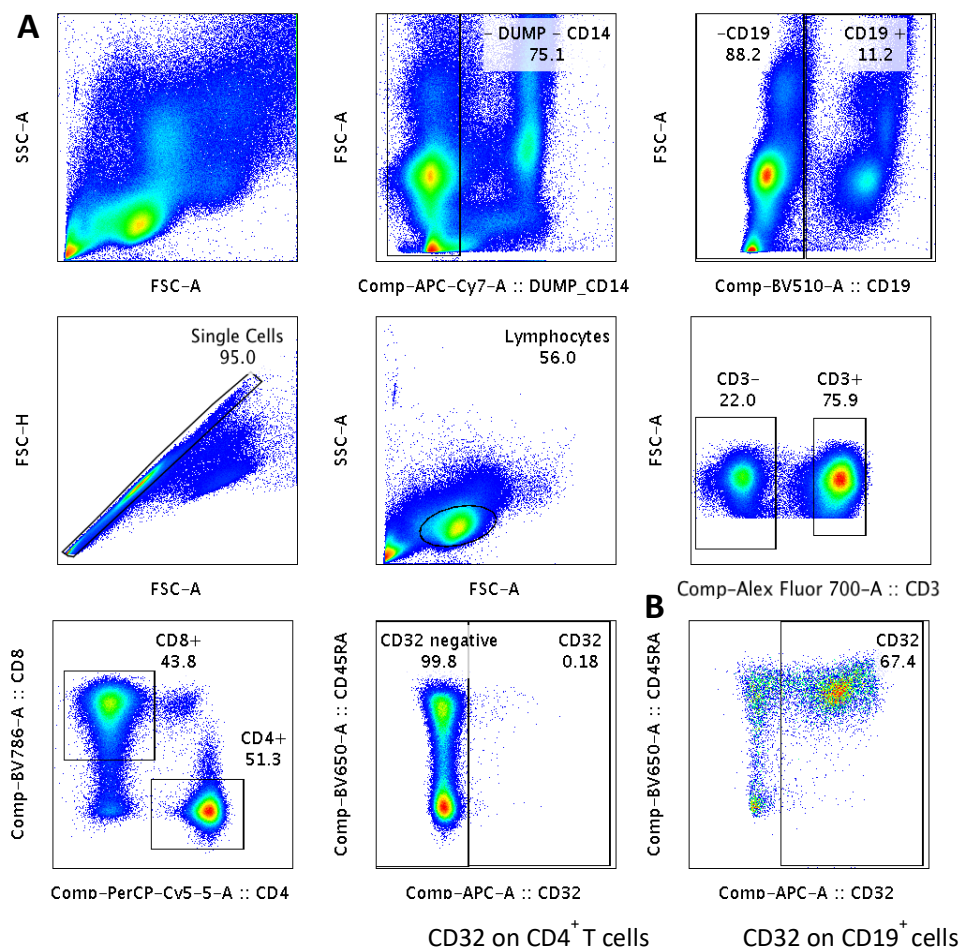


Supplementary Figure 2: Comparison of freshly processed and cryopreserved CD4⁺ T cells used for surface phenotyping. Healthy controls were directly stained without prior freezing (“fresh”). Part of these unstained PBMC were cryopreserved (“frozen”) and then stained for either CD32 (A) or α 4 β 7 (B). (B) PBMC were stained with a combination of an α 4-specific antibody (Clone 7.2R) and a β 7-specific antibody. Data from 6 (A) and 5 (B) healthy individuals. The right graphs show the correlation between the frequencies of fresh and cryopreserved CD4⁺ T cells as determined by linear regression. $Ns \geq 0.05$, as calculated by Wilcoxon matched-pairs signed rank test.

The analysis shows that neither CD32⁺ nor α 4 β 7⁺ CD4⁺ T cell frequencies changed significantly after cryopreservation. Although the correlation between fresh and cryopreserved, thawed CD32⁺ CD4⁺ T cells is quite weak ($R^2=0,2$; $p=0,367$), the frequencies of CD32⁺ CD4⁺ T cells still do not differ significantly. Since the overall frequencies of CD32⁺ CD4⁺ T cells are low, small differences have a larger impact than they do when analysing α 4 β 7⁺ CD4⁺ T cells, which are more stable and show less deviation. Taken together, the frequencies of CD32⁺ and α 4 β 7⁺ cryopreserved CD4⁺ T cells were not significantly different from cells that had been processed directly. This allowed for a substantial simplification of the process, as samples could be acquired over longer periods of time and then frozen down and measured in batches.

Gating strategy

The following **Supplementary Figure 3** illustrates the applied gating strategy that was applied for identification of CD4⁺ and CD8⁺ CD32⁺ T cells. Briefly, dead and CD14⁺ and CD19⁺ cells were excluded before single cells, lymphocytes, CD3⁺ and then either CD4⁺ or CD8⁺ cells were gated. To set the gates for CD32, fluorescence minus one (FMO) controls were applied.



Supplementary Figure 3: Gating strategy for CD4⁺/CD8⁺ CD32⁺ T cells. (A) Dead, CD14⁺ cells and CD19⁺ cells were excluded. After gating on single cells and lymphocytes, CD3⁺ cells were selected. Subsequent analysis was based on either CD8⁺ or CD4⁺ T cells. (B) “Positive control” of the CD32 antibody by gating on CD19⁺ cells.

6.1 List of abbreviations

Ahr	Aryl hydrocarbon receptor
AIDS	Acquired immunodeficiency syndrome
APC	Antigen presenting cells
APOBEC	Apolipoprotein B mRNA editing catalytic polypeptide-like
ART	Antiretroviral therapy
BV	Brilliant violet
BUV	Brilliant ultraviolet
CD	Cluster of differentiation
DC	Dendritic cells
CCL25	C-C motif chemokine ligand 25
DMSO	Dimethyl sulfoxide
dNTP	Deoxyribonucleotide triphosphate
CCR9	C-C motif chemokine receptor 9
CPT	Cell preparation tube
DNA	Deoxyribonucleic acid
EC	Elite controller
EDTA	Ethylenediaminetetraacetic acid
FACS	Fluorescence-activated cell sorting
FcR	Fc receptor
FITC	Fluorescein isothiocyanate
FCS	Foetal calf serum
FSC	Forward scatter
g	Gram/gravitational force equivalent
GALT	Gut-associated lymphoid tissue
GI	Gastrointestinal
HAART	Highly active antiretroviral therapy
HEPES	4-(2-hydroxyethyl)-1-piperazineethanesulfonic acid
h	Hour
HLA	Human leukocyte antigen
HIV	Human immunodeficiency virus
ICAM-1	Intercellular adhesion molecule-1
ICOS	Inducible costimulator
IFN- γ	Interferon- γ
IL	Interleukin
IU	International Units
LAG-3	Lymphocyte-activation gene 3
LNMC	Lymph node mononuclear cells
LPL	Lamina propria lymphocytes
LPS	Lipopolysaccharide
LRA	Latency-reversing agent
MAdCAM-1	Mucosal vascular addressin cell adhesion molecule-1
MAIT cells	Mucosal-associated invariant T cells
MFI	Mean fluorescence intensity

MHC	Major histocompatibility complex
M	Molar
mM	Millimolar
mL	Millilitre
MSM	Men who have sex with men
PBMC	Peripheral blood mononuclear cells
PBS	Phosphate buffered saline
PCR	Polymerase chain reaction
PD-1	Programmed cell death protein 1
PE	Phycoerythrin
PerCp-Cy5.5	Peridinin-chlorophyll-protein-complex-Cy5.5
PFA	Paraformaldehyde
QVOA	Quantitative viral outgrowth assay
RA	Retinoic acid
ROR γ t	Retinoic acid-related orphan receptor γ t
RPM	Rounds per minute
RPMI	Roswell Park Memorial Institute medium
RNA	Ribonucleic acid
RT	Room temperature
SAMHD1	Sterile a motif domain-, HD domain-containing protein 1
sCD14	Soluble CD14
SIV	Simian immunodeficiency virus
SSC	Side scatter
STR	Single tablet regimen
TCM	Central memory T cells
TCR	T-cell receptor
TEM	Effector memory T cells
TFH	T follicular helper cells
TGF- β	Transforming growth factor- β
TIGIT	T cell immunoreceptor with Ig and ITIM domains
Tim-3	T cell immunoglobulin and mucin domain-containing protein 3
TNF- α	Tumour necrosis factor- α
Treg	Regulatory T cells
TRM	Tissue-resident memory T cells
TTM	Transitional memory T cells
UC	Ulcerative colitis
VCAM-1	Vascular cell adhesion protein-1
VDZ	Vedolizumab
Vif	Viral infectivity factor
Vpu	Viral protein unknown
Vpx	Viral protein x
VL	Viral load
$^{\circ}$ C	Grad Celsius
μ G	Mikrogram
μ L	Mikroliter

6.2 References

1. Schulz, T. F., Boshoff, C. H. & Weiss, R. A. HIV infection and neoplasia. *Lancet* **348**, 587–591 (1996).
2. Fromentin, R. *et al.* CD4+ T Cells Expressing PD-1, TIGIT and LAG-3 Contribute to HIV Persistence during ART. *PLOS Pathog.* **12**, e1005761 (2016).
3. Banga, R. *et al.* PD-1+ and follicular helper T cells are responsible for persistent HIV-1 transcription in treated aviremic individuals. *Nat. Med.* **22**, 754–761 (2016).
4. Serra-Peinado, C. *et al.* Expression of CD20 after viral reactivation renders HIV-reservoir cells susceptible to Rituximab. *Nat. Commun.* **10**, (2019).
5. McGary, C. S. *et al.* CTLA-4+PD-1- Memory CD4+ T Cells Critically Contribute to Viral Persistence in Antiretroviral Therapy-Suppressed, SIV-Infected Rhesus Macaques. *Immunity* **47**, 776-788.e5 (2017).
6. Descours, B. *et al.* CD32a is a marker of a CD4 T-cell HIV reservoir harbouring replication-competent proviruses. *Nature* **543**, 564–567 (2017).
7. Gottlieb, M. S. *et al.* Pneumocystis carinii Pneumonia and Mucosal Candidiasis in Previously Healthy Homosexual Men: Evidence of a New Acquired Cellular Immunodeficiency. *N. Engl. J. Med.* **305**, 1425–1431 (1981).
8. Barre-Sinoussi, F. *et al.* Isolation of a T-lymphotropic retrovirus from a patient at risk for acquired immune deficiency syndrome (AIDS). *Science (80-.).* **220**, 868–871 (1983).
9. Clavel, F. *et al.* Isolation of a new human retrovirus from West African patients with AIDS. *Science (80-.).* **233**, 343–346 (1986).
10. Gao, F. *et al.* A Comprehensive Panel of Near-Full-Length Clones and Reference Sequences for Non-Subtype B Isolates of Human Immunodeficiency Virus Type 1. *J. Virol.* **72**, 5680–5698 (1998).
11. Spira, S., Wainberg, M. A., Loemba, H., Turner, D. & Brenner, B. G. Impact of clade diversity on HIV-1 virulence, antiretroviral drug sensitivity and drug resistance. *J. Antimicrob. Chemother.* **51**, 229–40 (2003).
12. Zhu, P. *et al.* Distribution and three-dimensional structure of AIDS virus envelope spikes. *Nature* **441**, 847–852 (2006).
13. Chan, D. C., Fass, D., Berger, J. M. & Kim, P. S. Core structure of gp41 from the HIV envelope glycoprotein. *Cell* **89**, 263–273 (1997).
14. Feng, Y., Broder, C. C., Kennedy, P. E. & Berger, E. A. HIV-1 entry cofactor: functional cDNA cloning of a seven-transmembrane, G protein-coupled receptor. *Science* **272**, 872–7 (1996).

15. Dragic, T. *et al.* HIV-1 entry into CD4+ cells is mediated by the chemokine receptor CC-CKR-5. *Nature* **381**, 667–73 (1996).
16. Deng, H. *et al.* Identification of a major co-receptor for primary isolates of HIV-1. *Nature* **381**, 661–6 (1996).
17. Zuckerman, R. A. *et al.* Higher concentration of HIV RNA in rectal mucosa secretions than in blood and seminal plasma, among men who have sex with men, independent of antiretroviral therapy. *J. Infect. Dis.* **190**, 156–61 (2004).
18. Kiviat, N. B. *et al.* Determinants of human immunodeficiency virus DNA and RNA shedding in the anal-rectal canal of homosexual men. *J. Infect. Dis.* **177**, 571–8 (1998).
19. Oleske, J. *et al.* Immune deficiency syndrome in children. *JAMA* **249**, 2345–9 (1983).
20. Blanche, S. *et al.* A Prospective Study of Infants Born to Women Seropositive for Human Immunodeficiency Virus Type 1. *N. Engl. J. Med.* **320**, 1643–1648 (1989).
21. Donegan, E. *et al.* Infection with Human Immunodeficiency Virus Type 1 (HIV-1) among Recipients of Antibody-Positive Blood Donations. *Ann. Intern. Med.* **113**, 733–739 (1990).
22. Carnathan, D. G. *et al.* Activated CD4+CCR5+ T cells in the rectum predict increased SIV acquisition in SIVGag/Tat-vaccinated rhesus macaques. *Proc. Natl. Acad. Sci. U. S. A.* **112**, 518–23 (2015).
23. Nisole, S. & Saïb, A. Early steps of retrovirus replicative cycle. *Retrovirology* **1**, (2004).
24. Myszka, D. G. *et al.* Energetics of the HIV gp120-CD4 binding reaction. *Proc. Natl. Acad. Sci. U. S. A.* **97**, 9026–9031 (2000).
25. Schuitemaker, H. *et al.* Biological phenotype of human immunodeficiency virus type 1 clones at different stages of infection: progression of disease is associated with a shift from monocyctotropic to T-cell-tropic virus population. *J. Virol.* **66**, 1354–60 (1992).
26. Fauci, A. S. The human immunodeficiency virus: Infectivity and mechanisms of pathogenesis. *Science* **239**, 617–622 (1988).
27. Ananworanich, J. *et al.* HIV DNA Set Point is Rapidly Established in Acute HIV Infection and Dramatically Reduced by Early ART. *EBioMedicine* **11**, 68–72 (2016).
28. Strain, M. C. *et al.* Effect of Treatment, during Primary Infection, on Establishment and Clearance of Cellular Reservoirs of HIV-1. *J. Infect. Dis.* **191**, 1410–1418 (2005).
29. Murphy, Kenneth M.; Travers, Paul; Walport, M. *Janeway Immunologie*. (Springer Berlin Heidelberg, 2014).
30. Tindall, B., Cooper, D. A., Burcham, J., Gold, J. & Penny, R. Clinical and immunologic sequelae of AIDS retrovirus infection. *Aust. N. Z. J. Med.* **16**, 749–755 (1986).

31. Cooper, D. A., Tindall, B., Wilson, E. J., Imrie, A. A. & Penny, R. Characterization of T Lymphocyte Responses During Primary Infection with Human Immunodeficiency Virus. *J. Infect. Dis.* **157**, 889–896 (1988).
32. Nicholson, J. K. A. *et al.* Exposure to human T-lymphotropic virus type III/lymphadenopathy-associated virus and immunologic abnormalities in asymptomatic homosexual men. *Ann. Intern. Med.* **103**, 37–42 (1985).
33. Moore, J. P., Cao, Y., Ho, D. D. & Koup, R. A. Development of the anti-gp120 antibody response during seroconversion to human immunodeficiency virus type 1. *J. Virol.* **68**, 5142–55 (1994).
34. Tomaras, G. D. *et al.* Initial B-Cell Responses to Transmitted Human Immunodeficiency Virus Type 1: Virion-Binding Immunoglobulin M (IgM) and IgG Antibodies Followed by Plasma Anti-gp41 Antibodies with Ineffective Control of Initial Viremia. *J. Virol.* **82**, 12449–12463 (2008).
35. Okoye, A. A. & Picker, L. J. CD4(+) T-cell depletion in HIV infection: mechanisms of immunological failure. *Immunol. Rev.* **254**, 54–64 (2013).
36. Klein, R. S. *et al.* Oral Candidiasis in High-Risk Patients as the Initial Manifestation of the Acquired Immunodeficiency Syndrome. *N. Engl. J. Med.* **311**, 354–358 (1984).
37. Sunderam, G. *et al.* Tuberculosis as a Manifestation of the Acquired Immunodeficiency Syndrome (AIDS). *JAMA J. Am. Med. Assoc.* **256**, 362–366 (1986).
38. Boshoff, C. & Weiss, R. Aids-related malignancies. *Nat. Rev. Cancer* **2**, 373–382 (2002).
39. Gringhuis, S. I. *et al.* HIV-1 exploits innate signaling by TLR8 and DC-SIGN for productive infection of dendritic cells. *Nat. Immunol.* **11**, 419–426 (2010).
40. Heil, F. *et al.* Species-Specific Recognition of Single-Stranded RNA via Toll-like Receptor 7 and 8. *Science (80-.).* **303**, 1526–1529 (2004).
41. Beignon, A. S. *et al.* Endocytosis of HIV-1 activates plasmacytoid dendritic cells via Toll-like receptor-viral RNA interactions. *J. Clin. Invest.* **115**, 3265–3275 (2005).
42. Floyd-Smith, G., Slattery, E. & Lengyel, P. Interferon action: RNA cleavage pattern of a (2'-5') oligoadenylate-dependent endonuclease. *Science (80-.).* **212**, 1030–1032 (1981).
43. Takaoka, A. *et al.* Integration of interferon- α/β signalling to p53 responses in tumour suppression and antiviral defence. *Nature* **424**, 516–523 (2003).
44. Geijtenbeek, T. B. H. *et al.* DC-SIGN, a dendritic cell-specific HIV-1-binding protein that enhances trans-infection of T cells. *Cell* **100**, 587–597 (2000).
45. Shen, R., Smythies, L. E., Clements, R. H., Novak, L. & Smith, P. D. Dendritic cells transmit HIV-1 through human small intestinal mucosa. *J. Leukoc. Biol.* **87**, 663–670 (2010).

46. Malim, M. H. & Bieniasz, P. D. HIV restriction factors and mechanisms of evasion. *Cold Spring Harb. Perspect. Med.* **2**, a006940–a006940 (2012).
47. Sheehy, A. M., Gaddis, N. C., Choi, J. D. & Malim, M. H. Isolation of a human gene that inhibits HIV-1 infection and is suppressed by the viral Vif protein. *Nature* **418**, 646–650 (2002).
48. Salter, J. D., Bennett, R. P. & Smith, H. C. The APOBEC Protein Family: United by Structure, Divergent in Function. *Trends in Biochemical Sciences* **41**, 578–594 (2016).
49. Sheehy, A. M., Gaddis, N. C. & Malim, M. H. The antiretroviral enzyme APOBEC3G is degraded by the proteasome in response to HIV-1 Vif. *Nat. Med.* **9**, 1404–1407 (2003).
50. Marin, M., Rose, K. M., Kozak, S. L. & Kabat, D. HIV-1 Vif protein binds the editing enzyme APOBEC3G and induces its degradation. *Nat. Med.* **9**, 1398–1403 (2003).
51. Laguette, N. *et al.* SAMHD1 is the dendritic- and myeloid-cell-specific HIV-1 restriction factor counteracted by Vpx. *Nature* **474**, 654–657 (2011).
52. Hrecka, K. *et al.* Vpx relieves inhibition of HIV-1 infection of macrophages mediated by the SAMHD1 protein. *Nature* **474**, 658–661 (2011).
53. Ahn, J. *et al.* HIV/simian immunodeficiency virus (SIV) accessory virulence factor Vpx loads the host cell restriction factor SAMHD1 onto the E3 ubiquitin ligase complex CRL4DCAF1. *J. Biol. Chem.* **287**, 12550–12558 (2012).
54. Neil, S. J. D., Zang, T. & Bieniasz, P. D. Tetherin inhibits retrovirus release and is antagonized by HIV-1 Vpu. *Nature* **451**, 425–430 (2008).
55. Van Damme, N. *et al.* The interferon-induced protein BST-2 restricts HIV-1 release and is downregulated from the cell surface by the viral Vpu protein. *Cell Host Microbe* **3**, 245–252 (2008).
56. Lederberg, J. Genes and Antibodies: Do antigens bear instructions for antibody specificity or do they select cell lines that arise by mutation? *Science (80-)*. **129**, 1649–1653 (1959).
57. Cocchi, F. *et al.* Identification of RANTES, MIP-1 alpha, and MIP-1 beta as the major HIV-suppressive factors produced by CD8+ T cells. *Science* **270**, 1811–5 (1995).
58. Schmitz, J. E. *et al.* Control of viremia in simian immunodeficiency virus infection by CD8+ lymphocytes. *Science (80-)*. **283**, 857–860 (1999).
59. Borrow, P. *et al.* Antiviral pressure exerted by HIV-1-specific cytotoxic T lymphocytes (CTLs) during primary infection demonstrated by rapid selection of CTL escape virus. *Nat. Med.* **3**, 205–11 (1997).
60. Matloubian, M., Concepcion, R. J. & Ahmed, R. CD4+ T cells are required to sustain CD8+ cytotoxic T-cell responses during chronic viral infection. *J. Virol.* **68**, 8056–8063 (1994).

61. Jones, R. B. *et al.* Tim-3 expression defines a novel population of dysfunctional T cells with highly elevated frequencies in progressive HIV-1 infection. *J. Exp. Med.* **205**, 2763–79 (2008).
62. Peretz, Y. *et al.* CD160 and PD-1 co-expression on HIV-specific CD8 T cells defines a subset with advanced dysfunction. *PLoS Pathog.* **8**, e1002840 (2012).
63. Wherry, E. J. T cell exhaustion. *Nat. Immunol.* **12**, 492–499 (2011).
64. Day, C. L. *et al.* PD-1 expression on HIV-specific T cells is associated with T-cell exhaustion and disease progression. *Nature* **443**, 350–354 (2006).
65. Kassu, A., Marcus, R. A., D’Souza, M. B., Kelly-McKnight, E. A. & Palmer, B. E. Suppression of HIV Replication by Antiretroviral Therapy Reduces TIM-3 Expression on HIV-Specific CD8⁺ T Cells. *AIDS Res. Hum. Retroviruses* **27**, 1–3 (2011).
66. Rehr, M. *et al.* Emergence of polyfunctional CD8⁺ T cells after prolonged suppression of human immunodeficiency virus replication by antiretroviral therapy. *J. Virol.* **82**, 3391–404 (2008).
67. Migueles, S. A. *et al.* Defective human immunodeficiency virus-specific CD8⁺ T-cell polyfunctionality, proliferation, and cytotoxicity are not restored by antiretroviral therapy. *J. Virol.* **83**, 11876–89 (2009).
68. Serrano-Villar, S. *et al.* HIV-infected individuals with low CD4/CD8 ratio despite effective antiretroviral therapy exhibit altered T cell subsets, heightened CD8⁺ T cell activation, and increased risk of non-AIDS morbidity and mortality. *PLoS Pathog.* **10**, e1004078 (2014).
69. Takata, H. *et al.* Delayed differentiation of potent effector CD8⁺ T cells reducing viremia and reservoir seeding in acute HIV infection. *Sci. Transl. Med.* **9**, eaag1809 (2017).
70. Migueles, S. A. *et al.* HLA B*5701 is highly associated with restriction of virus replication in a subgroup of HIV-infected long term nonprogressors. *Proc. Natl. Acad. Sci. U. S. A.* **97**, 2709–14 (2000).
71. Kaslow, R. A. *et al.* Influence of combinations of human major histocompatibility complex genes on the course of HIV-1 infection. *Nat. Med.* **2**, 405–411 (1996).
72. Samson, M. *et al.* Resistance to HIV-1 infection in caucasian individuals bearing mutant alleles of the CCR-5 chemokine receptor gene. *Nature* **382**, 722–5 (1996).
73. Landais, E. *et al.* Direct killing of Epstein-Barr virus (EBV)-infected B cells by CD4 T cells directed against the EBV lytic protein BHRF1. *Blood* **103**, 1408–1416 (2004).
74. Zaunders, J. J. *et al.* Identification of circulating antigen-specific CD4⁺ T lymphocytes with a CCR5⁺, cytotoxic phenotype in an HIV-1 long-term nonprogressor and in CMV infection. *Blood* **103**, 2238–2247 (2004).

75. Farber, D. L., Yudanin, N. A. & Restifo, N. P. Human memory T cells: Generation, compartmentalization and homeostasis. *Nature Reviews Immunology* **14**, 24–35 (2014).
76. Mosmann, T. R., Cherwinski, H., Bond, M. W., Giedlin, M. A. & Coffman, R. L. Two types of murine helper T cell clone. I. Definition according to profiles of lymphokine activities and secreted proteins. *J. Immunol.* **136**, 2348–57 (1986).
77. Veldhoen, M., Hocking, R. J., Atkins, C. J., Locksley, R. M. & Stockinger, B. TGF β in the Context of an Inflammatory Cytokine Milieu Supports De Novo Differentiation of IL-17-Producing T Cells. *Immunity* **24**, 179–189 (2006).
78. Sakaguchi, S., Sakaguchi, N., Asano, M., Itoh, M. & Toda, M. Immunologic self-tolerance maintained by activated T cells expressing IL-2 receptor alpha-chains (CD25). Breakdown of a single mechanism of self-tolerance causes various autoimmune diseases. *J. Immunol.* **155**, 1151–64 (1995).
79. Goswami, R. & Kaplan, M. H. A Brief History of IL-9. *J. Immunol.* **186**, 3283–3288 (2011).
80. Dardalhon, V. *et al.* IL-4 inhibits TGF- β -induced Foxp3⁺ T cells and, together with TGF- β , generates IL-9⁺ IL-10⁺ Foxp3⁽⁻⁾ effector T cells. *Nat. Immunol.* **9**, 1347–55 (2008).
81. Veldhoen, M. *et al.* Transforming growth factor- β ‘reprograms’ the differentiation of T helper 2 cells and promotes an interleukin 9-producing subset. *Nat. Immunol.* **9**, 1341–6 (2008).
82. Yu, D. *et al.* The Transcriptional Repressor Bcl-6 Directs T Follicular Helper Cell Lineage Commitment. *Immunity* **31**, 457–468 (2009).
83. Chtanova, T. *et al.* T follicular helper cells express a distinctive transcriptional profile, reflecting their role as non-Th1/Th2 effector cells that provide help for B cells. *J. Immunol.* **173**, 68–78 (2004).
84. Breitfeld, D. *et al.* Follicular B helper T cells express CXC chemokine receptor 5, localize to B cell follicles, and support immunoglobulin production. *J. Exp. Med.* **192**, 1545–52 (2000).
85. Marafioti, T. *et al.* The inducible T-cell co-stimulator molecule is expressed on subsets of T cells and is a new marker of lymphomas of T follicular helper cell-derivation. *Haematologica* **95**, 432–9 (2010).
86. Dorfman, D. M., Brown, J. A., Shahsafaie, A. & Freeman, G. J. Programmed death-1 (PD-1) is a marker of germinal center-associated T cells and angioimmunoblastic T-cell lymphoma. *Am. J. Surg. Pathol.* **30**, 802–10 (2006).
87. Perreau, M. *et al.* Follicular helper T cells serve as the major CD4 T cell compartment for HIV-1 infection, replication, and production. *J. Exp. Med.* **210**, 143–156 (2013).
88. Lindqvist, M. *et al.* Expansion of HIV-specific T follicular helper cells in chronic HIV infection. *J. Clin. Invest.* **122**, 3271–3280 (2012).

89. Grossman, W. J. *et al.* Differential expression of granzymes A and B in human cytotoxic lymphocyte subsets and T regulatory cells. *Blood* **104**, 2840–2848 (2004).
90. Collison, L. W. *et al.* IL-35-mediated induction of a potent regulatory T cell population. *Nat. Immunol.* **11**, 1093–1101 (2010).
91. Groux, H. *et al.* A CD4⁺T-cell subset inhibits antigen-specific T-cell responses and prevents colitis. *Nature* **389**, 737–742 (1997).
92. Seddon, B. P. & Mason, D. Regulatory T cells in the control of autoimmunity: The essential role of transforming growth factor β and interleukin 4 in the prevention of autoimmune thyroiditis in rats by peripheral CD4⁺CD45RC⁻ cells and CD4⁺CD8⁻ thymocytes. *J. Exp. Med.* **189**, 279–288 (1999).
93. Eller, K. *et al.* IL-9 Production by Regulatory T Cells Recruits Mast Cells That Are Essential for Regulatory T Cell-Induced Immune Suppression. *J. Immunol.* **186**, 83–91 (2011).
94. Chen, W. *et al.* Conversion of peripheral CD4⁺CD25⁻ naive T cells to CD4⁺CD25⁺ regulatory T cells by TGF- β induction of transcription factor Foxp3. *J. Exp. Med.* **198**, 1875–86 (2003).
95. Panzer, M. *et al.* Rapid in vivo conversion of effector T cells into Th2 cells during helminth infection. *J. Immunol.* **188**, 615–23 (2012).
96. Hegazy, A. N. *et al.* Interferons direct Th2 cell reprogramming to generate a stable GATA-3(+)T-bet(+) cell subset with combined Th2 and Th1 cell functions. *Immunity* **32**, 116–28 (2010).
97. Clerici, M. & Shearer, G. M. A TH1->TH2 switch is a critical step in the etiology of HIV infection. *Immunol. Today* **14**, 107–11 (1993).
98. Langrish, C. L. *et al.* IL-23 drives a pathogenic T cell population that induces autoimmune inflammation. *J. Exp. Med.* **201**, 233–240 (2005).
99. Gaffen, S. L., Jain, R., Garg, A. V & Cua, D. J. The IL-23-IL-17 immune axis: from mechanisms to therapeutic testing. *Nat. Rev. Immunol.* **14**, 585–600 (2014).
100. Moseley, T. A., Haudenschild, D. R., Rose, L. & Reddi, A. H. Interleukin-17 family and IL-17 receptors. *Cytokine and Growth Factor Reviews* **14**, 155–174 (2003).
101. Lee, J. S. S. *et al.* Interleukin-23-Independent IL-17 Production Regulates Intestinal Epithelial Permeability. *Immunity* **43**, 727–738 (2015).
102. Wang, C., Kang, S. G., Lee, J., Sun, Z. & Kim, C. H. The roles of CCR6 in migration of Th17 cells and regulation of effector T-cell balance in the gut. *Mucosal Immunol.* **2**, 173–83 (2009).
103. Sallusto, F. *et al.* T-cell trafficking in the central nervous system. *Immunol. Rev.* **248**, 216–227 (2012).

-
104. Acosta-Rodriguez, E. V *et al.* Surface phenotype and antigenic specificity of human interleukin 17–producing T helper memory cells. *Nat. Immunol.* **8**, 639–646 (2007).
 105. Zhou, L., Chong, M. M. W. & Littman, D. R. Plasticity of CD4+ T Cell Lineage Differentiation. *Immunity* **30**, 646–655 (2009).
 106. Ivanov, I. I. *et al.* The Orphan Nuclear Receptor ROR γ t Directs the Differentiation Program of Proinflammatory IL-17+ T Helper Cells. *Cell* **126**, 1121–1133 (2006).
 107. Yosef, N. *et al.* Dynamic regulatory network controlling Th17 cell differentiation. *Nature* **496**, 461 (2013).
 108. Brüstle, A. *et al.* The development of inflammatory TH-17 cells requires interferon-regulatory factor 4. *Nat. Immunol.* **8**, 958–966 (2007).
 109. Quintana, F. J. *et al.* Control of Treg and TH17 cell differentiation by the aryl hydrocarbon receptor. *Nature* **453**, 65–71 (2008).
 110. Brenchley, J. M. *et al.* Differential Th17 CD4 T-cell depletion in pathogenic and nonpathogenic lentiviral infections. *Blood* **112**, 2826–35 (2008).
 111. Khoury, G. *et al.* Persistence of integrated HIV DNA in CXCR3 + CCR6 + memory CD4R T cells in HIV-infected individuals on antiretroviral therapy. *AIDS* **30**, 1511–1520 (2016).
 112. El Hed, A. *et al.* Susceptibility of Human Th17 Cells to Human Immunodeficiency Virus and Their Perturbation during Infection. *J. Infect. Dis.* **201**, 843–854 (2010).
 113. Brandt, L. *et al.* Low Level of Regulatory T Cells and Maintenance of Balance Between Regulatory T Cells and TH17 Cells in HIV-1–Infected Elite Controllers. *JAIDS J. Acquir. Immune Defic. Syndr.* **57**, 101–108 (2011).
 114. Dandekar, S., George, M. D. & Bäumlner, A. J. Th17 cells, HIV and the gut mucosal barrier. *Curr. Opin. HIV AIDS* **5**, 173–178 (2010).
 115. Ciccone, E. J. *et al.* CD4+ T Cells, Including Th17 and Cycling Subsets, Are Intact in the Gut Mucosa of HIV-1-Infected Long-Term Nonprogressors. *J. Virol.* **85**, 5880 (2011).
 116. Smail, R. C. & Brew, B. J. HIV-associated neurocognitive disorder. in *Handbook of Clinical Neurology* **152**, 75–97 (Elsevier B.V., 2018).
 117. van Sighem, A., Gras, L., Reiss, P., Brinkman, K. & de Wolf, F. Life expectancy of recently diagnosed asymptomatic HIV-infected patients approaches that of uninfected individuals. *AIDS* **24**, 1527–1535 (2010).
 118. Ingle, S. M. *et al.* Impact of Risk Factors for Specific Causes of Death in the First and Subsequent Years of Antiretroviral Therapy Among HIV-Infected Patients. *Clin. Infect. Dis.* **59**, 287–297 (2014).
 119. Heron, J. E. *et al.* The prevalence and risk of non-infectious comorbidities in HIV-infected and non-HIV infected men attending general practice in Australia. *PLoS One* **14**, (2019).

120. Alikhani, A. *et al.* Association between lipodystrophy and length of exposure to ARTs in adult HIV-1 infected patients in Montreal. *BMC Infect. Dis.* **19**, (2019).
121. Nanni, M. G., Caruso, R., Mitchell, A. J., Meggiolaro, E. & Grassi, L. Depression in HIV Infected Patients: A Review. *Current Psychiatry Reports* **17**, 1–11 (2015).
122. Murphy, S. V. S. E. The history of antiretroviral therapy and of its implementation in resource-limited areas of the world. *Aids* **26**, 1231–1241 (2012).
123. Fischl, M. A. *et al.* The Efficacy of Azidothymidine (AZT) in the Treatment of Patients with AIDS and AIDS-Related Complex. *N. Engl. J. Med.* **317**, 185–191 (1987).
124. Kuritzkes, D. R. *et al.* Lamivudine in combination with zidovudine, stavudine, or didanosine in patients with HIV-1 infection. A randomized, double-blind, placebo-controlled trial. *AIDS* (1999). doi:10.1097/00002030-199904160-00009
125. Hammer, S. M. *et al.* A controlled trial of two nucleoside analogues plus indinavir in persons with human immunodeficiency virus infection and CD4 cell counts of 200 per cubic millimeter or less. *N. Engl. J. Med.* (1997). doi:10.1056/NEJM199709113371101
126. Palella, F. J. *et al.* Declining morbidity and mortality among patients with advanced human immunodeficiency virus infection. *N. Engl. J. Med.* (1998). doi:10.1056/NEJM199803263381301
127. Department of Health and Human Services. *Panel on Antiretroviral Guidelines for Adults and Adolescents. Guidelines for the Use of Antiretroviral Agents in Adults and Adolescents with HIV.* (2019).
128. Margolis, D. A. *et al.* Long-acting intramuscular cabotegravir and rilpivirine in adults with HIV-1 infection (LATTE-2): 96-week results of a randomised, open-label, phase 2b, non-inferiority trial. *Lancet* **390**, 1499–1510 (2017).
129. Achhra, A. C., Mwasakifwa, G., Amin, J. & Boyd, M. A. Efficacy and safety of contemporary dual-drug antiretroviral regimens as first-line treatment or as a simplification strategy: a systematic review and meta-analysis. *Lancet HIV* **3**, e351–e360 (2016).
130. Barrett, S. E. *et al.* Extended-duration MK-8591-eluting implant as a candidate for HIV treatment and prevention. *Antimicrob. Agents Chemother.* **62**, (2018).
131. Kerr, Z. Y., Miller, K. R., Galos, D., Love, R. & Poole, C. Challenges, Coping Strategies, and Recommendations Related to the HIV Services Field in the HAART Era: A Systematic Literature Review of Qualitative Studies from the United States and Canada. *AIDS Patient Care STDS* **27**, 85–95 (2013).
132. Svicher, V., Ceccherini-Silberstein, F., Antinori, A., Aquaro, S. & Perno, C. F. Understanding HIV Compartments and Reservoirs. *Curr. HIV/AIDS Rep.* **11**, 186–194 (2014).

133. Lamers, S. L. *et al.* HIV DNA Is Frequently Present within Pathologic Tissues Evaluated at Autopsy from Combined Antiretroviral Therapy-Treated Patients with Undetectable Viral Loads. *J. Virol.* **90**, 8968–83 (2016).
134. Gu, Z., Gao, Q., Li, X., Parniak, M. A. & Wainberg, M. A. Novel mutation in the human immunodeficiency virus type 1 reverse transcriptase gene that encodes cross-resistance to 2',3'-dideoxyinosine and 2',3'-dideoxycytidine. *J. Virol.* **66**, 7128–35 (1992).
135. St Clair, M. H. *et al.* Resistance to ddI and sensitivity to AZT induced by a mutation in HIV-1 reverse transcriptase. *Science* **253**, 1557–9 (1991).
136. Sengupta, S. & Siliciano, R. F. Targeting the Latent Reservoir for HIV-1. *Immunity* **48**, 872–895 (2018).
137. Chun, T. W. *et al.* Quantification of latent tissue reservoirs and total body viral load in HIV-1 infection. *Nature* **387**, 183–8 (1997).
138. Finzi, D. *et al.* Latent infection of CD4+ T cells provides a mechanism for lifelong persistence of HIV-1, even in patients on effective combination therapy. *Nat. Med.* **5**, 512–7 (1999).
139. Chomont, N. *et al.* HIV reservoir size and persistence are driven by T cell survival and homeostatic proliferation. *Nat. Med.* **15**, 893–900 (2009).
140. Sun, H. *et al.* Th1/17 Polarization of CD4 T Cells Supports HIV-1 Persistence during Antiretroviral Therapy. *J. Virol.* **89**, 11284–11293 (2015).
141. Bailey, J. R. *et al.* Residual Human Immunodeficiency Virus Type 1 Viremia in Some Patients on Antiretroviral Therapy Is Dominated by a Small Number of Invariant Clones Rarely Found in Circulating CD4+ T Cells. *J. Virol.* **80**, 6441–6457 (2006).
142. Buzon, M. J. *et al.* HIV-1 persistence in CD4+ T cells with stem cell-like properties. *Nat. Med.* **20**, 139–142 (2014).
143. Kumar, R. B., Maher, D. M., Herzberg, M. C. & Southern, P. J. Expression of HIV receptors, alternate receptors and co-receptors on tonsillar epithelium: Implications for HIV binding and primary oral infection. *Virol. J.* **3**, (2006).
144. Allers, K. *et al.* Evidence for the cure of HIV infection by CCR5Δ32/Δ32 stem cell transplantation. *Blood* **117**, 2791–2799 (2011).
145. Contreras, X. *et al.* Suberoylanilide hydroxamic acid reactivates HIV from latently infected cells. *J. Biol. Chem.* **284**, 6782–9 (2009).
146. Margolis, N. A. K. E. D. H. Expression of latent human immunodeficiency type 1 is induced by novel and selective histone deacetylase inhibitors. *Aids* **23**, 1799–1806 (2009).
147. Archin, N. M. *et al.* Expression of Latent HIV Induced by the Potent HDAC Inhibitor Suberoylanilide Hydroxamic Acid. *AIDS Res. Hum. Retroviruses* **25**, 207–212 (2009).

148. Perreau, M., Banga, R. & Pantaleo, G. Targeted Immune Interventions for an HIV-1 Cure. *Trends in Molecular Medicine* **23**, 945–961 (2017).
149. Ylisastigui, L., Archin, N. M., Lehrman, G., Bosch, R. J. & Margolis, D. M. Coaxing HIV-1 from resting CD4 T cells: Histone deacetylase inhibition allows latent viral expression. *AIDS* **18**, 1101–1108 (2004).
150. Siliciano, J. D. *et al.* Stability of the Latent Reservoir for HIV-1 in Patients Receiving Valproic Acid. *J. Infect. Dis.* **195**, 833–836 (2007).
151. Nixon, C. C. *et al.* Systemic HIV and SIV latency reversal via non-canonical NF- κ B signalling in vivo. *Nature* **578**, 160–165 (2020).
152. McBrien, J. B. *et al.* Robust and persistent reactivation of SIV and HIV by N-803 and depletion of CD8+ cells. *Nature* **578**, 154–159 (2020).
153. Zerbato, J. M., Purves, H. V, Lewin, S. R. & Rasmussen, T. A. Between a shock and a hard place: challenges and developments in HIV latency reversal. *Current Opinion in Virology* **38**, 1–9 (2019).
154. Brucklacher-Waldert, V., Carr, E. J., Linterman, M. A. & Veldhoen, M. Cellular plasticity of CD4+ T cells in the intestine. *Frontiers in Immunology* **5**, (2014).
155. Schneider, T. *et al.* Loss of CD4 T lymphocytes in patients infected with human immunodeficiency virus type 1 is more pronounced in the duodenal mucosa than in the peripheral blood. Berlin Diarrhea/Wasting Syndrome Study Group. *Gut* **37**, 524–9 (1995).
156. Veazey, R. S. *et al.* Gastrointestinal Tract as a Major Site of CD4+ T Cell Depletion and Viral Replication in SIV Infection. *Science (80-.)*. **280**, (1998).
157. Lim, S. G. *et al.* Loss of mucosal CD4 lymphocytes is an early feature of HIV infection. *Clin. Exp. Immunol.* **92**, 448–54 (1993).
158. Brenchley, J. M. *et al.* CD4+ T cell depletion during all stages of HIV disease occurs predominantly in the gastrointestinal tract. *J. Exp. Med.* **200**, 749–59 (2004).
159. Perrone, I. *et al.* MAdCAM signaling through integrin $\alpha_4\beta_7$ modulates surface expression of CCR5 and markers of CD4+ T cell activation. *J. Immunol.* **196**, 207.13 LP-207.13 (2016).
160. Sonnenberg, G. F., Fouser, L. A. & Artis, D. Border patrol: Regulation of immunity, inflammation and tissue homeostasis at barrier surfaces by IL-22. *Nature Immunology* **12**, 383–390 (2011).
161. Kawachi, I., Maldonado, J., Strader, C. & Gilfillan, S. MR1-restricted V alpha 19i mucosal-associated invariant T cells are innate T cells in the gut lamina propria that provide a rapid and diverse cytokine response. *J. Immunol.* **176**, 1618–27 (2006).
162. Le Bourhis, L. *et al.* MAIT Cells Detect and Efficiently Lyse Bacterially-Infected Epithelial Cells. *PLoS Pathog.* **9**, (2013).

163. Wong, E. B. *et al.* Low levels of peripheral CD161⁺⁺CD8⁺ Mucosal Associated Invariant T (MAIT) cells are found in HIV and HIV/TB co-infection. *PLoS One* **8**, (2013).
164. Cosgrove, C. *et al.* Early and nonreversible decrease of CD161⁺⁺/MAIT cells in HIV infection. *Blood* **121**, 951–961 (2013).
165. Eberhard, J. M. *et al.* CD161⁺ MAIT cells are severely reduced in peripheral blood and lymph nodes of HIV-infected individuals independently of disease progression. *PLoS One* **9**, e111323 (2014).
166. Luster, A. D., Alon, R. & von Andrian, U. H. Immune cell migration in inflammation: present and future therapeutic targets. *Nat. Immunol.* **6**, 1182–1190 (2005).
167. Iwata, M. *et al.* Retinoic Acid Imprints Gut-Homing Specificity on T Cells. *Immunity* **21**, 527–538 (2004).
168. Czarnewski, P. *et al.* Retinoic Acid and Its Role in Modulating Intestinal Innate Immunity. *Nutrients* **9**, 68 (2017).
169. Ley, K., Laudanna, C., Cybulsky, M. I. & Nourshargh, S. Getting to the site of inflammation: the leukocyte adhesion cascade updated. *Nat. Rev. Immunol.* **7**, 678–689 (2007).
170. Berlin, C. *et al.* $\alpha 4\beta 7$ integrin mediates lymphocyte binding to the mucosal vascular addressin MAdCAM-1. *Cell* **74**, 185–195 (1993).
171. Hynes, R. O. Integrins: Bidirectional, Allosteric Signaling Machines. *Cell* **110**, 673–687 (2002).
172. Nolte, M. A. & Margadant, C. Activation and suppression of hematopoietic integrins in hemostasis and immunity. *Blood* **135**, 7–16 (2020).
173. Makgoba, M. W. *et al.* ICAM-1 a ligand for LFA-1-dependent adhesion of B, T and myeloid cells. *Nature* **331**, 86–88 (1988).
174. Elices, M. J. *et al.* VCAM-1 on activated endothelium interacts with the leukocyte integrin VLA-4 at a site distinct from the VLA-4/Fibronectin binding site. *Cell* **60**, 577–584 (1990).
175. Denucci, C. C., Mitchell, J. S. & Shimizu, Y. Integrin function in T-cell homing to lymphoid and nonlymphoid sites: getting there and staying there. *Crit. Rev. Immunol.* **29**, 87–109 (2009).
176. Förster, R., Davalos-Miszlitz, A. C. & Rot, A. CCR7 and its ligands: balancing immunity and tolerance. *Nat. Rev. Immunol.* **8**, 362–371 (2008).
177. Connor, E. M., Eppihimer, M. J., Morise, Z., Granger, D. N. & Grisham, M. B. Expression of mucosal addressin cell adhesion molecule-1 (MAdCAM-1) in acute and chronic inflammation. *J. Leukoc. Biol.* **65**, 349–355 (1999).
178. Sivo, A. *et al.* Integrin $\alpha 4\beta 7$ expression on peripheral blood CD4⁺ T cells predicts HIV acquisition and disease progression outcomes. *Sci. Transl. Med.* **10**, eaam6354 (2018).

179. Kader, M. *et al.* $\alpha 4 + \beta 7$ hiCD4+ memory T cells harbor most Th-17 cells and are preferentially infected during acute SIV infection. *Mucosal Immunol.* **2**, 439–449 (2009).
180. Arthos, J. *et al.* HIV-1 envelope protein binds to and signals through integrin $\alpha 4 \beta 7$, the gut mucosal homing receptor for peripheral T cells. *Nat. Immunol.* **9**, 301–309 (2008).
181. Cicala, C. *et al.* The integrin $\alpha 4 \beta 7$ forms a complex with cell-surface CD4 and defines a T-cell subset that is highly susceptible to infection by HIV-1. *Proc. Natl. Acad. Sci. U. S. A.* **106**, 20877–82 (2009).
182. Guzzo, C. *et al.* Virion incorporation of integrin $\alpha 4 \beta 7$ facilitates HIV-1 infection and intestinal homing. *Sci. Immunol.* **2**, eaam7341 (2017).
183. Byraredy, S. N. *et al.* Sustained virologic control in SIV+ macaques after antiretroviral and $\alpha 4 \beta 7$ antibody therapy. *Science (80-.).* **354**, 197–202 (2016).
184. Brooks, D. G., Qiu, W. Q., Luster, A. D. & Ravetch, J. V. Structure and expression of human IgG FcRII(CD32). Functional heterogeneity is encoded by the alternatively spliced products of multiple genes. *J. Exp. Med.* **170**, 1369–85 (1989).
185. Hartnell, A., Moqbel, R., Walsh, G. M., Bradley, B. & Kay, A. B. Fc gamma and CD11/CD18 receptor expression on normal density and low density human eosinophils. *Immunology* **69**, 264–70 (1990).
186. Parren, P. W. H. I. *et al.* On the interaction of IgG subclasses with the low affinity Fc γ RIIa (CD32) on human monocytes, neutrophils, and platelets. Analysis of a functional polymorphism to human IgG2. *J. Clin. Invest.* **90**, 1537–1546 (1992).
187. Mantzioris, B. X., Berger, M. F., Sewell, W. & Zola, H. Expression of the Fc receptor for IgG (Fc gamma RII/CDw32) by human circulating T and B lymphocytes. *J. Immunol.* **150**, 5175–51784 (1993).
188. Smith, K. G. C. & Clatworthy, M. R. Fc γ RIIB in autoimmunity and infection: evolutionary and therapeutic implications. *Nat. Rev. Immunol.* **10**, 328–43 (2010).
189. Nimmerjahn, F. & Ravetch, J. V. Fc γ receptors as regulators of immune responses. *Nat. Rev. Immunol.* **8**, 34–47 (2008).
190. Lu, J. *et al.* Structural recognition and functional activation of Fc γ RIIb by innate pentraxins. *Nature* **456**, 989–92 (2008).
191. Forthal, D. N. *et al.* Fc γ RIIa Genotype Predicts Progression of HIV Infection. *J. Immunol.* **179**, (2007).
192. Kruize, Z. & Kootstra, N. A. The Role of Macrophages in HIV-1 Persistence and Pathogenesis. *Frontiers in Microbiology* **10**, (2019).
193. Soriano-Sarabia, N. *et al.* Peripheral V γ 9V δ 2 T Cells Are a Novel Reservoir of Latent HIV Infection. *PLOS Pathog.* **11**, e1005201 (2015).

194. Lee, G. Q. & Lichterfeld, M. Diversity of HIV-1 reservoirs in CD4+ T-cell subpopulations. *Current Opinion in HIV and AIDS* **11**, 383–387 (2016).
195. Harper, M. E., Marselle, L. M., Gallo, R. C. & Wong-Staal, F. Detection of lymphocytes expressing human T-lymphotropic virus type III in lymph nodes and peripheral blood from infected individuals by in situ hybridization. *Proc. Natl. Acad. Sci. U. S. A.* **83**, 772–776 (1986).
196. Morón-López, S. *et al.* Sensitive quantification of the HIV-1 reservoir in gut-associated lymphoid tissue. *PLoS One* **12**, e0175899 (2017).
197. Wittner, M. *et al.* CD32 Expression of Different Memory T Cell Subpopulations in the Blood and Lymph Nodal Tissue of HIV Patients and Healthy Controls Correlates With Immune Activation. *J. Acquir. Immune Defic. Syndr.* **77**, 345–349 (2018).
198. Wittner, M. *et al.* Comparison of the integrin $\alpha 4\beta 7$ expression pattern of memory T cell subsets in HIV infection and ulcerative colitis. *PLoS One* **14**, e0220008 (2019).
199. Rouzioux, C. & Richman, D. How to best measure HIV reservoirs? *Curr. Opin. HIV AIDS* **8**, 170–5 (2013).
200. Dunay, G. A. *et al.* Assessment of the HIV-1 reservoir in CD4+ regulatory T cells by a Droplet Digital PCR based approach. *Virus Res.* **240**, 107–111 (2017).
201. Noto, A. *et al.* CD32 + and PD-1 + Lymph Node CD4 T Cells Support Persistent HIV-1 Transcription in Treated Aviremic Individuals. *J. Virol.* **92**, e00901-18 (2018).
202. Yu, X. *et al.* The surface protein TIGIT suppresses T cell activation by promoting the generation of mature immunoregulatory dendritic cells. *Nat. Immunol.* **10**, 48–57 (2009).
203. Chew, G. M. *et al.* TIGIT Marks Exhausted T Cells, Correlates with Disease Progression, and Serves as a Target for Immune Restoration in HIV and SIV Infection. *PLOS Pathog.* **12**, e1005349 (2016).
204. Arthos, J. *et al.* The Role of Integrin $\alpha 4\beta 7$ in HIV Pathogenesis and Treatment. *Current HIV/AIDS Reports* **15**, 127–135 (2018).
205. Ungar, B. *et al.* Association of Vedolizumab Level, Anti-Drug Antibodies, and $\alpha 4\beta 7$ Occupancy With Response in Patients With Inflammatory Bowel Diseases. *Clin. Gastroenterol. Hepatol.* **16**, 697-705.e7 (2018).
206. Wang, X. *et al.* Monitoring $\alpha 4\beta 7$ integrin expression on circulating CD4+ T cells as a surrogate marker for tracking intestinal CD4+ T-cell loss in SIV infection. *Mucosal Immunol.* **2**, 518–526 (2009).
207. Perciani, C. T. *et al.* $\alpha E\beta 7$, $\alpha 4\beta 7$ and $\alpha 4\beta 1$ integrin contributions to T cell distribution in blood, cervix and rectal tissues: Potential implications for HIV transmission. *PLoS One* **13**, e0192482 (2018).

-
208. Sallusto, F., Langenkamp, A., Geginat, J. & Lanzavecchia, A. Functional subsets of memory T cells identified by CCR7 expression. in *Current Topics in Microbiology and Immunology* **251**, 167–171 (2000).
 209. Michie, C. A., McLean, A., Alcock, C. & Beverley, P. C. L. Lifespan of human lymphocyte subsets defined by CD45 isoforms. *Nature* **360**, 264–265 (1992).
 210. Mora, J. R. *et al.* Generation of gut-homing IgA-secreting B cells by intestinal dendritic cells. *Science* **314**, 1157–60 (2006).
 211. Uzzan, M. *et al.* Anti- $\alpha 4\beta 7$ therapy targets lymphoid aggregates in the gastrointestinal tract of HIV-1-infected individuals. *Sci. Transl. Med.* **10**, eaau4711 (2018).
 212. Kim, C. J. *et al.* Mucosal Th17 cell function is altered during HIV infection and is an independent predictor of systemic immune activation. *J. Immunol.* **191**, 2164–73 (2013).
 213. Alzahrani, J. *et al.* Inflammatory and immunometabolic consequences of gut dysfunction in HIV: Parallels with IBD and implications for reservoir persistence and non-AIDS comorbidities. *EBioMedicine* **46**, 522–531 (2019).
 214. Brenchley, J. M. *et al.* Microbial translocation is a cause of systemic immune activation in chronic HIV infection. *Nat. Med.* **12**, 1365–1371 (2006).
 215. Vujkovic-Cvijin, I. *et al.* Dysbiosis of the gut microbiota is associated with HIV disease progression and tryptophan catabolism. *Sci. Transl. Med.* **5**, 193ra91 (2013).
 216. Ott, S. J. *et al.* Reduction in diversity of the colonic mucosa associated bacterial microflora in patients with active inflammatory bowel disease. *Gut* **53**, 685–693 (2004).
 217. Knox, T. A., Spiegelman, D., Skinner, S. C. & Gorbach, S. Diarrhea and abnormalities of gastrointestinal function in a cohort of men and women with HIV infection. *Am. J. Gastroenterol.* **95**, 3482–3489 (2000).
 218. Villinger, F. & Ansari, A. A. Role of IL-12 in HIV infection and vaccine. *European Cytokine Network* **21**, 215–218 (2010).
 219. Papadakis, K. A. *et al.* The role of thymus-expressed chemokine and its receptor CCR9 on lymphocytes in the regional specialization of the mucosal immune system. *J. Immunol.* **165**, 5069–76 (2000).
 220. Bruel, T. & Schwartz, O. Markers of the HIV-1 reservoir. *Curr. Opin. HIV AIDS* **13**, 383–388 (2018).
 221. Badia, R. *et al.* CD32 expression is associated to T-cell activation and is not a marker of the HIV-1 reservoir. *Nat. Commun.* **9**, 2739 (2018).
 222. Martin, G. E. *et al.* CD32-expressing CD4 T cells are phenotypically diverse and can contain proviral HIV DNA. *Front. Immunol.* **9**, (2018).

-
223. Thornhill, J. P. *et al.* CD32 expressing doublets in HIV-infected gut-associated lymphoid tissue are associated with a T follicular helper cell phenotype. *Mucosal Immunol.* **12**, 1212–1219 (2019).
 224. Iglesias-Ussel, M., Vandergeeten, C., Marchionni, L., Chomont, N. & Romerio, F. High Levels of CD2 Expression Identify HIV-1 Latently Infected Resting Memory CD4+ T Cells in Virally Suppressed Subjects. *J. Virol.* **87**, 9148–9158 (2013).
 225. Vásquez, J. J. *et al.* CD32-RNA Co-localizes with HIV-RNA in CD3+ Cells Found within Gut Tissues from Viremic and ART-Suppressed Individuals. *Pathog. Immun.* **4**, 147–160 (2019).
 226. Darcis, G. *et al.* CD32+CD4+ T Cells Are Highly Enriched for HIV DNA and Can Support Transcriptional Latency. *Cell Rep.* **30**, 2284-2296.e3 (2020).
 227. Grau-Expósito, J. *et al.* A Novel Single-Cell FISH-Flow Assay Identifies Effector Memory CD4(+) T cells as a Major Niche for HIV-1 Transcription in HIV-Infected Patients. *MBio* **8**, e00876-17 (2017).
 228. Abdel-Mohsen, M. *et al.* CD32 is expressed on cells with transcriptionally active HIV but does not enrich for HIV DNA in resting T cells. *Sci. Transl. Med.* **10**, eaar6759 (2018).
 229. Bertagnolli, L. N. *et al.* The role of CD32 during HIV-1 infection. *Nature* **561**, E17–E19 (2018).
 230. Pérez, L. *et al.* Conflicting evidence for HIV enrichment in CD32+ CD4 T cells. *Nature* **561**, E9–E16 (2018).
 231. García, M. *et al.* CD32 Expression is not Associated to HIV-DNA content in CD4 cell subsets of individuals with Different Levels of HIV Control. *Sci. Rep.* **8**, 15541 (2018).
 232. Dhummakupt, A. *et al.* The Latent Human Immunodeficiency Virus (HIV) Reservoir Resides Primarily in CD32-CD4+ T Cells in Perinatally HIV-Infected Adolescents With Long-Term Virologic Suppression. *J. Infect. Dis.* **219**, 80–88 (2019).
 233. Engelhardt, W., Matzke, J. & Schmidt, R. E. Activation-dependent expression of low affinity IgG receptors Fc gamma RII(CD32) and Fc gamma RIII(CD16) in subpopulations of human T lymphocytes. *Immunobiology* **192**, 297–320 (1995).
 234. McLain, L. & Dimmock, N. J. A human CD4+ T-cell line expresses functional CD64 (Fc gamma RI), CD32 (Fc gamma RII), and CD16 (Fc gamma RIII) receptors but these do not enhance the infectivity of HIV-1-IgG complexes. *Immunology* **90**, 109–14 (1997).
 235. Morrow, W. J. W., Wharton, M., Stricker, R. B. & Levy, J. A. Circulating immune complexes in patients with acquired immune deficiency syndrome contain the AIDS-associated retrovirus. *Clin. Immunol. Immunopathol.* **40**, 515–524 (1986).
 236. Brouwer, K. C. *et al.* Polymorphism of Fc receptor IIa for IgG in infants is associated with susceptibility to perinatal HIV-1 infection. *AIDS* **18**, 1187–1194 (2004).

237. Horiike, M. *et al.* Lymph nodes harbor viral reservoirs that cause rebound of plasma viremia in SIV-infected macaques upon cessation of combined antiretroviral therapy. *Virology* **423**, 107–118 (2012).
238. Spiegel, H., Herbst, H., Niedobitek, G., Foss, H. D. & Stein, H. Follicular dendritic cells are a major reservoir for human immunodeficiency virus type 1 in lymphoid tissues facilitating infection of CD4⁺ T-helper cells. *Am. J. Pathol.* **140**, 15–22 (1992).
239. Lorenzo-Redondo, R. *et al.* Persistent HIV-1 replication maintains the tissue reservoir during therapy. *Nature* **530**, 51–56 (2016).
240. Klatt, N. R., Chomont, N., Douek, D. C. & Deeks, S. G. Immune Activation And Hiv Persistence: Implications For Curative Approaches To Hiv Infection. *Immunol. Rev.* **254**, 326–342 (2013).
241. Soler, D. *et al.* The binding specificity and selective antagonism of vedolizumab, an anti- $\alpha 4\beta 7$ integrin therapeutic antibody in development for inflammatory bowel diseases. *J. Pharmacol. Exp. Ther.* **330**, 864–75 (2009).
242. Wyant, T., Yang, L. & Fedyk, E. In vitro assessment of the effects of vedolizumab binding on peripheral blood lymphocytes. *MAbs* **5**, 842–850 (2013).
243. Zeissig, S. *et al.* Vedolizumab is associated with changes in innate rather than adaptive immunity in patients with inflammatory bowel disease. *Gut* **68**, 25–39 (2019).
244. Ling, L. *et al.* Vedolizumab-mediated integrin $4\beta 7$ blockade does not control HIV-1SF162 rebound after combination antiretroviral therapy interruption in humanized mice. *AIDS* **33**, F1–F12 (2019).
245. Abbink, P. *et al.* Lack of therapeutic efficacy of an antibody to $\alpha 4\beta 7$ in SIVmac251-infected rhesus macaques. *Science (80-.)*. **365**, 1029–1033 (2019).
246. Di Mascio, M. *et al.* Evaluation of an antibody to $\alpha 4\beta 7$ in the control of SIVmac239-nef-stop infection. *Science (80-.)*. **365**, 1025–1029 (2019).
247. Iwamoto, N. *et al.* Blocking $\alpha 4\beta 7$ integrin binding to SIV does not improve virologic control. *Science (80-.)*. **365**, 1033–1036 (2019).
248. Sneller, M. C. *et al.* An open-label phase 1 clinical trial of the anti- $\alpha 4\beta 7$ monoclonal antibody vedolizumab in HIV-infected individuals. *Sci. Transl. Med.* **11**, eaax3447 (2019).
249. Nawaz, F. *et al.* MAdCAM costimulation through Integrin- $\alpha 4\beta 7$ promotes HIV replication. *Mucosal Immunol.* **11**, 1342–1351 (2018).
250. Ishida, Y., Agata, Y., Shibahara, K. & Honjo, T. Induced expression of PD-1, a novel member of the immunoglobulin gene superfamily, upon programmed cell death. *EMBO J.* **11**, 3887–95 (1992).

-
251. Cimbri, R. *et al.* IL-7 induces expression and activation of integrin $\alpha 4\beta 7$ promoting naive T-cell homing to the intestinal mucosa. *Blood* **120**, 2610–9 (2012).
 252. Lord, J. D. *et al.* Circulating integrin $\alpha 4/\beta 7$ lymphocytes targeted by vedolizumab have a pro-inflammatory phenotype. *Clin. Immunol.* **193**, 24–32 (2018).
 253. Trivedi, P. J. *et al.* Intestinal CCL25 expression is increased in colitis and correlates with inflammatory activity. *J. Autoimmun.* **68**, 98–104 (2016).
 254. McGuinty, M., J. Angel, A. Kumar, R. Sy, S. Murthy, D. Kilby, N. Tremblay, E. Lavoie, S. B. Schinkel, and S. N. B. Seeking suppression in havarti: Viremia and T cells after vedolizumab and analytical treatment interruption in HIV/ART. in *Conference on Retroviruses and Opportunistic Infections (CROI)* 4–7 (2019).
 255. Thornhill, J. P. *et al.* Vedolizumab use and the associations between $\alpha 4\beta 7$ expression and HIV reservoir in the gut during treated primary HIV infection. *AIDS* **33**, 2268–2271 (2019).
 256. Chun, T. W. *et al.* Early establishment of a pool of latently infected, resting CD4(+) T cells during primary HIV-1 infection. *Proc. Natl. Acad. Sci. U. S. A.* **95**, 8869–73 (1998).
 257. Sills, J. Editorial expression of concern. *Science* **365**, 991 (2019).
 258. Kelley, C. F. *et al.* Differences in expression of gut-homing receptors on CD4+ T cells in black and white HIV-negative men who have sex with men. *AIDS* **30**, 1305–8 (2016).
 259. Costantini, A. *et al.* Effects of cryopreservation on lymphocyte immunophenotype and function. *J. Immunol. Methods* **278**, 145–155 (2003).
 260. Rockstroh, J. & Hoffmann, C. *HIV-Buch.* (Medizin Fokus Verlag, Hamburg, 2011).

7 Acknowledgements

Ich möchte mich zunächst bei meinem Doktorvater PD Dr. med. Julian Schulze zur Wiesch für die Überlassung des Themas und die unermüdliche Unterstützung bedanken. Außerdem für die vielen Möglichkeiten, die mir gegeben wurden.

Des Weiteren gilt mein Dank Prof. Dr. Dobner für die Betreuung und die Möglichkeit, meine Ergebnisse auch außerhalb meiner Arbeitsgruppe zu diskutieren.

Besonderer Dank gilt allen Patienten und Freiwilligen, die selbstlos Blut und Gewebe gespendet haben.

Ich möchte allen in meiner Arbeitsgruppe von ganzem Herzen für die tolle Arbeitsatmosphäre und die besondere Kollegialität danken und dafür, dass ihr mich so schnell und gut aufgenommen habt.

Christin, fürs Team! Für deine Hilfe beim Korrekturlesen und für dein verlässliches Teamwork; egal ob beim Lymphknoten schneiden oder Anträge schreiben. Außerdem für deine Unterstützung während des Schlussspurts.

Johanna, riesen Dank für alles, was du mir beigebracht hast und die schöne Zeit.

Robin, danke für deine Hilfe im Labor und für Michael J., die Lamas und jederzeit das passende Gif. Dit war dit-hamwa!

Silke, ich danke dir für dein offenes Ohr, den Spaß an und neben der Bench und dafür, dass du mich betüddelt und mir so viel geholfen hast. Bist halt die Beste.

Vero, Dankeschön fürs ausdauernde Proben jagen und deine Unterstützung bei allem anderen.

Zum Schluss ein riesiges Dankeschön an meine Familie: Dafür, dass ihr euch für meine Arbeit interessiert, euch mit mir gefreut und Daumen gedrückt habt. Bernd und Peter, danke für den Telefonsupport, Steffi fürs Vorträge üben und Mama und Papa, danke für „Das machst du schon“.